

Papers Written on DNA by Franklin and R. G. Gosling and Correspondence

Shelfmark: FRKN 1/3
Reference number: b19832060
Persistent URL: <https://wellcomelibrary.org/item/b19832060>
Catalogue record: https://search.wellcomelibrary.org/iii/encore/record/C__Rb1983206

This digital version has been supplied by the Wellcome Library under the following Conditions of Use:

You have permission to make copies of this work under a Creative Commons, Attribution, Non-commercial license.

Non-commercial use includes private study, academic research, teaching, and other activities that are not primarily intended for, or directed towards, commercial advantage or private monetary compensation. See the Legal Code for further information.

Image source should be attributed as specified in the full catalogue record. If no source is given the image should be attributed to Wellcome Library.

This material has been provided by **Churchill Archives Centre, Churchill College, Cambridge** where the originals may be consulted.



Wellcome Library
183 Euston Road
London NW1 2BE UK
T +44 (0)20 7611 8722
E library@wellcome.ac.uk
<https://wellcomelibrary.org>

HEADING TO PLATES I TO V

I. 3 fibres of NaDNA, diameters 18-30 μ , specimen-film distance 15 mm, exposure 116 hours. R.H. 75%

II. Bundle of fine fibres. Specimen-film distance 15 mm.

Exposure 6 hours R.H. 92%.

III. Bundle of fine fibres. Specimen-film distance 15 mm, exposure 3 $\frac{1}{2}$ hours. R.H. 84%.

IV. Single fibre, diameter 50 μ , specimen-film distance 15 mm, exposure 62 hours. R.H. 75%. This specimen had previously given photographs similar to Plate I.

V. a) Single fibre, diameter 120 μ , specimen-film distance 15 mm, exposure 22 hours. R.H. ?

b) Specimen as above, exposure 19 hours. R.H. ?

c) Specimen as above, exposure 24 hours. Dried over P_2O_5 at room temperature.

d) Bundle of about 30 fine fibres. Specimen-film distance 30 mm (Unicam camera). Specimen dried by heating in hydrogen 50 - 80°C before and during exposure.

VI. Specimen and conditions as for IV. Exposure 62 hours.

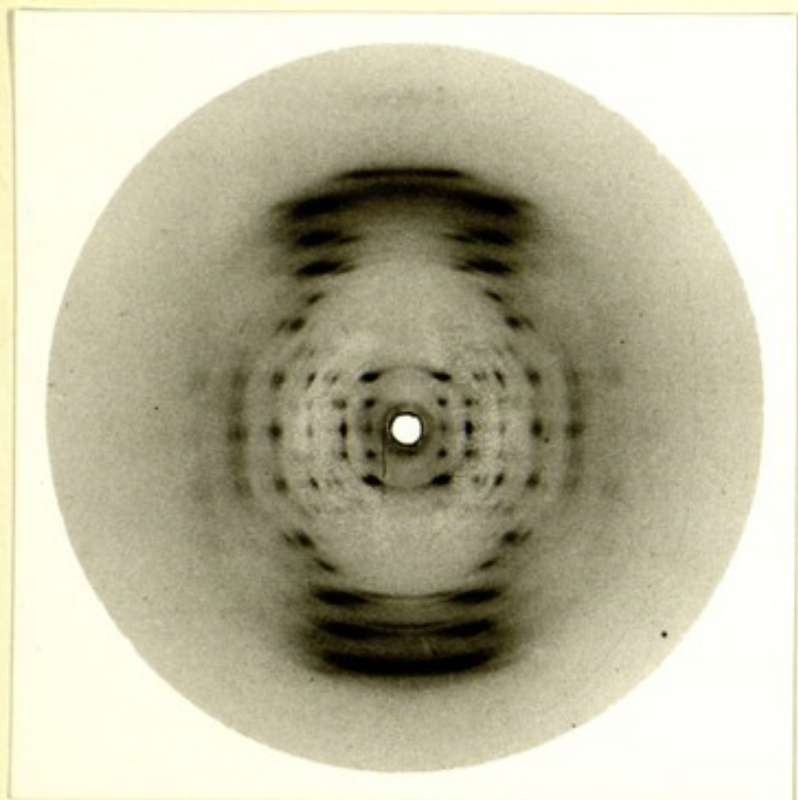


Plate 1

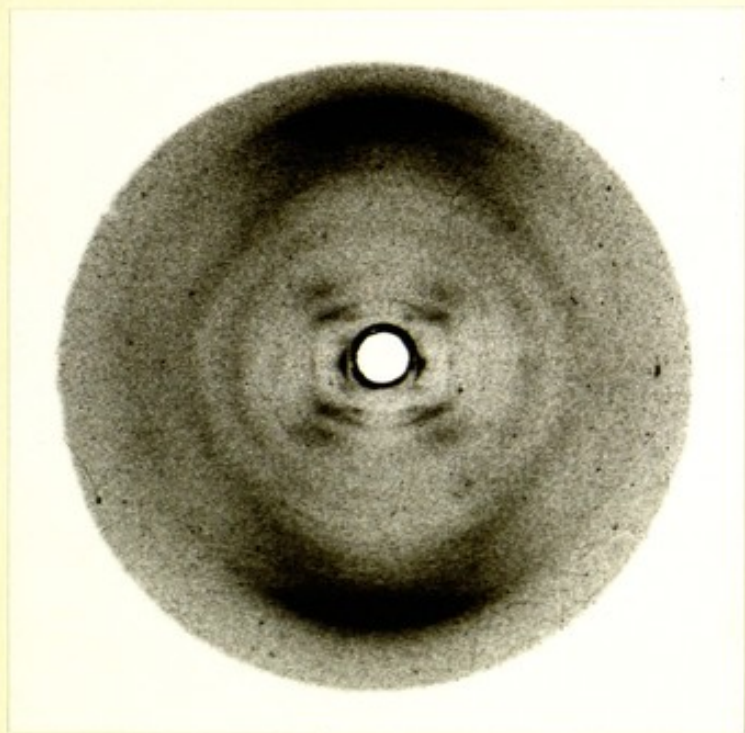


Plate 2

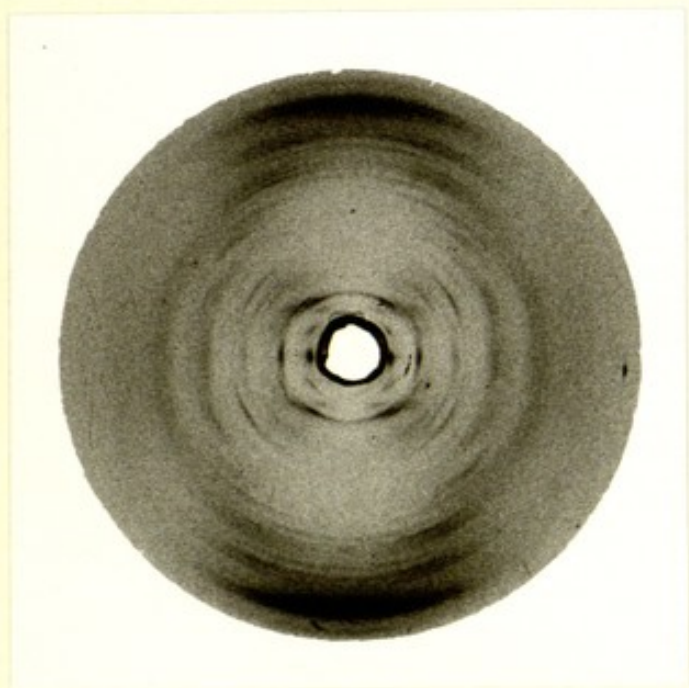
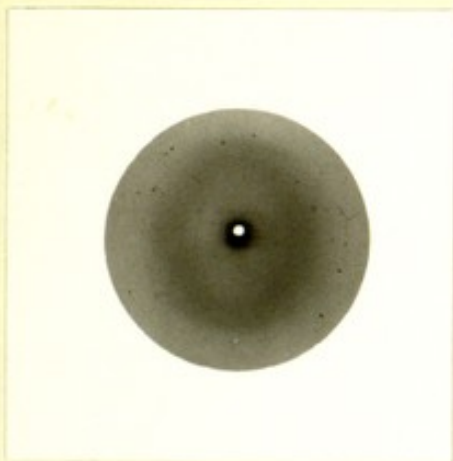
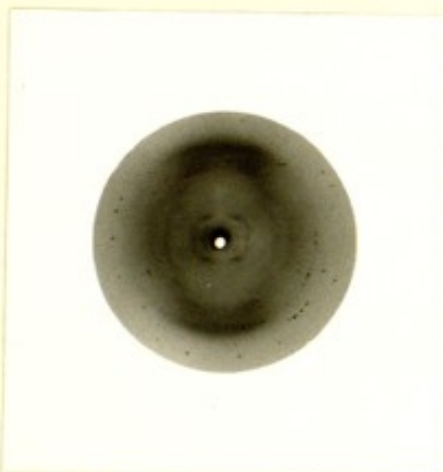
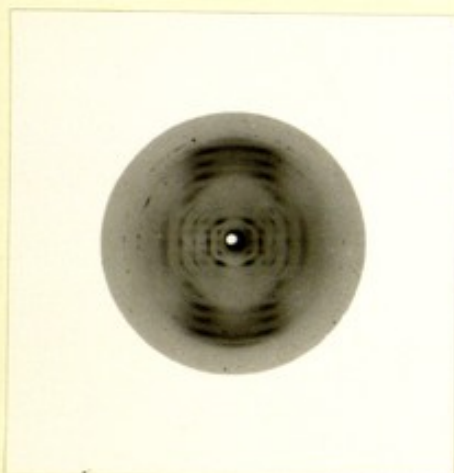


Fig 3

CaHPO₄ ?

Na₂U (3.24 vol)
2.81

Salv ~ 3.32 A }
2.9 A }



From 609

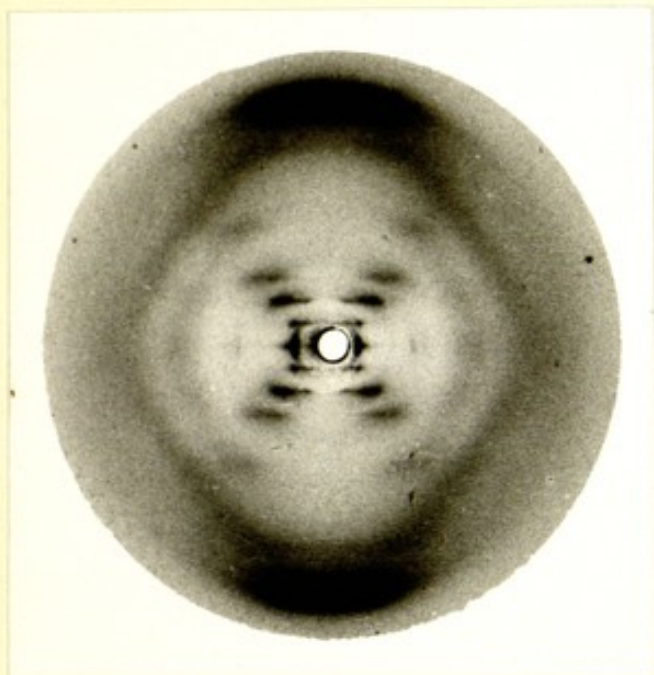


Plate 4

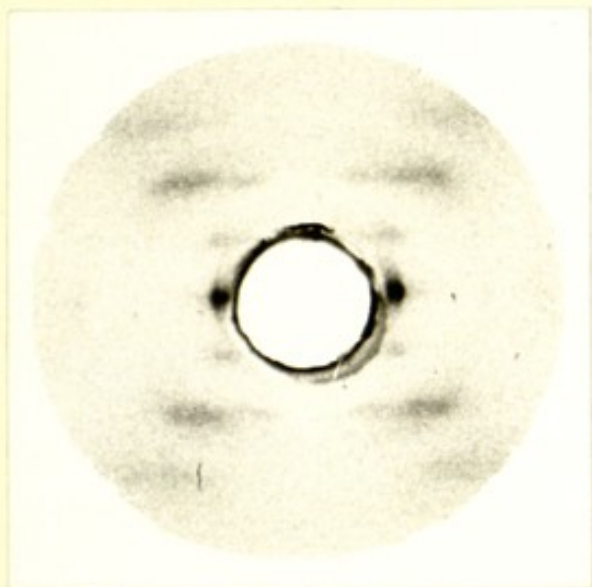


Plate 6

FIBRE DIAGRAMS OF SODIUM THYMONUCLEATE

I. THE INFLUENCE OF WATER CONTENT

Rosalind E. Franklin and R. G. Gosling

Wheatstone Physics Laboratory,
King's College London.

S U M M A R Y

A qualitative survey has been made of the types of X-ray diagram given by highly orientated specimens of sodium thymonucleate at different humidities. From the nature of the structural changes that occur when the humidity is varied, certain general conclusions have been drawn concerning both the way in which the sodium thymonucleate molecules are bound to one another and the part played by water in the structure.

INTRODUCTION

The fundamental substance of cell nuclei, nucleoprotein, consists of a fairly loose conjugation of desoxyribose nucleic acid (DNA) and simple proteins. The nucleic acid component can be separated from the protein and precipitated in the form of its sodium salt by a mild process (Signer and Schwander, 1949). A knowledge of the structure of DNA would therefore not only be interesting on its own account, but might well prove to be a valuable aid in the study of the nucleoproteins.

DNA is known to exist in the form of long-chain molecules of very high molecular weight; when sufficient precautions to avoid degradation are taken, values up to 8 million are obtained (Signer and Schwander, 1949; Katz, 1952). The chains are believed to be un-branched or nearly so. They are built up of four different nucleotides, each nucleotide being the phosphoric ester of a nucleoside, and each nucleoside the desoxypentose derivative of an amino-purine or amino-pyrimidine. The phosphate group is linked to two nucleotides through the C_3' and C_5' positions on the sugar ring (Davidson, 1950).

It was for some time believed that DNA contained the four bases, adenine and guanine (purines) and cytosine and thymine (pyrimidines) in equal proportions, and the suggestion was made that the fundamental unit was a tetranucleotide. However, careful analyses by Chargaff and ^{co-workers} Visher (1949) have shown this to be untrue and their results, together with the more recent studies of Sinsheimer and Koerner (1952) and of Markham and Smith (1952) of the fragments obtained by enzymatic digestion of DNA, suggest that the sequence of nucleotides in the chain may be complicated.

Sodium thymonucleate, the sodium salt of the nucleic acid extracted from calf thymus (referred to below as Na DNA), is

a fibrous solid which is capable of taking up large quantities of water to form a gel. By means of suitable mechanical treatment and drying, this gel can be used to obtain highly orientated specimens of Na DNA and these give characteristic X-ray fibre-diagrams (Astbury, 1947; Wilkins et al, 1953). The X-ray powder photographs of non-orientated aqueous systems of Na DNA have been studied by Riley & Oster. (1951).

None of the X-ray diagrams obtained from Na DNA shows discrete reflections at angles corresponding to spacings smaller than 2.5A. Even a complete quantitative study will not, therefore, be capable of yielding the atomic positions in the structure. But, since the chemical composition and structure of the constituent sugar and base components are well-established, this need not necessarily prove an insuperable obstacle to structure-determination. It was felt that, in any case, a comparative study of the different diagrams obtained under different conditions, combined with a detailed quantitative investigation of those diagrams which show the highest degree of crystalline order, should yield a certain amount of new information.

In particular, the diagrams show that the structure is highly sensitive to the humidity of the surrounding atmosphere. A general qualitative survey of this effect is described in the present paper. We believe that it throws some light on the way in which the long-chain molecules are bound to one another in the structure and this, in turn, may possibly have some bearing on the way in which nucleic acid and protein are united in nucleoprotein.

A quantitative study of the fibre diagram given by Na DNA in its most highly ordered state will be described in later papers.

Preparation of Fibres

The material used throughout this investigation was the highly purified sodium salt of calf thymus desoxyribose nucleic acid, which was kindly supplied to us by Professor Signer.

Fibres were prepared by the method of Wilkins (1953); sufficient distilled water is added to a small piece of the fibrous solid to form a stiff gel and a needle-point is then placed in the gel and slowly withdrawn. By suitably varying the speed of withdrawal and the water-content of the gel, fibres of diameter from about 100μ to less than 1μ can be obtained at will.

In general, the smaller the diameter of the fibre the greater the degree of orientation obtained.

Apparatus and Method

The first photographs (Wilkins et al 1953) were taken with a Unicam single-crystal camera and a Raymax tube, using a bundle of about 30 fibres of diameter $10-30\mu$ prepared as described above. Under suitable conditions (see below) fibre diagrams showing a high degree of crystallinity were obtained. It soon became evident, however, that a photographic system of higher resolving power might be expected to show more fine-structure in the diagram. Moreover, the bundle of fibres could not easily be maintained in perfect parallel alignment, and it was evidently desirable to be able to work with a single fibre of diameter not greater than 40μ .

In order to use such a small specimen and a photographic system of high resolving power, and yet to avoid prohibitive exposure times, a well-collimated micro-beam of high intensity was required. This was provided by an Ehrenberg-Spear fine-focus X-ray tube (1951), used in conjunction with a North-American Phillips micro-camera. The tube, which gives a focal spot of

about 40 μ diameter, was run at 35-40 KV and 0.4 m.a. The Phillips camera consists essentially of a lead-glass capillary collimator of length 10 mm and bore 100 μ or 50 μ , and a flat plate carrying the film. The latter can be set at either 10 mm or 15 mm from the end of the collimator.

For most of the work the 100 μ collimator and 15 mm specimen-film distance were used, together with nickel-filtered copper radiation. The specimen generally consisted of a single fibre placed directly over the front face of the collimator and fixed with cellulose glue.

When single fibres of 30-40 μ diameter were used, exposure times were of the order of 50 to 100 hours. For fibres of diameter about 100 μ , showing, in general, less good orientation than the finer fibres, exposure times were 20 hours or less.

In using such small specimens of weakly diffracting material it is important to eliminate scattering by air. Throughout each experiment a steady stream of hydrogen was therefore passed through the camera. The moisture content of the specimen was controlled by operating at constant humidity. For this purpose the hydrogen, before entering the camera, was bubbled through a saturated solution of a suitable inorganic salt, a little of the same saturated solution being placed in a small container inside the camera. Each specimen was left for at least one hour in the camera at constant humidity before starting the exposure.

RESULTS

Wilkins and co-workers (1953) observed that high humidity was required in order to obtain from the Na DNA fibres a photograph showing a high degree of crystallinity. Attempts to achieve a further increase in crystallinity by working at still higher R.H. resulted in the observation that at very high humidities a well-defined structural change occurs, leading to a

new type of fibre-diagram. The two types of diagram are shown in Plates 1 and 2. The structures represented by these two diagrams will be referred to in what follows as structures A and B.

Plate 1 was taken at 75% R.H. and Plate 2 at 92% R.H. It must be emphasized, however, that the type of diagram obtained depends not only on the relative humidity but also on the past history of the specimen. A strong hysteresis is observed, both in the quantity of water taken up by the bulk Na DNA and in the structural change in the fine fibres. A diagram of type A may frequently be obtained at 92% R.H. if the specimen has previously been subjected to prolonged drying over P_2O_5 .

On passing from structure A to structure B the layer-line spacing increases from 28A to 34A, and this is accompanied by a similar increase in the macroscopic length of the fibre.

With some samples of calf thymus Na DNA, although it is possible to obtain well-orientated fibres (as shown by optical birefringence and X-ray diagrams), it has so far not been found possible to obtain structure A. Fibres from such samples give diagrams resembling Plate 2 at all R.H. above about 60%. The failure to obtain structure A in these specimens may possibly be due to excessive degradation during extraction of the DNA, or to the presence of some impurity. But, for specimens in which structure A can be obtained the change from A to B is, in general, reversible. When R.H. 75% is approached from the dry side, structure A is obtained, and when R.H. 92% is approached from the wet side the resulting diagram is always that of structure B. Intermediate states consist of a mixture of A and B. An example of this is shown in Plate III.

Here a further reservation must, however, be made. It sometimes happens that a fibre which has been in use in the camera for some days or even weeks, and which has passed through

the reversible $A \rightleftharpoons B$ transformation a number of times, suddenly passes irreversibly to structure B. Such a fibre then behaves subsequently like those mentioned above, from which structure A cannot be obtained. The photograph shown in Plate IV was obtained at R.H. 75% from a fibre which had passed irreversibly to structure B. The difference between Plates II and IV is probably mainly due to the difficulty of photographing a very wet fibre in a highly oriented state. The reversible change $A \rightarrow B$ is accompanied by a length increase of about 25%. It is therefore necessary to attach the fibre to the collimator at points so close to the collimator hole that it cannot move out of the direct beam. This results in some buckling of the fibre in the wet state, and consequent deterioration of the quality of the photograph. No such difficulty is experienced with fibres which do not give structure A.

If, with a specimen showing structure A, the humidity in the camera is reduced appreciably below 75%, the intensity of the reflections decreases relative to that of the diffuse background. This effect increases progressively with decreasing humidity and is accompanied by a slight lateral shrinkage of the structure. This is illustrated in Plate V. After prolonged drying at room temperature only a broad diffuse ring is observed, and after drying at 80° C even this fades out and there remains only a diffuse scattering at low angles. The change from the crystalline state A to this disordered state represented in Plate V is wholly reversible (Wilkins et al, 1953).

DISCUSSION

Quantitative work, both on the water-uptake in relation to crystallinity and on the structure of the most highly ordered state, is still in progress. Nevertheless, the above qualitative observations of the structural changes that occur when the water content of Na DNA fibres is varied suggest certain

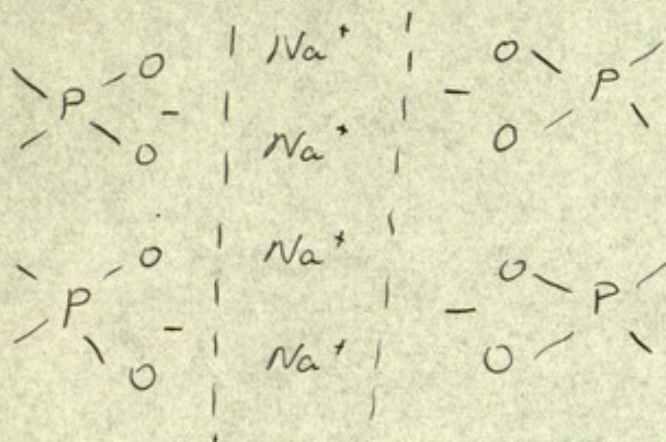
general ideas which we tentatively put forward here.

The most highly ordered state is structure A, obtained at 75% R.H. and clearly possessing a high degree of crystallinity. This state has previously been obtained, in non-orientated form, by Riley and Oster (1951); the spacings reported by them for the "crystalline" structure in Signer and Schwander's preparation agree to within 0.1 Å with those of strong spots or of the mean values of doublets or triplets in the fibre diagram of structure A. Riley and Oster also observed that the transition from this state to the "wet gel" was reversible, but they made no measurements in the high-angle region with "wet gel" or "moist crystalline" specimens, and therefore did not observe structure B.

The equilibrium water content of the bulk sodium thymonucleate at 25°C and 75% R.H., for a specimen which has previously been thoroughly dried, is about 40% to 45% of the dry weight. It is not, of course, certain that this represents the water content of the crystallites, but the value is fairly constant for a number of different specimens and is therefore probably similar in the actual fibres examined. There may well be excess water in layers on the surface of the crystallites or in non-crystalline, inter-crystallite regions. 45% is therefore a maximum possible value for the structural water of the crystallites in structure A. This value corresponds to about 8 molecules of water per nucleotide.

The most polar part of the Na DNA molecule lies in the phosphate groups, and it is with these that we should expect the water molecules to be associated. We may note, for example, that the compounds $(C_2H_5O)_2 PO_2Na$ and $(C_3H_7O)_2 PO_2Na$, in which the bonding of the phosphorus is similar to that in nucleic acid, are hygroscopic (Drushel and Felty, 1918). For the same reason we should expect a tendency for the phosphate groups to associate with one another in the structure, just as carboxyl groups are

associated in the structures of organic acids and their salts. We should, in fact, expect to find an inter-molecular arrangement of the type



This type of back-to-back bonding of chains through their phosphate groups leads one to expect that, in the crystalline structure, the purine and pyrimidine groups will be linked to similar groups of neighbouring chains by hydrogen bonds.

Thus we may assume that in Structure A the main inter-molecular forces are phosphate-phosphate bonds together with hydrogen bonding between base groups. In the gel state and in solution there is evidence for the existence of small stable aggregates of molecules linked by hydrogen bonds between their base groups, and having their phosphate groups exposed to the aqueous medium. In particular, while the phosphate groups in DNA can be titrated in the normal way, the $-NH_2$ and $-CO$ groups remain inaccessible unless the pH is taken above 11 or below 5 (Gulland and Jordan 1947).

Since the change from the crystalline structure to the wet state is readily and rapidly reversible, it seems reasonable to suppose that the small molecular aggregates of the wet state can be easily derived from the grouping existing in the crystal structure. This suggests that in structure A we may expect to find a small group of chains held together as a unit by hydrogen bonds between their base groups, and these units linked in

crystalline array by phosphate-phosphate bonds.

The transformation from the crystalline structure to the molecular aggregates of the wet state, in which the phosphate groups are believed to lie near the outside, must necessarily involve some breaking of phosphate-phosphate bonds. The extreme rapidity with which water is taken up or lost by Na DNA fibres when the humidity of the surrounding atmosphere is changed, the large quantity of water which can be absorbed, and the continuity of the process which leads ultimately to gel formation and solution, all clearly indicate that the phosphate groups with which the water is associated are in a relatively accessible part of the structure. Since we are dealing with long-chain molecules in which the phosphate groups occur at regular and frequent intervals along the chain, the phosphate-phosphate bonds and associated water molecules will lie on lines or surfaces which extend throughout the structure, and hydration, swelling and solution will result from the distention of these polar regions.

When the water content of Na DNA fibres in state A is sufficiently increased, structure B always results. It is clear from the X-ray diagrams that structure B has a lower degree of order than structure A. This suggests that the additional water has in some way weakened the directional property of the phosphate-phosphate link, probably by directly associating itself with the sodium ions and forming a new intermediate in the link. This would make possible some degree of inter-molecular displacement in the direction of the fibre axis, as well as an intra-molecular re-arrangement. Here we may note that the photograph shown in Plate IV is strongly characteristic of the type of diagram shown by Cochran, Crick and Vand (1952) to result from a single helical structure.

Further support for these general ideas is provided by the photograph shown in Plate VI. Here the equatorial reflection

at about 22Å, which is a prominent feature of structure B, appears as a well-resolved doublet. The spacings corresponding to this doublet are 22.1 and 24.6Å. The difference between these spacings, 2.5Å, is approximately equal to the thickness of a single layer of water molecules, and seems to indicate, therefore, the possible coexistence in the structure of two different hydration states.

The water content of fibres showing structure B may vary within wide limits, and it is probable that structure B can co-exist with a large quantity of inter-crystallite or inter-micellar water. Increasing the water-content beyond the lower limit necessary for the passage from structure A to structure B results in increased lateral swelling of the fibre, but this is not accompanied by any further appreciable length change.

It is perhaps worth pointing to the analogy which exists between the type of bonding and hydration suggested here and that which is known to occur in the clays (Hendricks and Jefferson, 1938) and in graphitic acid (Hofmann, 1931). In each case a surface rich in -CH or -OM (where M is a cation) groups is separated from a neighbouring similar surface by a layer of water only a few molecules thick, the actual thickness of the layer depending on the ambient humidity. The existence of the water layer probably permits some degree of dis-alignment between the neighbouring structural units.

The above ideas seem incompatible with a structure recently proposed for DNA by Pauling and Corey (Proc. Nat. Acad. Sci. 1953). These authors suggest a 3-strand helical structure in which the phosphate groups form a dense core. It is hard to see how the swelling and solution of DNA in water could be explained in terms of such a structure. Moreover, if such a structure existed in the crystalline state, it would be necessary to assume a radical inter-molecular re-arrangement in passing from the crystalline to the wet state. For in the wet state

one must explain not only the accessibility of the phosphate groups and inaccessibility of the $-NH_2$ and $-CO$ groups during titration, but also, and far more important, the availability of phosphate groups for interaction with proteins. Since, as we have seen, the transition from the crystalline to the wet state is readily and rapidly reversible, such a radical change in structure seems unlikely.

The influence of drying

When water is progressively removed from the crystalline structure by drying, the sharp X-ray reflections gradually fade out and the general diffuse scattering increases. There is no sign of the formation of a new ordered state in the dry substance, and the crystalline state is restored immediately on exposure to a moist atmosphere. Indeed, a more perfect crystallinity in a specimen can frequently be attained by strong drying followed by re-wetting. It seems, therefore, that drying does not break the phosphate-phosphate links but, if anything, cements them more strongly. The removal of water stresses and distorts the structure, destroying its regularity, while leaving the basic 3-dimensional skeleton intact. The effect on the X-ray diagrams may be compared with that of strong thermal agitation.

The diffuse low-angle scattering observed after strong drying (Plate Vd) ^{suggests} ~~shows~~ that complete removal of the water results in the formation of holes in the structure.

Sequence of nucleotides

All X-ray photographs of Na DNA show a rather strong background of diffuse scattering. While it is possible that this is merely due to the presence of small non-crystalline regions separating the crystallites, an alternative explanation might be suggested. We have supposed that phosphate-phosphate bonds are responsible for the inter-molecular order in the crystalline state, and that they form a rigid skeleton strong enough not to

be disrupted even by the strains produced by intensive drying. It may be that, while the phosphate groups form a truly crystalline array, the base groups of the nucleotides do not, possibly owing to different bases occupying equivalent crystallographic positions.

Wilkins ^{and co-workers} ~~et al~~ (1953) have shown that fibre diagrams similar to that of structure B may be obtained from Na DNA from a variety of sources other than calf thymus. In these, the content of the different nucleotides is known to vary considerably. It seems, therefore, that in structure B all nucleotides may be crystallographically equivalent.

Structure A, on the other hand, has been obtained only from calf thymus Na DNA, and it is natural to enquire, therefore, whether this structure is dependent on a particular nucleotide sequence. Here one obvious difficulty arises. If structure A is truly crystalline - that is, if a given position in the unit cell is always occupied by the same nucleotide - then the sequence of nucleotides in calf thymus DNA must be simple and invariable; its repeat unit must lie within the bounds of a single unit cell. In view of the biological properties generally attributed to DNA, this seems unlikely. On the other hand it also seems improbable that purine and pyrimidine groups, which differ from one another considerably in shape and size, could be interchangeable in a structure as highly ordered as structure A. A possible ^{so/u} relation, therefore, is that in structure A cytosine and thymine are interchangeable and adenine and guanine are interchangeable, while a purine and a pyrimidine are not. This is suggested by the remarkably similar crystal structures found by Miss Broomehead (1951) for adenine and guanine hydrochlorides. In this way an infinite variety of nucleotide sequences would be possible, to explain the biological specificity of DNA, while the existence of a crystalline structure in calf thymus Na DNA would be attributed

to a particular purine-pyrimidine sequence.

CONCLUSIONS

The structural changes which occur in Na DNA fibres when their water content is varied suggest that the fundamental structural unit is a group of molecules so arranged that the phosphate groups are exposed and accessible to water. This is entirely consistent with the work of Gulland and Jordan (1947), who concluded that the hydrogen-bond-forming -OH and -NH₂ groups, which lie at the opposite end of the nucleotides from the phosphate groups, are inaccessible to water in aqueous solutions of Na DNA at pH between 5.0 and 11.0. Presumably, hydrogen bonds link neighbouring chains through their -OH and -NH₂ groups and form a stable aggregate of molecules which survives as a micelle in aqueous solution.

Such a group of molecules, in which the hydrogen-bonded groups are turned inwards and the phosphate groups outwards, explains the ready availability of phosphate groups for interaction with proteins. Moreover, since both the protein in nucleo-proteins and the water in Na DNA fibres are believed to be associated with the phosphate groups, it is conceivable that the Na DNA structure might exist without great modification in the nucleic acid of nucleoproteins, the protein taking the place of the structural water.

It is hoped that further X-ray work will yield some knowledge of the precise form of the apparently stable group of Na DNA molecules.

ACKNOWLEDGMENTS

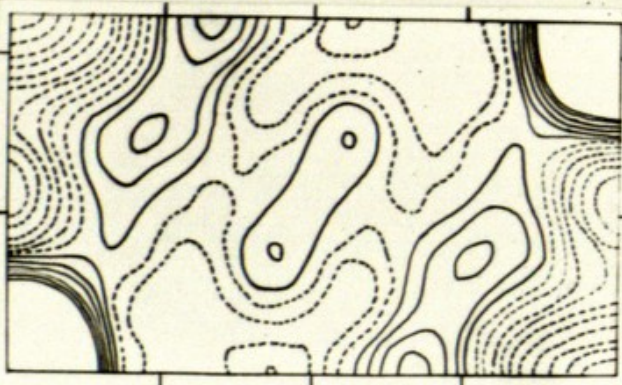
The authors are grateful to Professor J. T. Randall, F.R.S., for his interest and advice, and to M. H. F. Wilkins and A. R. Stokes for discussions.

One of us (R.E.F.) acknowledges the award of a Turner and Newall Fellowship.

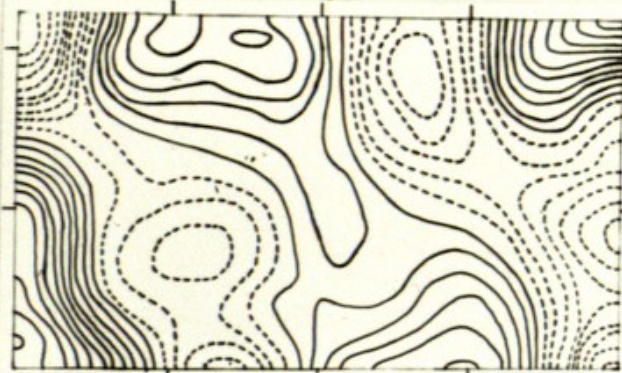
REFERENCES

- Astbury, W. T., (1947) Cold Spring Harbour Symp. on Quant. Biology, p.56.
- Broomhead, June M., (1951) Acta Cryst. 4, 92.
- Chargaff, E., et al (1949) J. Chem. 177, 405
- Cochran, W., Crick, F. H. C. and Vand, V., (1952) Acta Cryst. 5, 581
- Davidson, J. N. (1950) The Biochemistry of the Nucleic Acids (Methuen London) p.32
- Drushel, W. A., and Felty, A. R. (1918) Chem. Zentralblatt., 89, 1016
- Ehrenberg, W. and Spear, W. E., (1951) Proc. Phys. Soc. B 64, 67
- Gulland, J. M., and Jordan, D.O. (1947) Cold Spring Harbour Symp. on Quant. Biology, p.5
- Hendricks, S. B. and Jefferson (W.E.) (1938) Amer. Min. 23, 863
- Hofmann, U., (1931) Z. Elektrochem., 37, 613
- Katz, S., (1952) J. Amer. Chem. Soc., 74, 2238
- Markham, R., and Smith, J. D., (1952) Nature, 170, 120
- Pauling, L., and Corey, R. B. (1953), Proc. Nat. Acad. Sci.
- Riley, D. P., and Oster. G., (1951) Biochem. Biophys. Acta, 7, 526
- Signer, R., and Schwander, H. (1949) Helvet. Chim. Acta., 32, 854
- Sinsheimer, R. L. and Koerner, J. F. (1952) J. Amer. Chem. Soc. 74, 283
- Wilkins, M. H. F., et al, (1953)

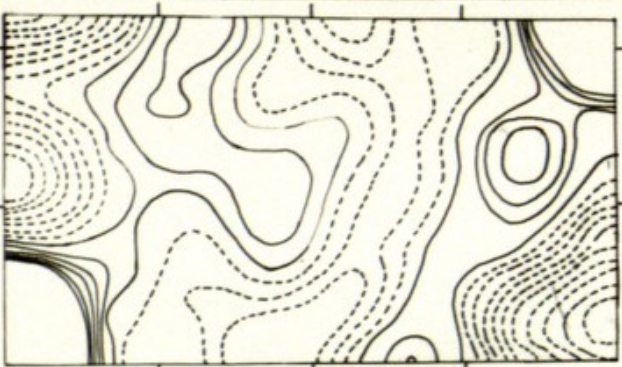
0



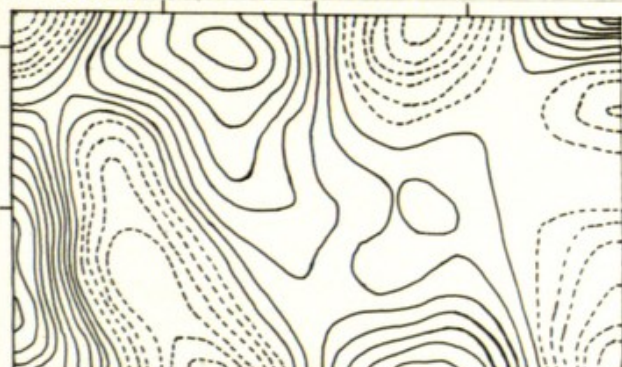
4



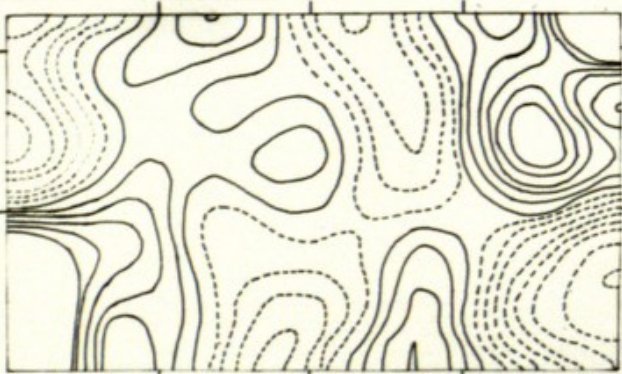
1



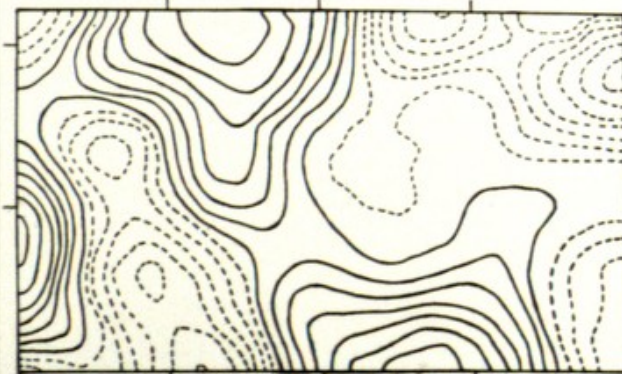
5



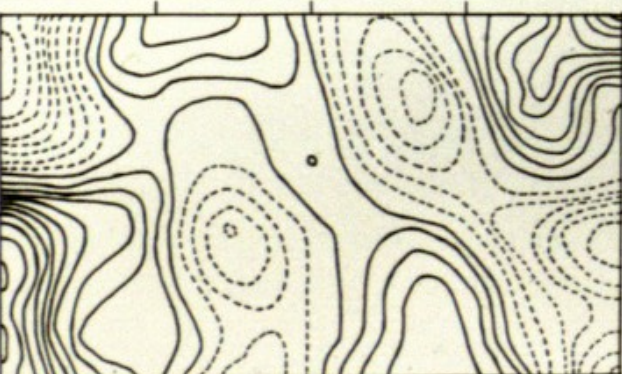
2



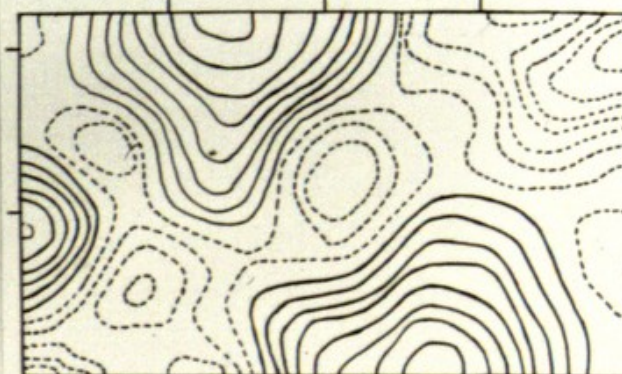
6



3

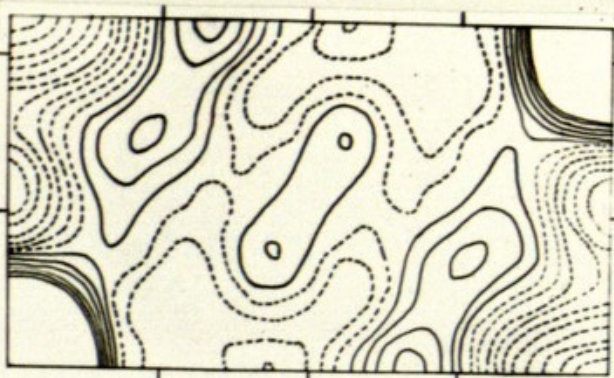


7

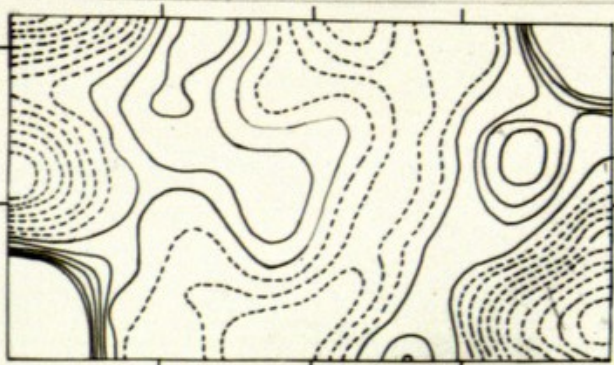


Q873

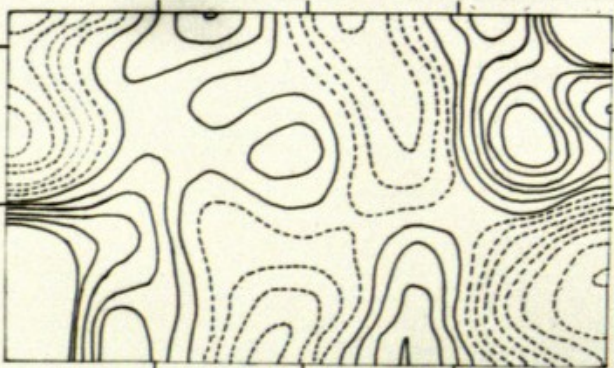
0



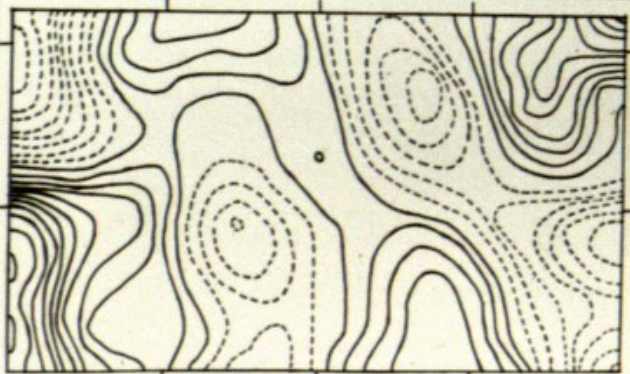
1



2



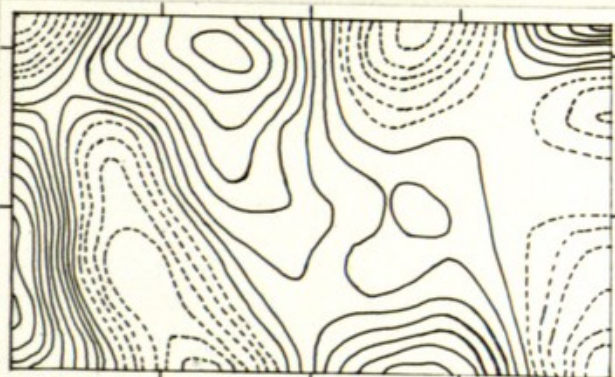
3



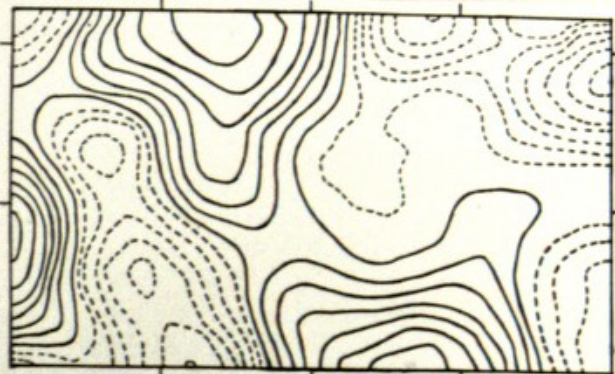
4



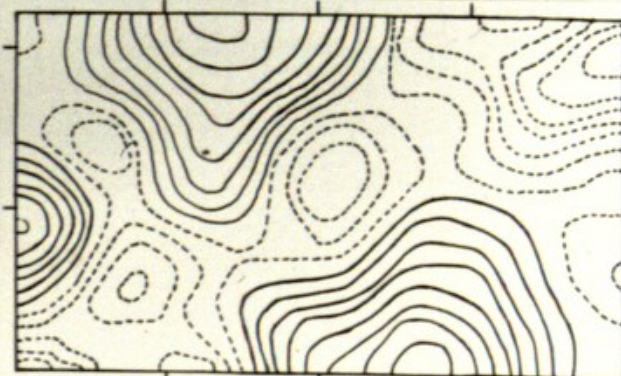
5



6

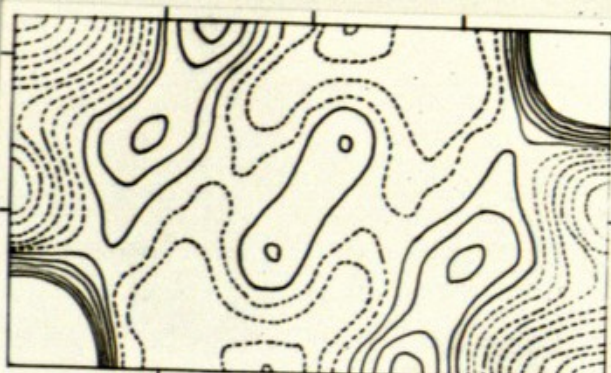


7

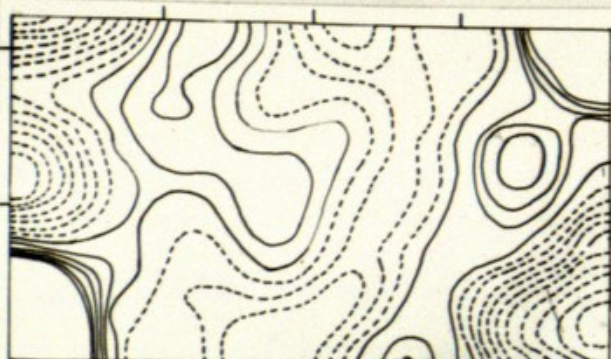


Q873

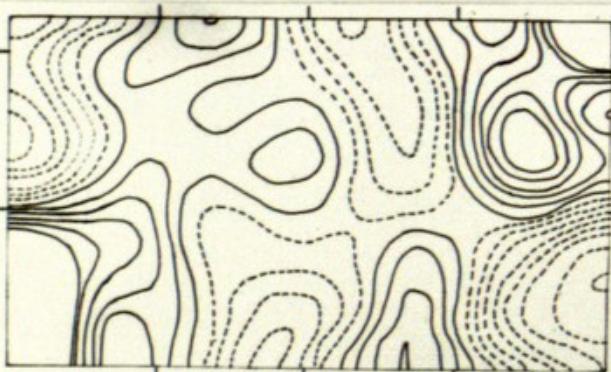
0



1



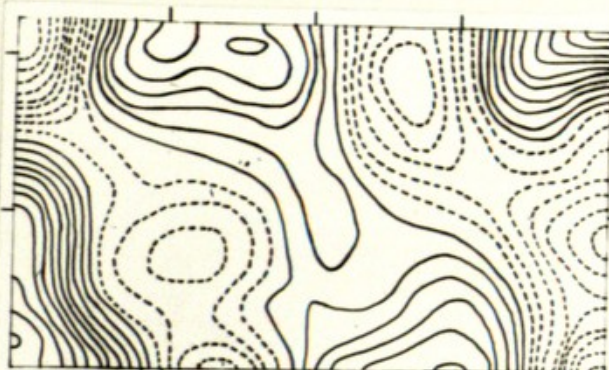
2



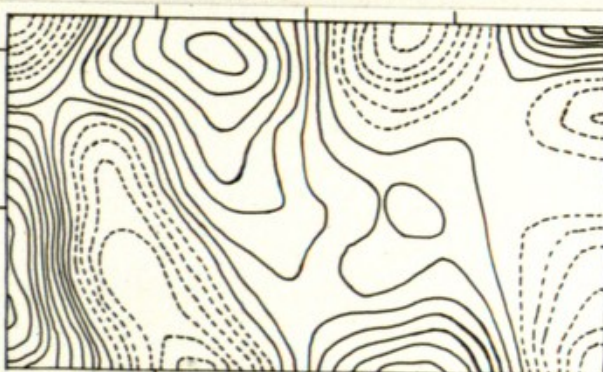
3



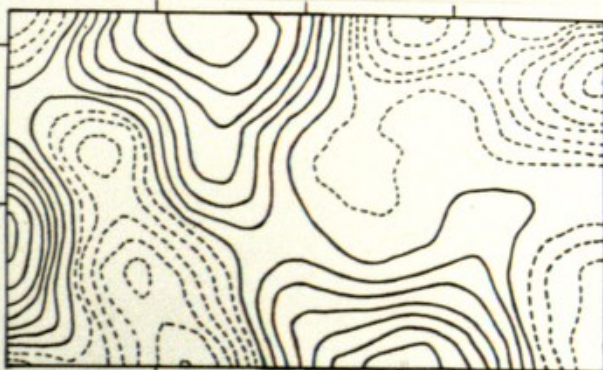
4



5



6

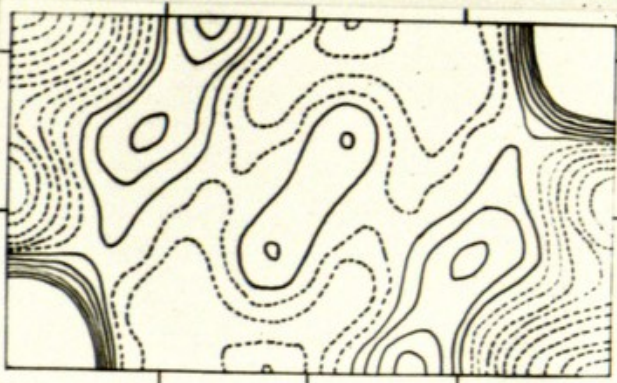


7

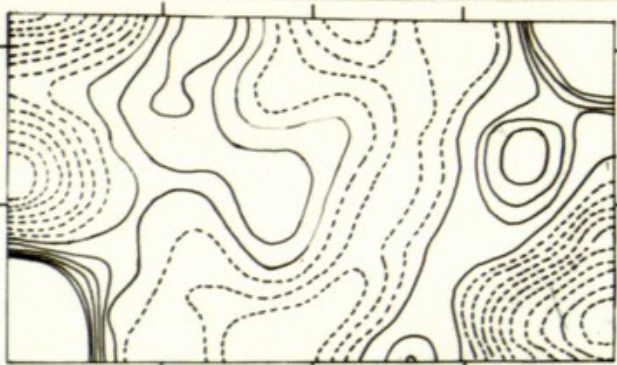


Q873

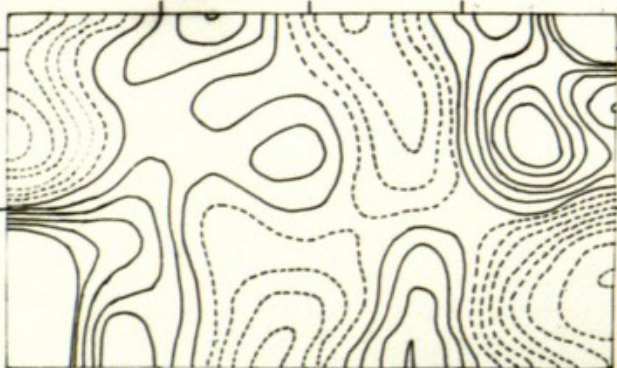
0



1



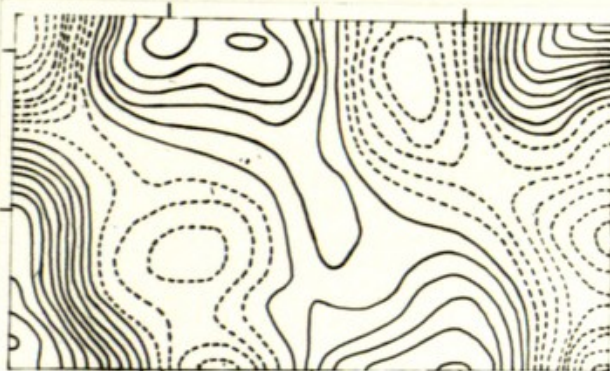
2



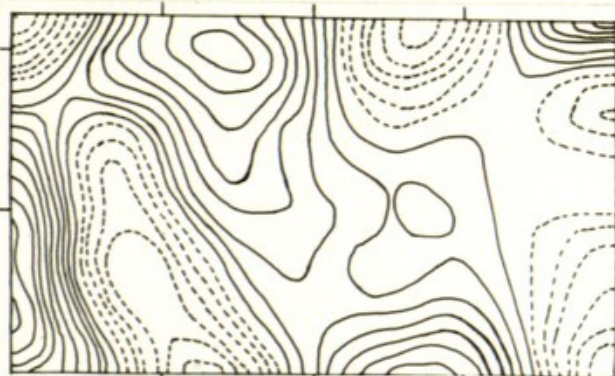
3



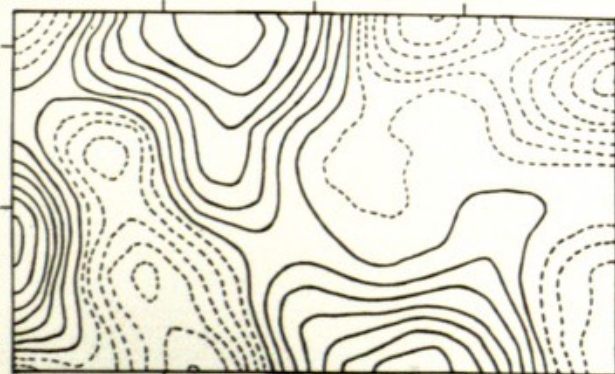
4



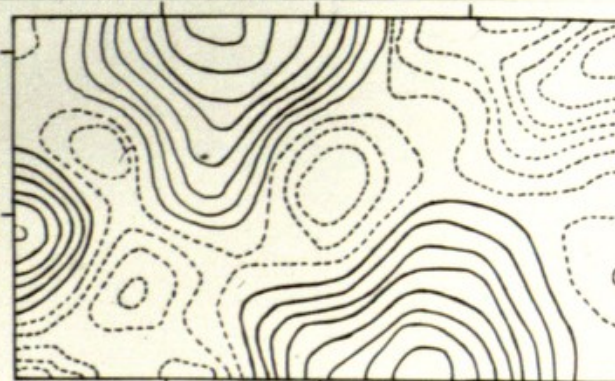
5



6

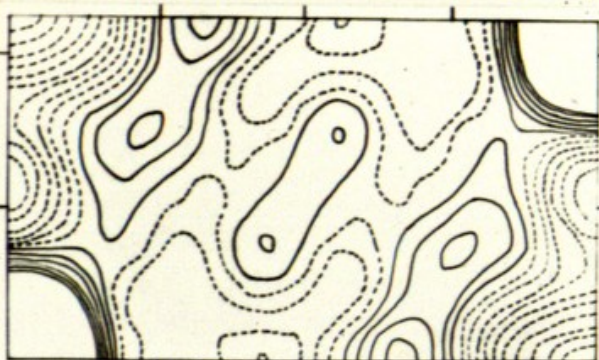


7

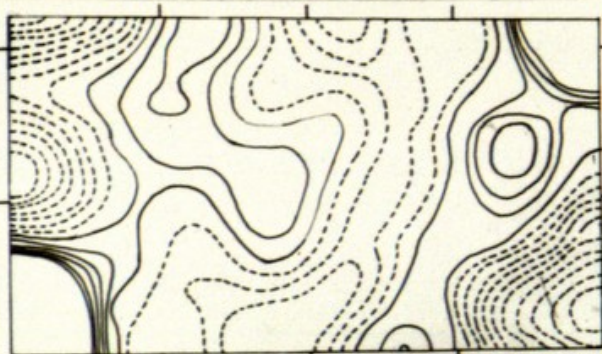


Q873

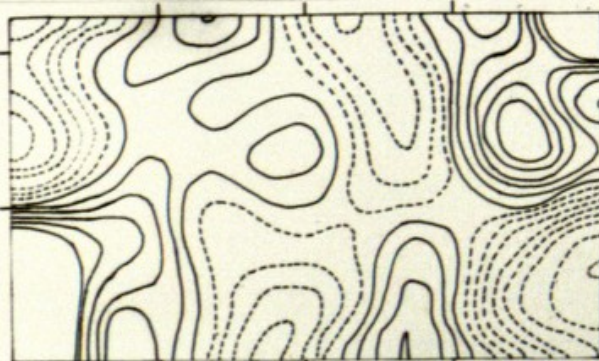
0



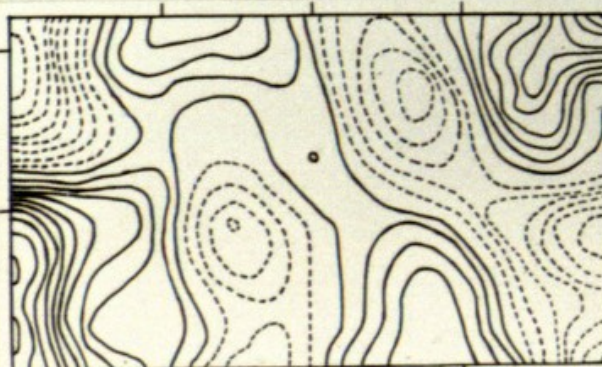
1



2



3



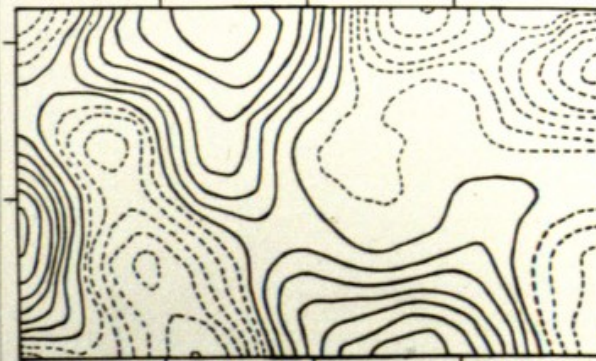
4



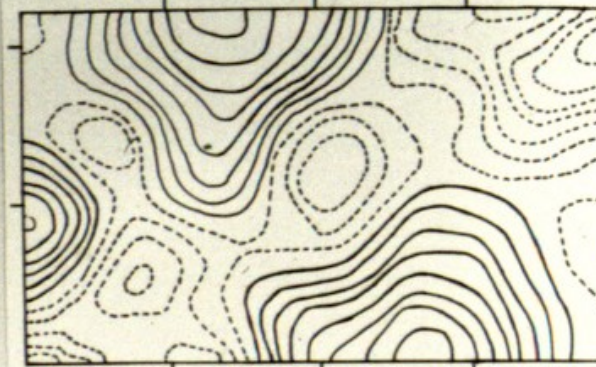
5



6

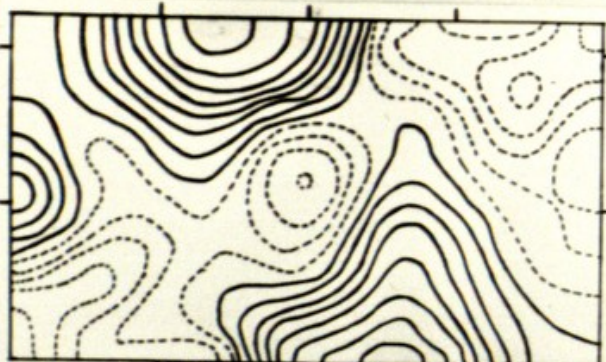


7



Q872

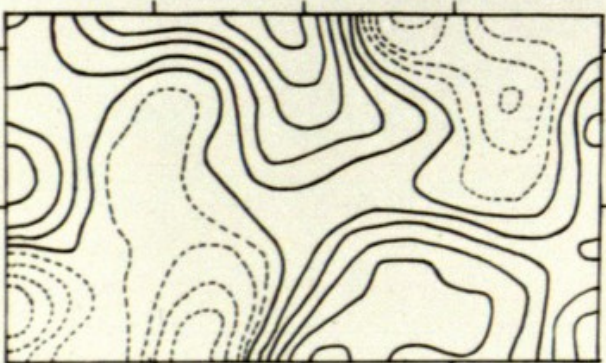
8



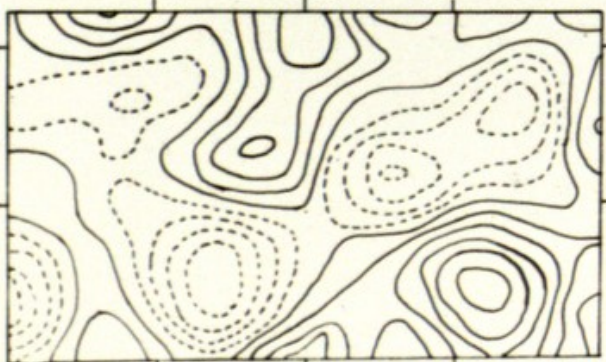
9



10



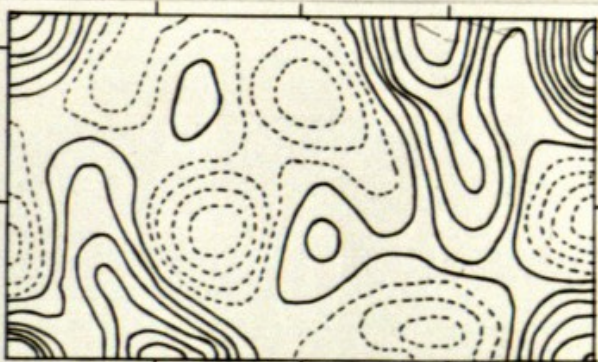
11



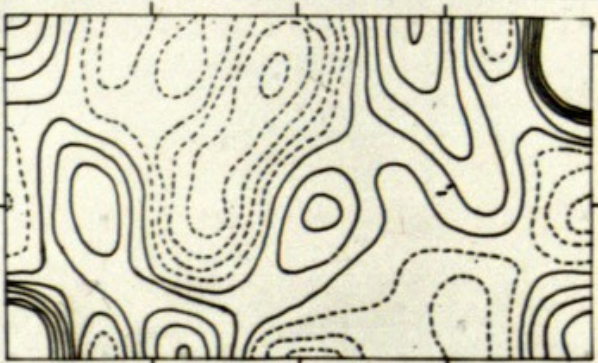
12



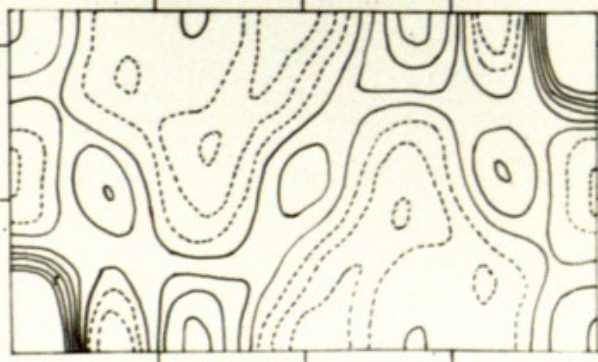
13



14

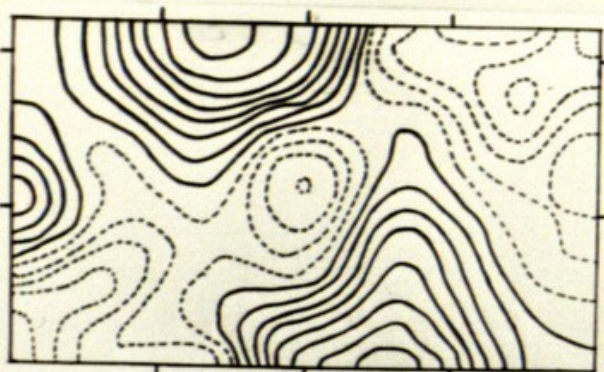


15

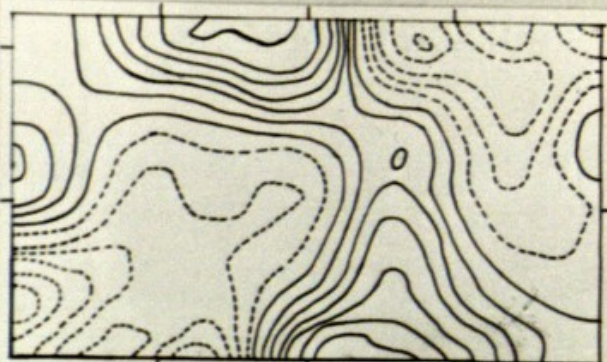


Q 874

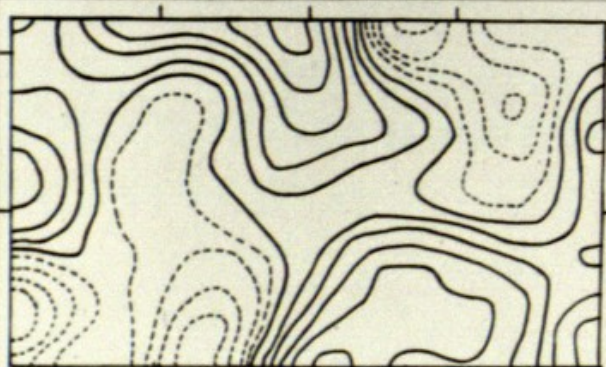
8



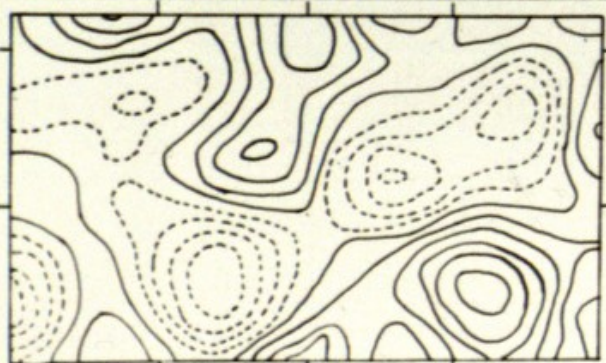
9



10



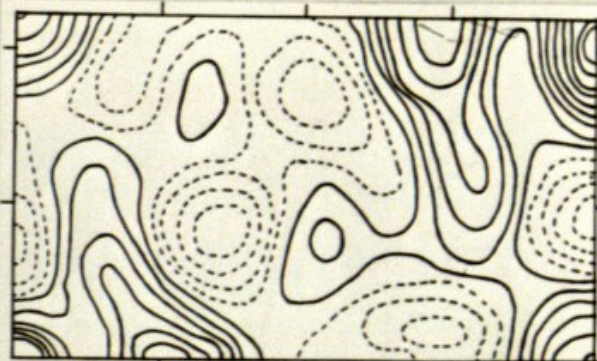
11



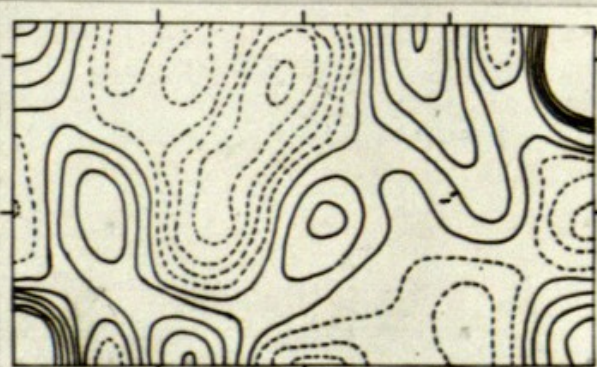
12



13



14

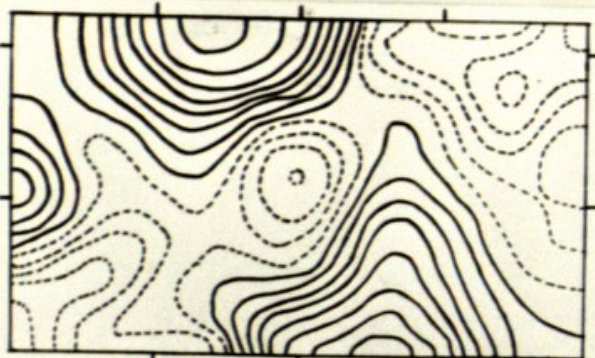


15

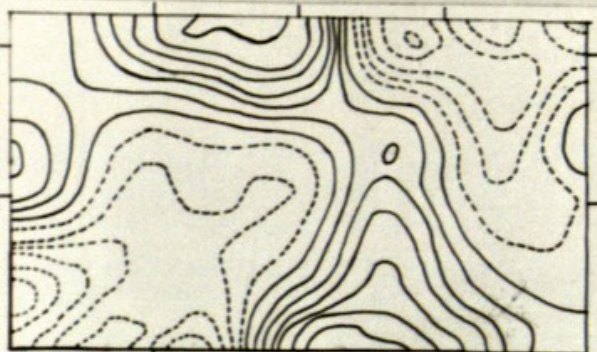


Q274

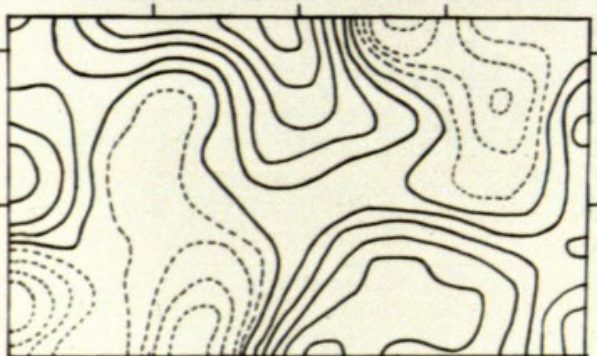
8



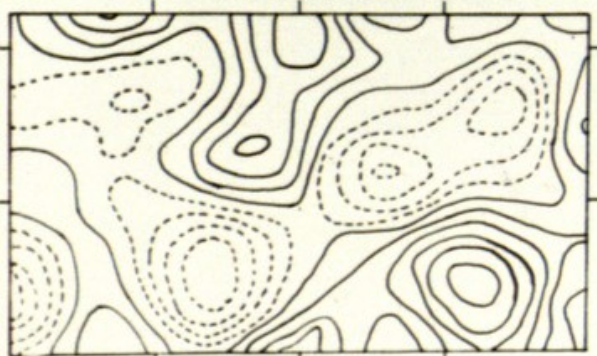
9



10



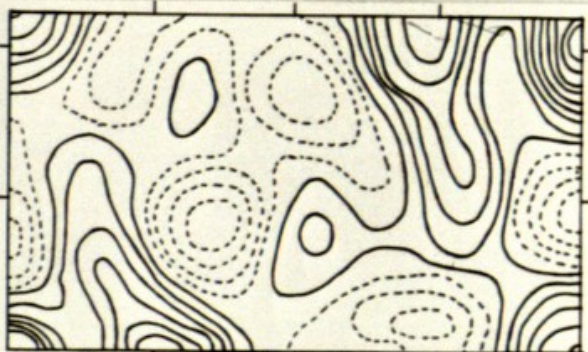
11



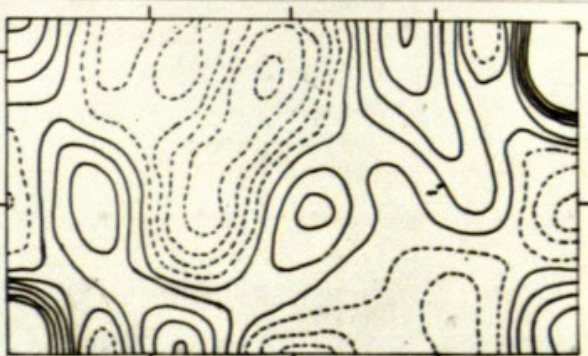
12



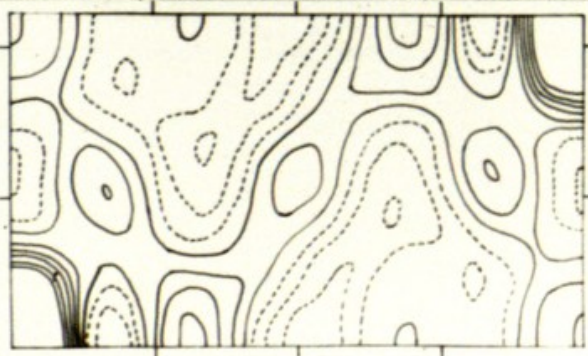
13



14

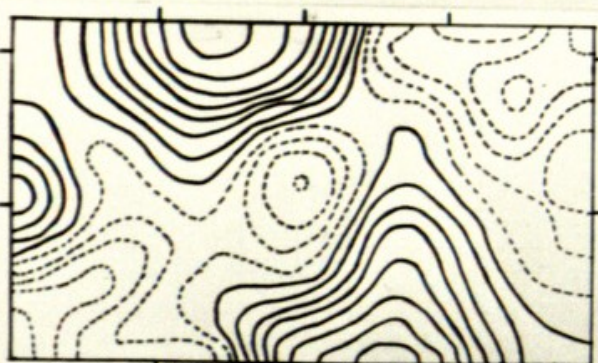


15

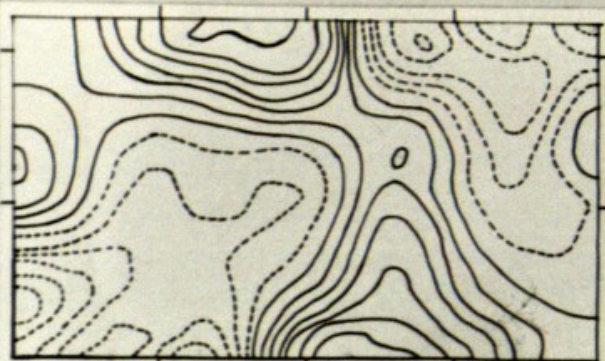


Q877

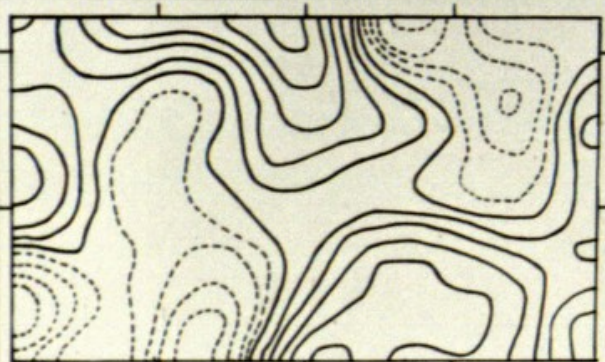
8



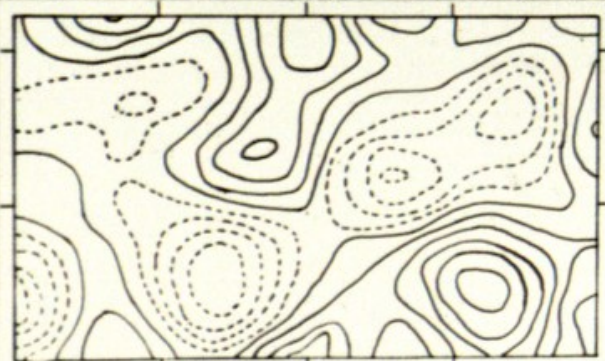
9



10



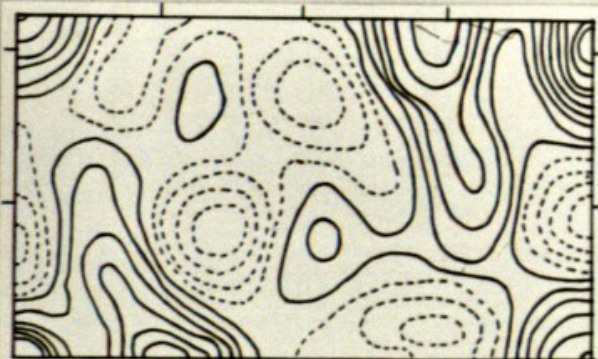
11



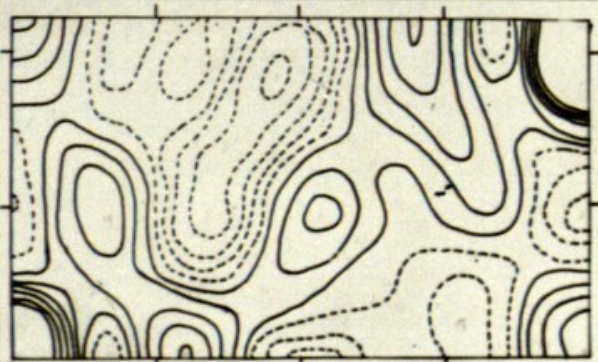
12



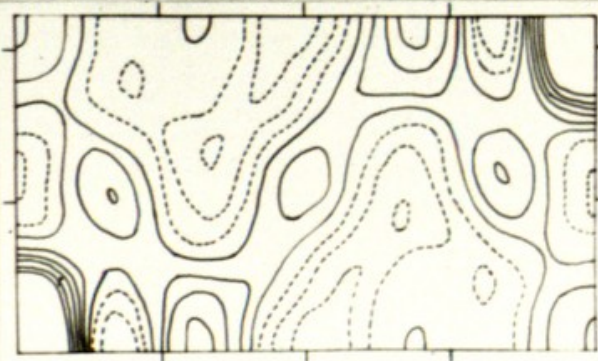
13



14

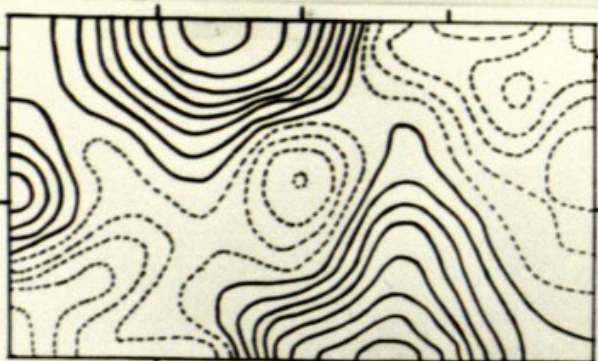


15

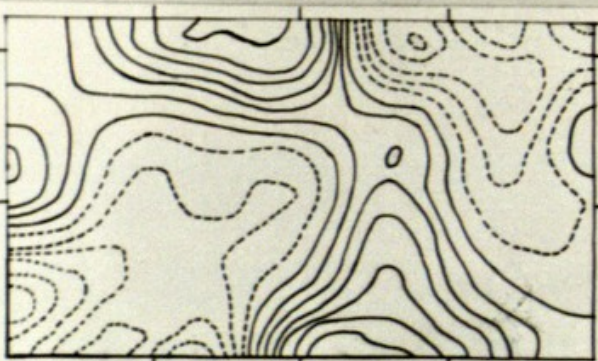


Q 874

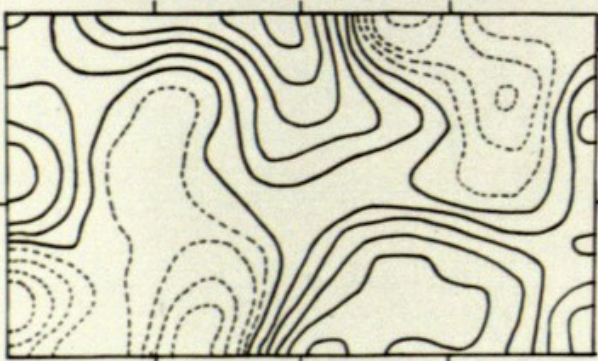
8



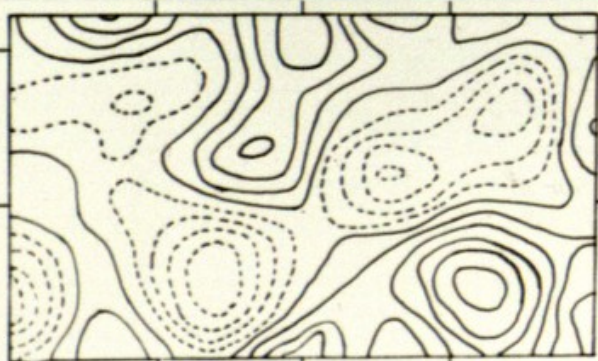
9



10



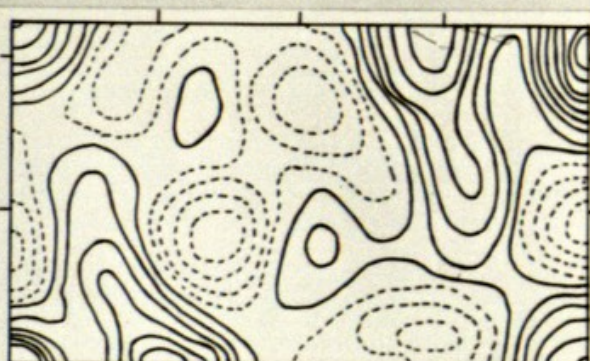
11



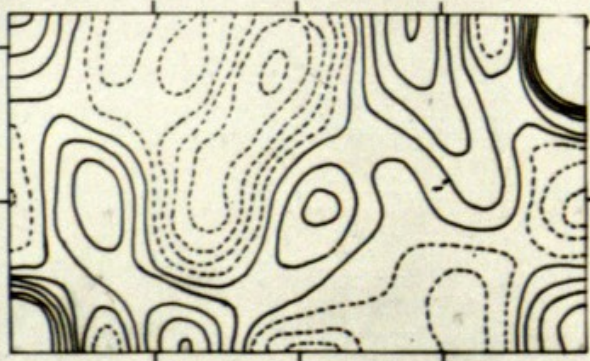
12



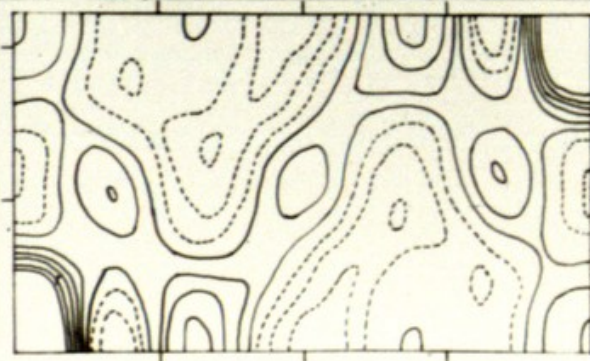
13



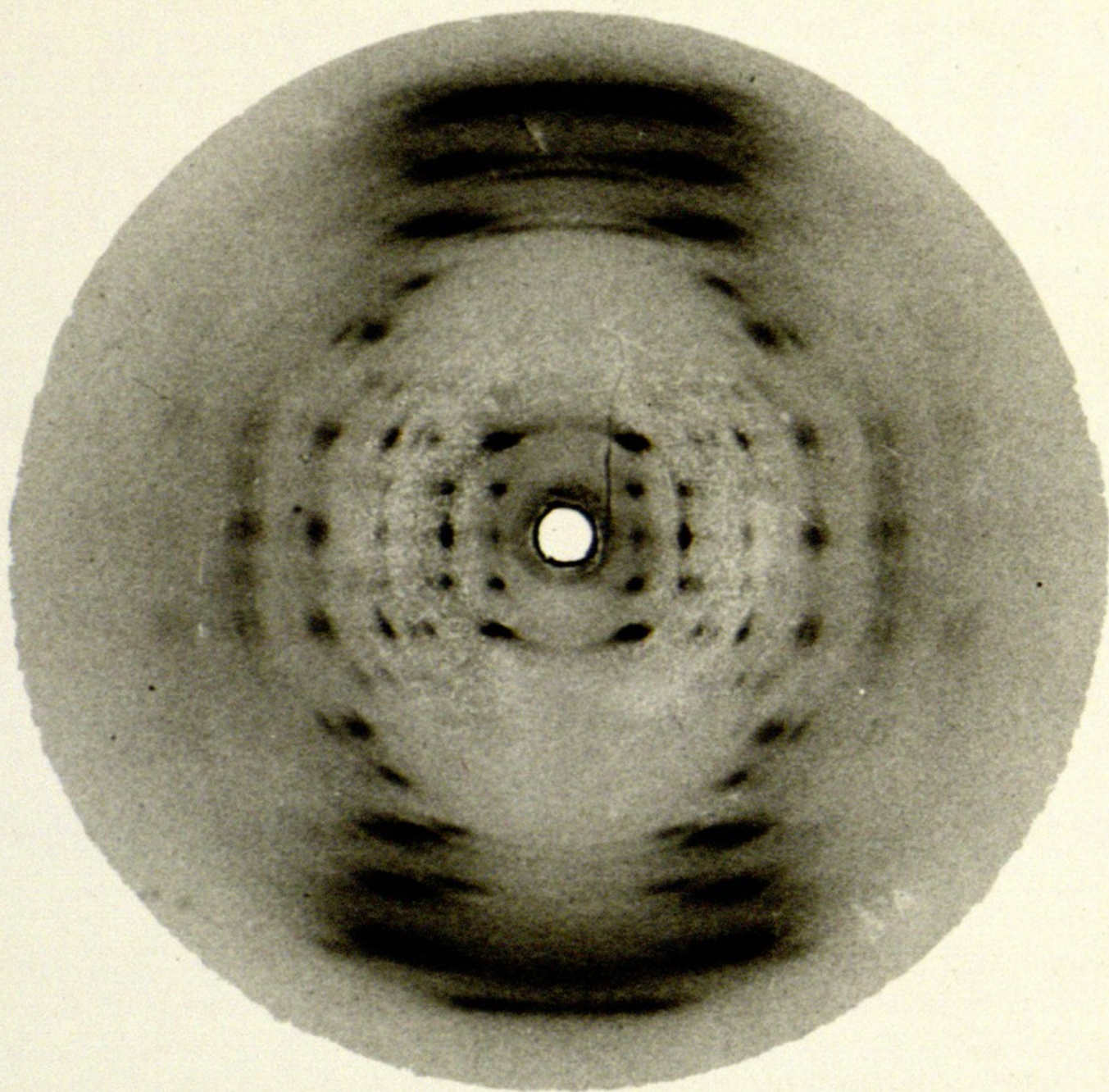
14



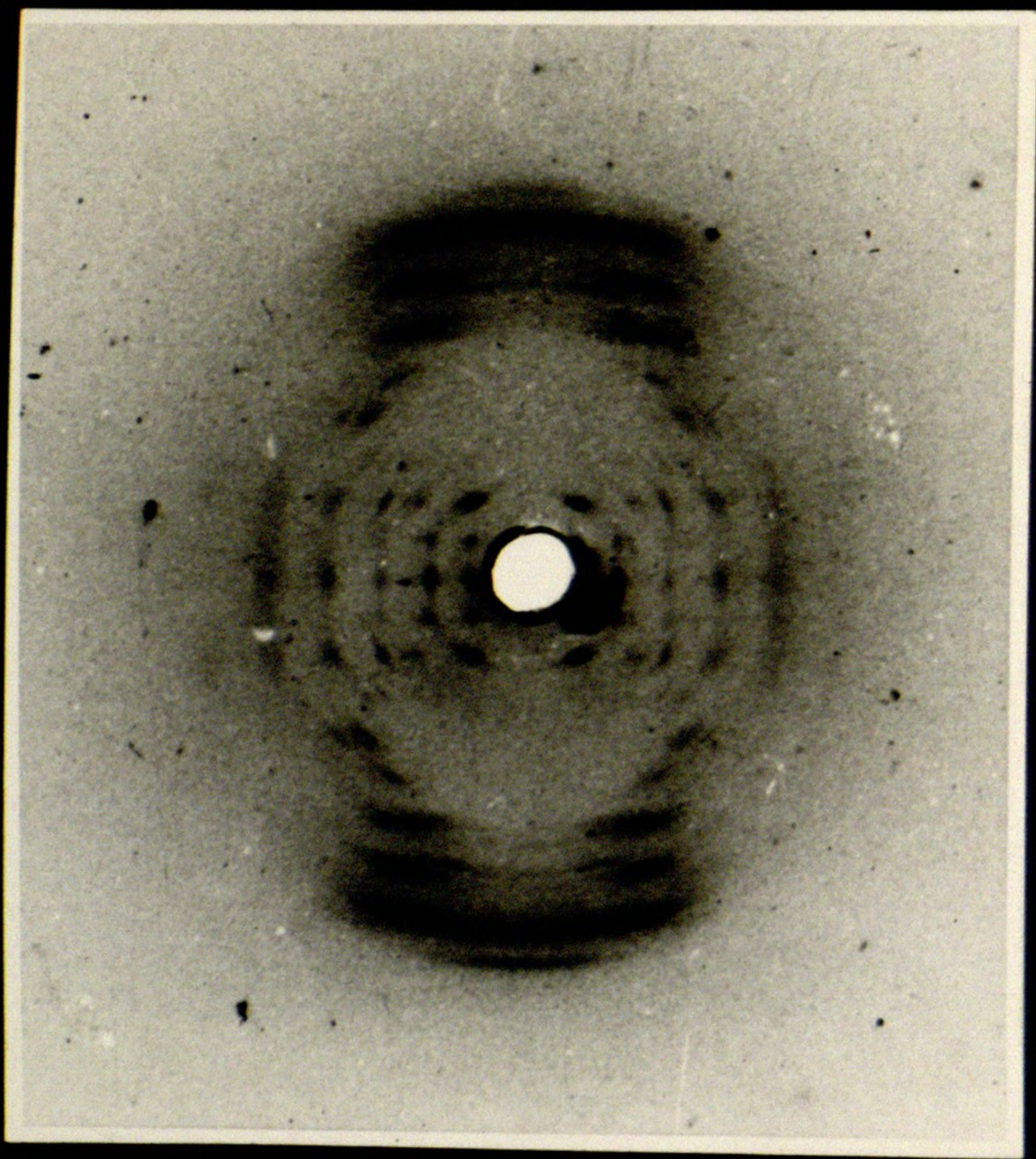
15



Q874



574



THE STRUCTURE OF SODIUM THYMONUCLEATE FIBRES

II. THE CYLINDRICALLY SYMMETRICAL PATTERSON FUNCTION

Rosalind E. Franklin and R. G. Gosling

Wheatstone Physics Laboratory
King's College London

SUMMARY

The positions and maximum photographic intensities of reflections have been measured on X-ray microphotographs of highly crystalline sodium thymonucleate fibres. A procedure is described for deducing from these measurements the integrated intensities of the reflections. These have been used to calculate the cylindrically symmetrical Patterson function. From this Patterson function it was possible to obtain the unit cell and hence to allot indices to all the 66 observed reflections. Confirmation of the correctness of the indexing was obtained from photographs of a single fibre which showed double orientation of the crystallites.

INTRODUCTION

In the preceding paper it was shown that by varying the water content of highly orientated fibres of sodium de-oxy-ribonucleate (NaDNA) different structural modifications could be obtained. The most highly ordered structure was that obtained when operating at about 75% R.H. (structure A). This has therefore been selected for a systematic quantitative study.

The fibre diagram of this crystalline structure (Franklin and Gosling, 1953, Plate I) shows 66 independent reflections distributed on nine well-defined layer-lines. During the course of attempts to index the reflections it became fairly clear that the unit cell was monoclinic c-face-centred, with the c-axis parallel to the fibre axis. However, owing to the inevitable errors of measurement, and to the ambiguities of indexing reflections at large angles of diffraction, it was not found possible, by direct inspection, to establish all the cell parameters with certainty. It was therefore decided to calculate the cylindrically symmetrical Patterson function described by MacGillavry and Bruins (1948). This function contains all the information which can be obtained from the fibre diagram without allotting to the reflections any indices other than their layer-line numbers, and is therefore periodic in the c-direction only. It is the function which would result from taking the true three-dimensional Patterson function, giving it cylindrical symmetry

2.
by rotating it about an axis through the origin and parallel to the fibre axis, and then taking a section through the axis of rotation.

The principal periodicities, or lattice translations, other than that corresponding to the layer-plane spacing, will be revealed as important peaks in this aperiodic Patterson function. They will, in general, be distinguished from other Patterson peaks in that their second (and higher) orders will be observed.

MacGillavry and Bruins (1948) have shown that the cylindrically symmetrical Patterson function $\phi(z, x)$ is given by the equations

$$\phi_\ell(x) = \frac{2\pi}{NV} \int_0^\infty H(\ell, \xi') J_0(2\pi \xi' x) \xi' d\xi' \quad (1)$$

and

$$\phi(z, x) = \sum_\ell \phi_\ell(x) \cos 2\pi \ell z. \quad (2)$$

Here $\xi' = \xi/\lambda$, where ξ is the

Bernal coordinate. z and λ is the wavelength of the incident radiation.

$H(\ell, \xi')$ is the intensity on the ℓ th layer-line at a distance ξ' from the fibre axis in R-space

$J_0(u)$ is the zero order Bessel function of u

and $\frac{V}{N}$ is the volume irradiated
is the total number of periods in the fibre direction.

MacGillavry and Bruins refer to ξ' (their ξ) as the Bernal coordinate, but we have preferred to use Bernal's original notation in the discussion which follows, and so have introduced it here.

If each layer-line shows only discrete reflections whose integrated intensities can be measured, the integral in equation

(1) may be replaced by a summation, and

$$\phi'_l(x) = \sum_{\xi'} I(l, \xi') J_0(2\pi \xi' x). \quad (3)$$

where $I(l, \xi')$ is the integrated intensity of a reflection occurring on the l th layer-line at a distance ξ' from the fibre axis,

and

$$\phi'_l(x) = NV \cdot \phi_l(x).$$

EXPERIMENTAL

Measurements were made on photographs taken with a specimen-film distance of 15 mm. using the Phillips micro-camera and an Ehrenberg-Spear fine-focus tube as described in the preceding paper. A constant stream of hydrogen at 75% relative humidity was passed through the camera during the exposures.

In order to search for further reflections on or near the fibre-axis direction, photographs were also taken with the fibre inclined to the X-ray beam at a series of angles in the range 85° to 70° . A micro-camera was designed specifically for this purpose and will be described elsewhere. The specimen-film distance and collimator dimensions were the same as those of the Phillips micro-camera.

These photographs revealed only one reflection not observed with the fibre perpendicular to the X-ray beam. This reflection lies on the 11th layer-line on, or close to, the fibre-axis direction. It is, however, a weak reflection and in the quantitative work described here its intensity,

when corrected for geometrical factors, is negligibly small.

For the measurement of the R-space co-ordinates and the intensities of the 66 independent reflections standard methods could not be applied owing to the small size of the photographs, and to the variety of shapes and sizes of the photographic spots. A description of the methods used is given below.

Measurement of R-space co-ordinates

For the measurement of the positions of reflections the microphotographs were projected on a white cardboard screen using a magnification of about 10. The centres of the reflections were then marked on the card and their x and y co-ordinates measured. For the outer reflections an indication of the length of the arcs was also recorded. The use of the projector rather than a travelling microscope was found not only to be much less fatiguing, but also to provide a more reliable estimate of the positions of weak reflections and a more convenient method of making measurements on curved^{ed} layer-lines.

For calibration of the scale of the projected photographs, photographs taken with a Unicam single-crystal camera were used. In this way, the very strong equatorial reflection was shown to correspond to a spacing of 11.3A. Using this value, the appropriate demagnification factor for converting the measured x and y co-ordinates to the scale of a Bernal chart was calculated, and hence the ξ and η values of each reflection were obtained.

Correction for tilting of the fibre axis

A correction must be applied to the measured ξ and η values owing to the fact that it is almost impossible to place the fibre

exactly perpendicular to the X-ray beam.

Fig. 1 (a) illustrates the diffraction conditions when the fibre-axis deviates from the ideal position by a small angle γ . A plane parallel to the layer-lines and at a distance from the R-space origin 0 given by $\gamma_s = \sin \gamma$ will give a straight line h_s on the flat film. Layer planes above γ_s will form layer lines which are less curved and have reflections more widely separated than if the fibre were normal to the direct beam. Layer planes lying below γ_s will form layer-lines more highly curved having reflections closer to the meridian. The general form of the layer lines will be as indicated in Fig.1 (b).

Let γ_1 and γ_2 be the apparent γ -values measured above and below the equator respectively for a given set of reflections corresponding to a spacing $d = 1/\rho$. It can be shown that the required value of γ for the perpendicular fibre is given by

$$\gamma = \gamma_1 \cos \gamma + \frac{1}{2} \rho^2 \sin \gamma = \gamma_2 \cos \gamma - \frac{1}{2} \rho^2 \sin \gamma. \quad (4)$$

whence $\tan \gamma = (\gamma_2 - \gamma_1) / \rho^2$

(5)

and

$$\gamma = \cos \gamma \cdot (\gamma_2 + \gamma_1) / 2$$

(6)

Measurements of γ_1 , γ_2 and ρ can therefore be used to determine γ .

Most of our measurements were made on photographs for which γ was found to be about 8° . Values of γ obtained with the aid of equations (4) and (5) from measurements made on reflections in the first 9 layer-lines are shown in Table 1. Each value is a mean of measurements on at least 3 reflections. Neglecting the value obtained for the 3rd layer-

line, where the reflections are weak and difficult to measure accurately, the mean value of γ is 0.0547. This gives c , the fibre-axis repeat period, as 28.1A.

TABLE I

L :	1	2	3	4	5	6	7	8	9
γ :	.0550	.0540	.0533	.0545	.0552	.0548	.0545	.0546	.0551

Having established in this way the layer-line spacing, values of ξ can now be obtained with improved accuracy for reflections on the higher layer-lines. For these, the most accurately observable parameter is the radius of the circle on which the four equivalent photographic spots must lie. This gives $\rho (= \lambda/d)$, and ξ -values were therefore determined from the relationship

$$\xi^2 = \rho^2 - \left(\frac{d\lambda}{c}\right)^2$$

Measurement of intensities

The variety of shapes and sizes of the photographic spots makes it impossible to estimate directly the integrated photographic intensity. It is necessary therefore either to explore each spot photometrically, or to estimate its maximum intensity and to consider separately the question of spot size and shape. The latter alternative was adopted. Not only would the photometric method involve a very large amount of work, but, in the micro-photographs available, the grain-size is too large in relation to the spot-size for photometry to be applied with any degree of accuracy. Use of fine-grain films would lead to excessive exposure times and thus remove the advantage gained from the use of the micro-technique.

The maximum intensity of each spot was estimated visually by comparison with a standard scale. For the preparation of this scale the ultra-fine collimating system of a low-angle camera * (slit width 8μ) was used to photograph the direct beam, with exposure times varying from 3 to 90 seconds. A set of streaks of width comparable with that of the spots on the micro-photographs was obtained. The fibre-photograph was projected, as for the measurement of the positions of reflections, and the scale displaced by hand across the photograph in the projector. The standard streaks were placed as close as possible to the spot whose intensity was being measured in order to eliminate, as far as possible, the effect of varying intensity of the background.

We must now consider how the measured values of photographic maximum intensity are related to the R-space integrated intensities of reflections. The relationship will depend on the following factors:-

(i) True diffraction breadth The breadth of the reflections, measured along a line joining the reflection to the origin, is approximately constant over the whole photograph. It may therefore be assumed that the true diffraction breadth is everywhere small compared with the geometrical broadening (direct beam size) and can be neglected.

(ii) Spread of reflections in R-space due to disorientation of the crystallites

(a) If the crystallites are perfectly aligned with respect to the fibre axis but in random orientation about this axis, each reflection will be spread over a circle of radius $\frac{e}{\lambda}$. Maximum intensities must therefore

be multiplied by in order * Designed by K.P.Norris.

be multiplied by ξ/λ in order to relate them to integrated intensities. (This accounts for the factor $2\pi\xi' = 2\pi\xi/\lambda$ which occurs in Equation (1) but not in Equation (3)).

(b) Imperfect alignment of the crystallites with respect to the fibre axis results in a small angular spread, ϕ , (fig. 2) of each reflection along an arc of a circle with centre at the origin and the fibre axis as diameter. The length of this arc in R-space is equal to $S\phi$, where S is its distance from the origin. The R-space maximum intensity must therefore be multiplied by S to relate it to the integrated intensity.

(iii) Geometrical factors involved in the transfer of R-space effects to the photographic film

We have seen that each reflection will be spread, in R-space, over a small volume of circular symmetry with mean radius ξ/λ , and axis on the fibre axis. An axial section of this volume (Fig. 2) shows two elements each of area $ds \cdot dl$ where ds is the true diffraction breadth of the reflection and dl , the length of the arc resulting from disorientation of the crystallites with respect to the fibre axis. We must now consider the effect on the photographic maximum intensity of the oblique intersection of ds and dl with the reflecting sphere.

When a reflection intersects the reflecting sphere obliquely two extreme effects are possible.

(a) If the diffraction breadth is much less than the geometrical breadth then the photographic spot-size is independent of the diffraction breadth, and oblique intersection leads only to increased photographic intensity. This is normally true in single-crystal work and is corrected for in the Lorentz factor.

(b) If the diffraction breadth is much greater than the geometrical breadth then oblique intersection with the reflecting sphere leads to increased spot breadth on the film but does not influence the maximum intensity.

In the present case we have seen that (a) is true for the dimension ds . Since ds makes an angle θ with the surface of the reflecting sphere, the observed maximum intensity must be multiplied by $\cos \theta$ to relate it

to the integrated intensity.

In general, the effect of oblique intersection of dl with the reflecting sphere is important for all reflections which occur at a large angular displacement from the equator. However, in the present work it happens that all such reflections occur at diffraction angles large enough for the length of the photographic arcs to be much greater than the geometrical broadening (direct beam size). Oblique intersection of dl and the reflecting sphere is therefore without effect on the maximum intensity for these reflections (see iii (b) above) and no special correction is required.

For reflections at small diffraction angles and small angular displacement from the equator, the influence, on the photographic maximum intensity of the geometrical broadening in the direction of dl is important. dl is given by $s\phi$ where ϕ is the angular spread due to disorientation. To obtain ϕ a visual estimate was made of the $\frac{1}{2}$ -peak length of the arcs for equatorial reflections at large θ . (Since the value of the correction to be applied is in any case small, this method of estimation was considered adequate).

This value of ϕ was then used to obtain the R-space lengths, dl , of arcs occurring at small θ . The lengths dl' , of the photographic arcs for reflections at small θ were then obtained, from the dl values and the ^{known} ~~known~~ diameter of the direct beam (by the method of Jones (1938)). If the effect of oblique intersection be neglected, the ratio of the R-space maximum intensity to the photographic maximum intensity is given by dl'/dl . The measured maximum intensity values must therefore be multiplied by this factor.

It is shown below that any error introduced by neglecting the obliquity correction for the reflections at small θ has little effect on the resulting Patterson function.

We are now in a position to list all the corrections which must be applied to the observed maximum intensity values. They are as follows:

1. Multiply by s/λ (see (ii) a above)
2. Multiply by $\cos \theta$ (see (iii) a above)
3. Multiply by s (see (ii) b above)

4. For reflections at small θ , multiply by dI'/dI
5. Multiply by the polarisation factor $1/(1 + \cos^2 2\theta)$
6. Correction for the influence of the angle of incidence of the diffracted X-rays on the film (Cox and Shaw, 1930).
7. Correction for variation of specimen-film distance with θ for a flat film.
8. Absorption correction

Correction 8. was negligible throughout. Moreover, in the range of θ used in this study, corrections 2, 5, 6 and 7 taken together never exceed 10%, which is well within the limit of experimental error of our intensity measurements. Only corrections 1, 3 and 4 were therefore used.

For the complete set of intensity measurements 12 films were used. These were obtained from two exposures on each of two different specimens, using three films for each exposure. The total range of intensities measured in this way was from 1 to 96, and agreement obtained between different sets of measurements was better than 20% for all except a few of the weakest reflections. Some slight further error may have been introduced by the approximations involved in obtaining integrated from maximum intensities, but such error will vary only smoothly and slowly with s and will not, therefore, have a major influence on the main feature of the Patterson diagram.

Artificial temperature factor

Since the corrected intensities showed little, if any, tendency to decrease with increasing θ an "artificial temperature factor" was applied. Intensities were multiplied by $e^{-a^2 s^2}$ where $a = 0.456$, a value chosen to reduce to 0.3 of its value the intensity of the furthest equatorial reflection observed.

Calculation of the cylindrical Patterson function

Values of $J_0(u)$ were available only for values of u up to 40 (Brit. Asso. 1937, Clapp, 1937). In order to cover the desired range of $2\pi \xi x$ in the present work, values of $J_0(u)$ for u up to 76 were required. These were calculated from the approximation formula

$$J_0(u) = \frac{\sin u + \cos u}{\sqrt{\pi u}}$$

The results obtained are tabulated in the Appendix.

Values of the corrected intensities, $I(\ell, \xi)$, were then assembled for each layer-line, ℓ , and the summations of equation (3) were carried out at intervals of 1A in x in the range $x = 0$ to 50A. For each value of x , the required Patterson function is then given as a function of χ^2 by the cosine series of equation (2).

RESULTS

The resulting cylindrically symmetrical Patterson function is shown in Fig. 3.

Before seeking in any way to interpret this function it seemed desirable to have some idea of the extent to which it might be influenced by possible errors in the intensity measurements. The greatest possible source of error lies in the two strongest spots, those at 11.3A on the equator and at 12.4A on the 2nd layer-line. Each of these is clearly an unresolved doublet, a fact which was allowed for only by making a visual estimate of the breadth of the arc. Moreover, in the case of the 2nd layer-line doublet, no correction was made for oblique intersection with the reflecting sphere (see above) and the intensity value adopted was therefore somewhat too high. It was estimated that, for these reflections, the maximum possible error from all sources was about 30%. The Patterson function was therefore calculated for values of x up to 26A for these two doublets alone, and one-third of it subtracted from the function shown in Fig. 4. It is clear that the principal features of the function are substantially unaltered by this procedure, and that the effect of experimental error in intensity measurements is therefore not important.

The Patterson function shows a number of strong, well-defined peaks, and among these we must look for the lattice translations,

The first important region of high density occurs at $x = 12 - 14A$ and $\chi = 5 - 9A$. However, it can readily be shown that it is impossible to index the equatorial reflections on the basis of a unit cell in which one parameter has an x -component of about 13A.

The peaks around $x = 22A$, $\chi = 2A$, and $x = 40A$, $\chi = 0$ were next selected as possibly containing lattice vectors. These agreed well with the $\frac{b}{a} \cdot \sin \beta$ ratio of 1.82 indicated by the application of a Bunn chart to the equatorial reflections, and led to the satisfactory indexing of all the

66 observed reflections on the basis of a face-centred monoclinic unit cell having the following parameters

$$a = 22.0\text{\AA}$$

$$b = 39.8\text{\AA}$$

$$c = 28.1\text{\AA}$$

$$\text{and } \beta = 96.5$$

Agreement between calculated and observed values of δ was generally better than 1%, and in no case worse than 2%.

It was found that for the larger values of θ on the equator and the first and second layer-lines no reflection could be indexed unambiguously; reflections which should have been well-resolved and single were absent. This result is clearly not fortuitous. It seems to imply that the presence or absence of observable reflections in this region is not of great significance; single reflections are not strong enough to be distinguished from the rather strong diffuse background, and only where the geometry of the reciprocal lattice is such that two or more reflections reinforce one another can a photographic effect be observed. On this account the introduction of an "artificial temperature factor" mentioned above is more than usually important.

When all possible indices of the observed reflections are taken into account the total number of reflections is increased from 66 to 92.

Space group

Owing to the relatively small number of reflections observed, and to the ambiguity of indexing the reflections at large θ , systematic absences cannot be detected with certainty. However, since the asymmetric carbon atoms of the sugar rings preclude the existence of a plane of symmetry, C2 is the only space-group possible.

Double orientation

A fortunate accident provided a rather satisfactory confirmation of the correctness of the indexing scheme. One fibre, of diameter about 40μ , was found to give a photograph showing strong double orientation. That is, the crystallites were not in random orientation about the fibre

axis, and gave, as a result, something intermediate between a rotation and an oscillation photograph. This photograph is shown in Plate I. It will be seen that many pairs of equivalent reflections in adjacent quadrants have markedly different intensities.

A list was drawn up in which those reflections which were strongest in the top left-hand quadrant of this photograph were labelled L and those strongest in the top right-hand quadrant were labelled R. It was then found that all reflections labelled L had been allotted indices $hk\bar{l}$ whereas all R reflections had indices $hk\bar{l}$. The distribution of the observed reflections among the different quadrants in R-space as determined independently by the process of allotting indices is thus directly confirmed by comparison with the distribution revealed in this photograph.

It was thought that the double orientation shown in Plate I was probably due either to a mechanical accident to the fibre, or to preferential orientation of the crystallites which lie near the surface.

Two. The series of attempts to reproduce the effect in other fibres have, however, been unsuccessful. Firstly, single fibres were placed on a glass slide and flattened by rolling a glass rod along the direction of the fibre-axis. When air-dried fibres were used this resulted in a transformation to the unstable, optically positive state (Wilkins et al, 1951) which is highly disordered; that is, it had the same effect as excessive stretching. If, on the other hand, the fibres were rolled while at 75% relative humidity they remained optically negative but showed subsequently the less highly ordered structure B (Franklin and Gosling, 1953, Plate 4). Secondly, X-ray photographs were taken of single fibres displaced with respect to the collimator in such a way that only a small region near the surface of the fibre was exposed to the X-rays. In this way several well-orientated photographs of structure A were obtained, but they showed no trace of double orientation.

Density Determination

The density of NaDNA at various humidities was measured by the following method.

Homogeneous lumps of dry Na DNA were prepared by allowing pieces of swollen gel to dry slowly, stirring them gently at first to allow trapped

14.

air to escape. The lumps were then dried over P_2O_5 at room temperature for several weeks. To measure the density of the dry substance, each lump was placed in CCl_4 in a test-tube, and the temperature allowed to rise slowly from below $-10^\circ C$ until the lump just sank. In this way a density range of about 1.65 to 1.58 g/cc, corresponding to temperatures from -10 to $25^\circ C$, can be satisfactorily covered. The density of dry Na DNA was found to be 1.625 ± 0.002 g/cc at $4 \pm 1^\circ C$, in good agreement with Astbury's value of 1.63 g/cc. (Asbury 1947).

By using, in the same temperature range, $CHCl_3$ in place of CCl_4 densities between about 1.54 and 1.48 g/cc can be measured. Lumps of Na DNA were maintained at the required relative humidity until equilibrium was reached, then immersed in the appropriate liquid (CCl_4 or $CHCl_3$) the temperature of which was rapidly adjusted to give a density measurement. In this way the density of Na DNA at 75% R. H. was found to be 1.52 ± 0.002 g/cc (corresponding to a temperature of $2^\circ C$ to $4^\circ C$ in $CHCl_3$). The water uptake of the lumps at 75% R.H. was 32 - 42%.

Number of nucleotides per unit cell

We are now in a position to assign upper and lower limits to the number of nucleotides per unit cell. The value cannot be fixed precisely owing to the uncertainty in the quantity of water in the crystallites (Franklin and Gosling 1953); this in turn leads to some uncertainty in the density of the crystallites, which may well be slightly greater than the value measured for the bulk material at 75% R.H.

In Table 2 we show the number of nucleotides per face-centred unit cell, calculated for water contents of the crystallites corresponding to from 4 to 8 molecules of water per nucleotide, and assuming a density of 1.52 g/cc for the crystallites.

DISCUSSION

It has been shown that the use of the cylindrically symmetrical Patterson function has enabled the unit cell to be established for the most highly ordered state of the sodium desoxy-ribonucleate obtained from calf thymus. For subsequent stages in the elucidation of this

structure, methods used in the determination of structure of single crystals can therefore be applied. Work on the three-dimensional Patterson function is now in progress and will be described in a later paper. Since this is a much more powerful instrument than the cylindrical function, no attempt will be made to introduce hypotheses concerning details of structure at the present stage. A few comments of a general nature may, however, be made.

The Patterson function shows rather few peaks of remarkably high intensity relative to that of the peak at the origin. Since the unit cell contains a very large number of atoms (of the order of 1000 excluding hydrogen and water) it seems probable that the main features of the function represent phosphate - phosphate interactions, these being the heaviest group in the structure.

It will be observed that the face-centred monoclinic unit cell is near-hexagonal in projection. Nevertheless, there is evidence to suggest that the symmetry of the structural unit itself is far from cylindrical. Although the nature of the accident which produced double orientation of the crystallites in a fibre (Plate I) is unknown, it seems unlikely that it could have occurred at all if the individual crystallites had a high degree of symmetry about the fibre axis. Moreover, when the reflections are indexed it is found that nearly all the strong spots have indices $(hk\bar{l})$; the total intensity in $(hk\bar{l})$ reflections is about twice that in the (hkl) 's.

Note by A.K.

Omitted in published paper.

(but finds an echo in the King's later 1953 paper)

Williams et al Nature 172 759 (1953)

See section entitled "Circular Symmetry ---"

REFERENCES

- Astbury, W.T., (1947) Cold Spring Harbour Symp. on Quant. Biology, p. 56.
- British Association for the Advancement of Science, (1937), Mathematical Tables Vol. 6 Part 1. Cambridge University Press.
- Clapp, M.M., (1937), J. Maths and Phys., 16, 76.
- Cox, E.G. and Shaw, W. F. B., (1930), Proc. Roy. Soc., A 127, 71.
- Franklin, R.E. and Gosling, R. G., (1953), Acts Crystallographica.
- Jones, F.W., (1938), Proc. Roy. Soc., A166, 16.
- MacGillavry and Bruins, (1948), Acts Crystallographica 1 156.

TABLE 2

Number of nucleotides per unit cell

Mean molecular weight of dry nucleotide = 330			
Density of NaDNA at R.H. 75% = 1.521			
No. molecules water per nucleotide	Mol. Wt. nucleotide and water	Water content, per cent	No. nucleotides per unit cell
4	402	21.8	55.8
5	420	27.3	53.5
6	438	33.0	51.2
7	456	38.2	49.1
8	474	43.6	47.4

HEADINGS TO FIGURES

1. a) Diagram showing reciprocal lattice planes and reflecting sphere for tilted fibre .

1. b) Appearance of photograph for diffraction conditions shown in 1a).

$\frac{1}{2}\pi$

λ = position of equivalent reflections with fibre normal to X-ray beam .

\bullet = position of equivalent reflections for fibre inclined at $(90 - \gamma)$ to X-ray beam .

2. Diagram illustrating spread of reflection in reciprocal space .
3. Cylindrical Patterson function of NaDNA (structure A) .
4. Function shown in Fig. 3, with contribution of strong reflections reduced by one third.

HEADING TO PLATES

Plate 1. Single fibre, about 40μ diameter. Specimen-film distance 15 mm. Exposure about 100 hours. Photograph showing double orientation.

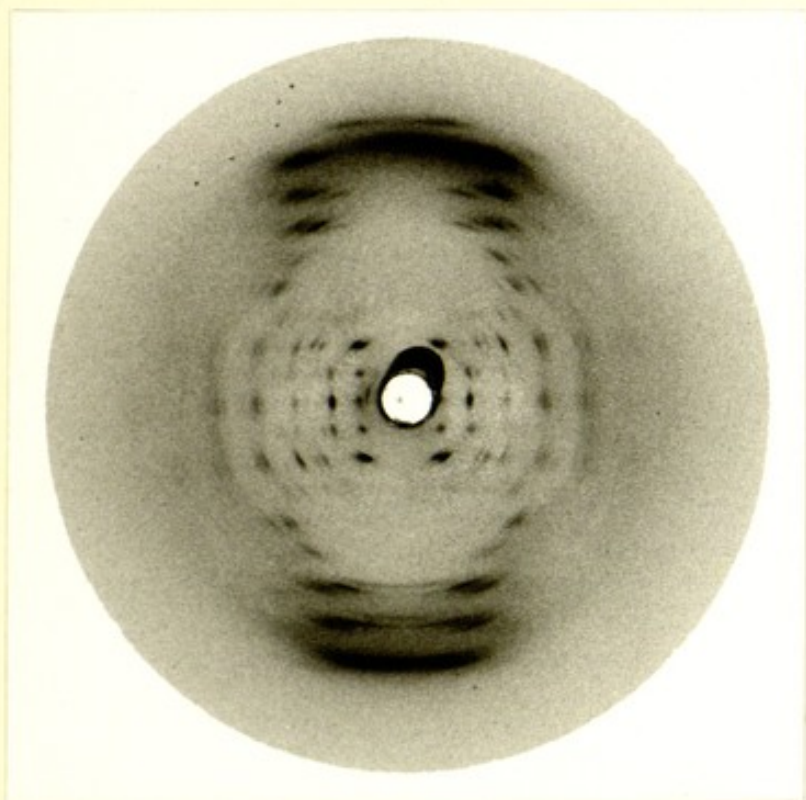


Plate 1

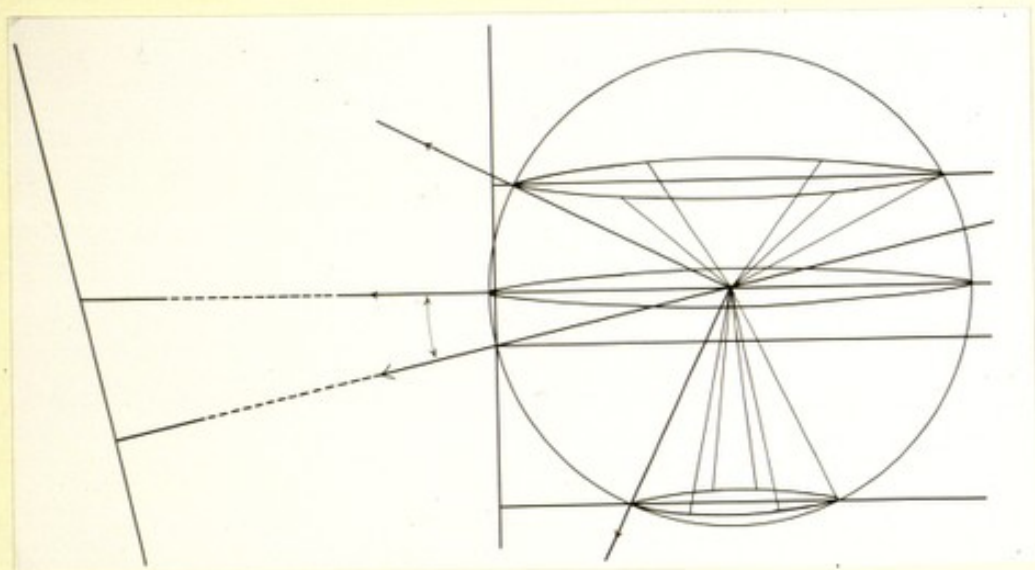


Fig 1a

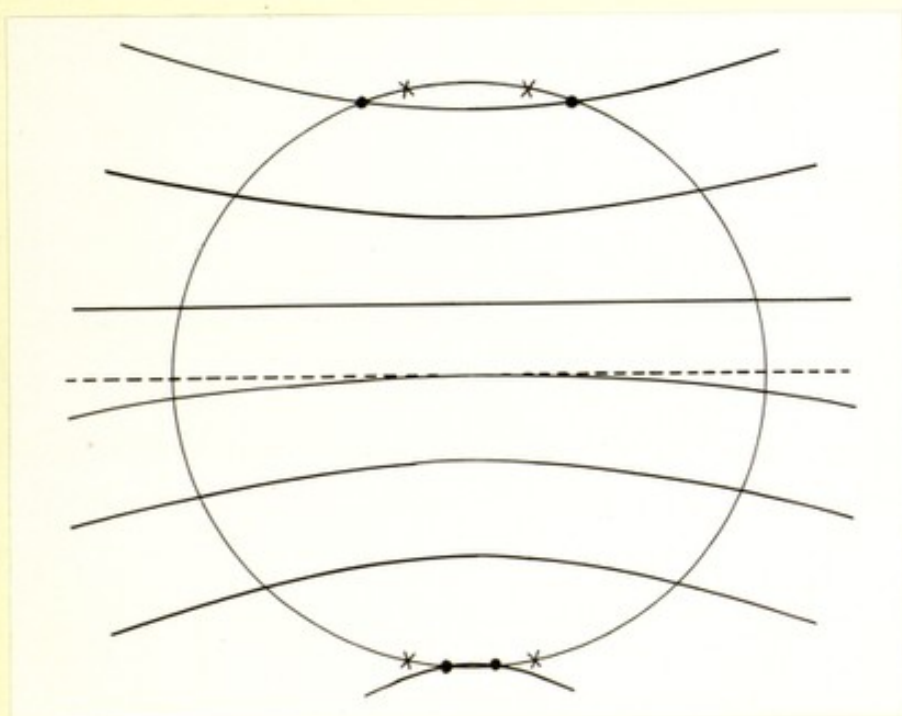


Fig 1b

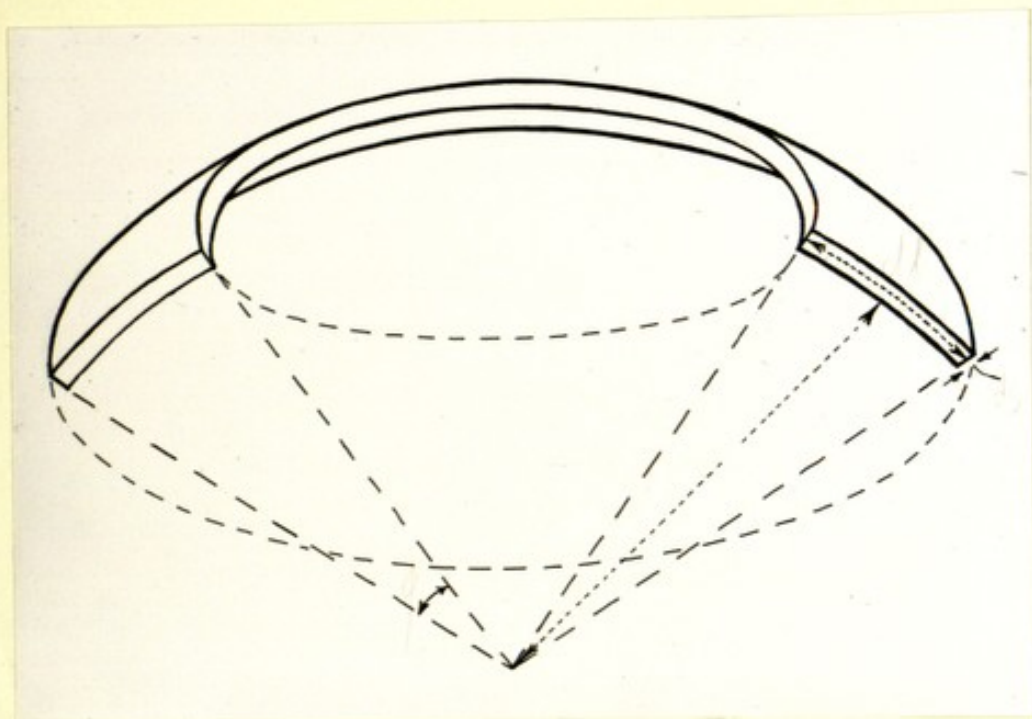


Fig 2

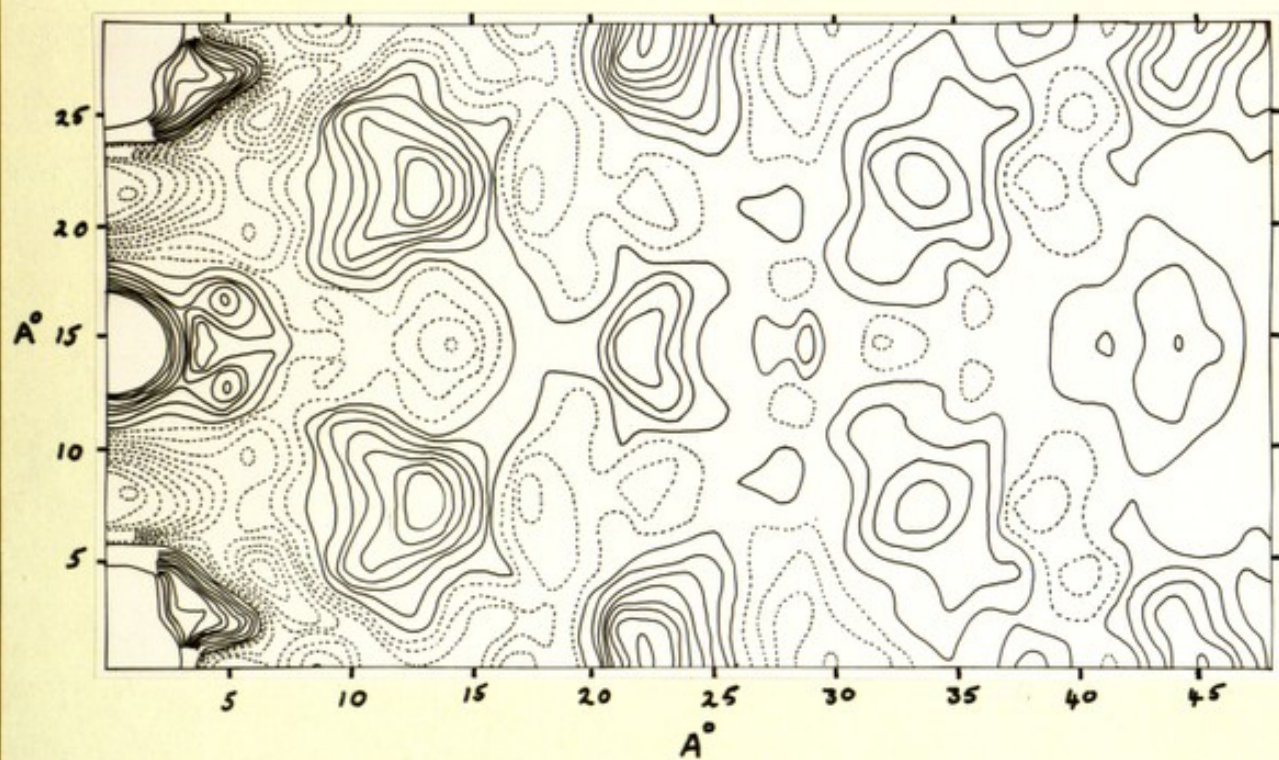


Fig 3

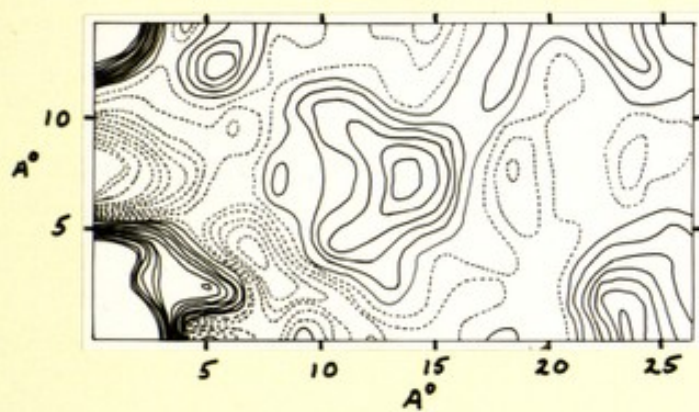


Fig 4

1008/1

§: "Durnal w. ordinate"

5/18/10

Zero Layer hkl I_{obs}
(corrected) I_{obs}
Temp. Factor

2 m 0/1

0528	5.25	110	10	9
0880	8.80	130		
0900	9.00	200	(157	134 ¹⁰⁴ ₋₃₀
1001	10.01	040	4	3
1052	10.52	220	5	4
1325	13.25	150	19	13
1380	13.8	240		
1575	15.75	310	17	11 ⁵² ₋₅₂
1755	17.55	330	9	5
1820	18.20	260	17	9
1885	18.85	170		
2000	20.00	400	42	21 ¹⁴ ₋₇
2080	20.80	350		
2200	22.10	420	25	12 ⁴ ₋₈
2285	22.85	080	17	7
2400	24.00	440	12	5
		280		
		370	33	12 ⁶ ₋₆
		510		
		190	63	21 ¹⁰ ₋₁₀
		530	46	14

1st Layer

0604	4.89	111	24	22
0658	5.53	111	12	11
0928	8.57	131	46	39
0973	9.06	131	28	23
1071	10.1	221	13	10
136	13.12	151	24	11
157	15.3	331	11	7
165	16.1	331	12	7
229	22.6	511		
		371	28	10 ⁶ ₋₄
238	23.51	461		
		531	30	9 ⁴ ₋₅

2nd Layer

0824-084-062	4.57	112	(99	85
0862-043	4.90	022		
0939-047	5.90	112	35	29
1215-067	9.80	222	27	20
1314-066	11.16	222		
148-074	13.00	242		
186-093	17.20	312	67	42 ¹⁴ ₋₁₄
		262	64	31
194-097	18.05	352		
		172	59	27 ⁹ ₋₉
212-107	20.00	262		
		082	11	5 ²⁶ ₋₂₆
230	21.90	442		
		372	36	12 ⁶ ₋₆
240	22.9	282		
		372		
		192	51	16 ⁵³ ₋₅₃
275	26.6	462		
		482		
		552	19	4 ¹ ₋₁
288	27.90	2,10,2		
		602		
		1,11,2		
		572	21	3 ¹² ₋₁₂

2 m8/λ	$5/\lambda_{10}^{obs} + 2$	hkl	I _{obs} (corrected)	I _{obs} Temp. factor	3
<u>3rd Layer</u>					
.167	12.8	243	13	7 $\begin{smallmatrix} 3 \\ -3 \end{smallmatrix}$.1068
.180	14.54	313	13	7 $\begin{smallmatrix} 4 \\ -3 \end{smallmatrix}$	
.184	14.95	063	16	8 $\begin{smallmatrix} 4 \\ -4 \end{smallmatrix}$	
.225	19.80	443	6	2	
.240	21.48	283	7	2	

<u>4th Layer</u>					
.096 .194	12.35	314	7	3 $\begin{smallmatrix} 1 \\ -1 \end{smallmatrix}$.1429
.101 .201	14.10	154	43	19 $\begin{smallmatrix} 10 \\ -9 \end{smallmatrix}$	
.107 .214	14.95	244	64	27 $\begin{smallmatrix} 13 \\ -13 \end{smallmatrix}$	
.111 .221	16.90	264	50	18 $\begin{smallmatrix} 14 \\ -4 \end{smallmatrix}$	
.257	21.45	374	22	5 $\begin{smallmatrix} 2 \\ -2 \end{smallmatrix}$	
.268	22.75	284	24	5 $\begin{smallmatrix} 2 \\ -3 \end{smallmatrix}$	

<u>5th Layer</u>					
.107 .213 .214	11.9	315	33	12	.1780
.109 .218 .217	12.4	245	33	12 $\begin{smallmatrix} 6 \\ -6 \end{smallmatrix}$	
.226	14.0	155	9	3	

<u>6th Layer</u>					
.230 .115	8.4	226	35	12	.2137
.238 .119	10.4	046	92	28 $\begin{smallmatrix} 14 \\ -14 \end{smallmatrix}$	
.243 .122	11.7	316	69	12	
.250 .125	12.75	156	69	12	
.253 .127	13.47	336	79	21	

<u>7th Layer</u>					
.261 .261 .737	7.9	117	39	9 $\begin{smallmatrix} 4 \\ -5 \end{smallmatrix}$.2492
.273 .273 .737	11.0	317	56	11	
.279 .279 .440	12.1	207	56	10 $\begin{smallmatrix} 5 \\ -5 \end{smallmatrix}$	
.284 .284 .442	13.2	337	56	10 $\begin{smallmatrix} 4 \\ -6 \end{smallmatrix}$	
		227			

<u>8th Layer</u>					
.215 .224 .304 .305	10.8	318	129	16 $\begin{smallmatrix} 10 \\ -6 \end{smallmatrix}$.2848
.277 .311 .311	12.5	158	133	15 $\begin{smallmatrix} 9 \\ -6 \end{smallmatrix}$	
.325	15.7	428	39	3	

<u>9th Layer</u>					
.163 .225	5.7	209	105	2	.3203

$\frac{5}{\lambda}$ obs 10 ⁻²	hkl	I obs (corrected)	I obs Temp Factor	$\frac{5}{\lambda}$ obs 10 ⁻²	hkl	I obs (corrected)	I obs Temp Factor
<u>ZERO LAYER</u>							
5.25	110	10	9	9.80	222	21	20
8.80	130	(157)	134	11.16	222	27	19
9.00	200			13.00	242	67	42
10.01	040	4	3		312		
10.52	220	5	4	17.20	262	64	31
13.25	150	19	13		352	59	27
				18.05	172		
13.8	240	17	11		262		
	310						
15.15	330	9	5		082	11	5
17.55	260	17	9	20.00	442		
18.20	170	12	21	21.90	372	36	12
	400				282		
18.75	500	25	12	22.9	372	51	16
	400				112		
20.00	040	17	7		462		
20.40	440	12	5	26.6	552	19	4
					210.2		
22.10	280	33	12		602		
	370						
22.85	510	63	21	27.70	1112	21	3
	190				512		
24.00	530	46	14	<u>3rd LAYER</u>			
<u>1st LAYER</u>							
4.89	111	24	22	12.8	243	13	7
5.58	111	12	11		313		
8.57	131	46	39	14.54	243	13	7
9.06	131	28	23		333		
10.1	221	18	10	14.75	063	16	8
13.12	151	24	11		313		
15.3	331	11	7	14.70	443	6	2
16.1	351	12	7	21.48	283	7	2
				<u>4th LAYER</u>			
22.6	511	28	10				
	371			12.35	314	7	3
					244		
23.51	461	30	9		154	43	19
	531			14.10	334		
<u>2nd LAYER</u>					244	64	27
4.57	112	(14)	85	14.45	064		
4.90	022			16.10	264	50	18
5.90	112	35	29		334		
				21.45	374	22	5
					284		

$\frac{I_{obs}}{\lambda} 10^{-2}$	<u>hkl</u>	$\frac{I_{obs}}{(\text{corrected})}$	$\frac{I_{obs} \times}{\text{Temp. Factor}}$	$\frac{I_{obs}}{\lambda} 10^{-2}$	<u>hkl</u>	$\frac{I_{obs}}{(\text{corrected})}$	$\frac{I_{obs} \times}{\text{Temp. Factor}}$
<u>4th LAYER</u>				<u>9th LAYER</u>			
22.15	281 114	24	5	5.7	209	105	2
<u>5th LAYER</u>							
11.9	315	33	12				
12.4	215 225	33	12				
14.0	155	9	3				
<u>6th LAYER</u>							
8.4	226	35	12				
10.4	046 136	92	26				
11.7	316	69	12				
12.75	156	69	12				
13.47	356	79	21				
<u>7th LAYER</u>							
7.1	117 137	39	9				
11.0	117	56	11				
12.4	207 247	56	10				
13.2	337 227	56	10				
<u>8th LAYER</u>							
10.6	317 136	121	16				
12.5	158 208	133	15				
15.7	428	39	3				

Fibres of human Na deoxyribonucleate and nucleoprotein studied
in polarized light by a single method

G.C. White & P.C. Flores

(Manuscript, June '51)

Drying solⁿ in NaCl gives fibres ~~not~~ oriented within NaCl crystals
nucleoprotein prepared in this way shows -ve birefringence

Na nucleate

rapid extraction 5°C with N-NaOH \rightarrow (+ve) fibres within xtal

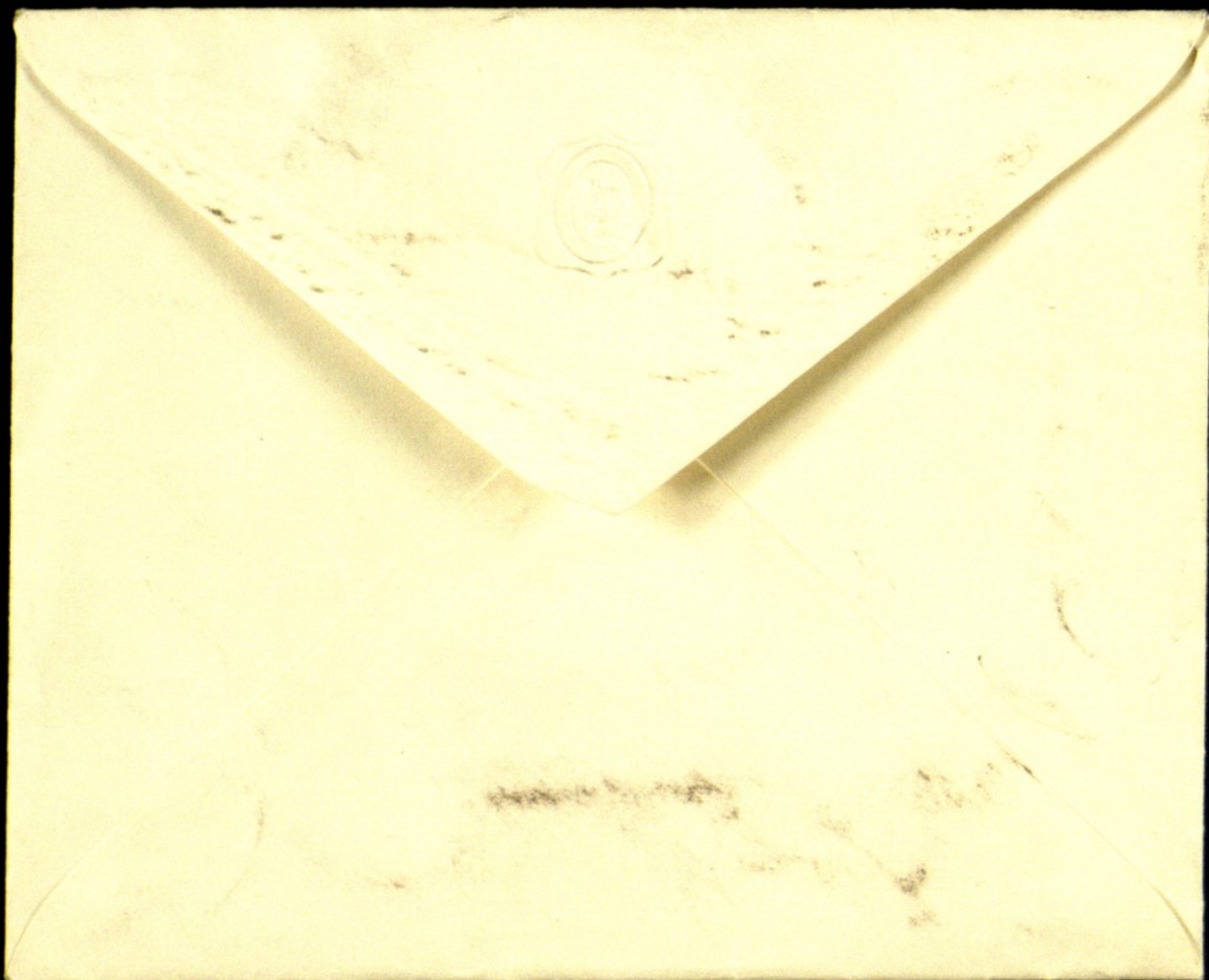
Removal of NaCl by MeOH

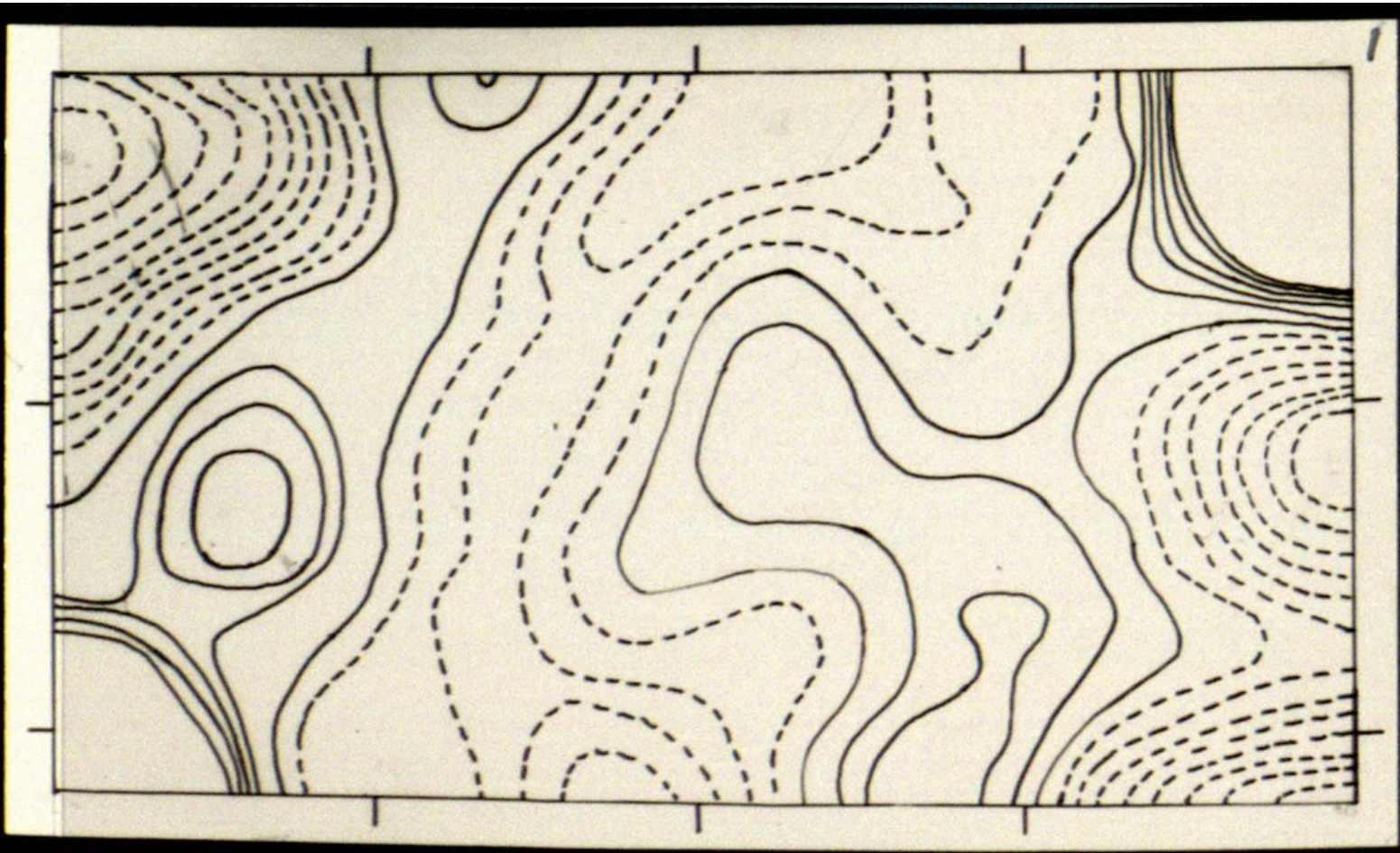
-ve fibres stay -ve at first, then \rightarrow +ve then birefringence decreases

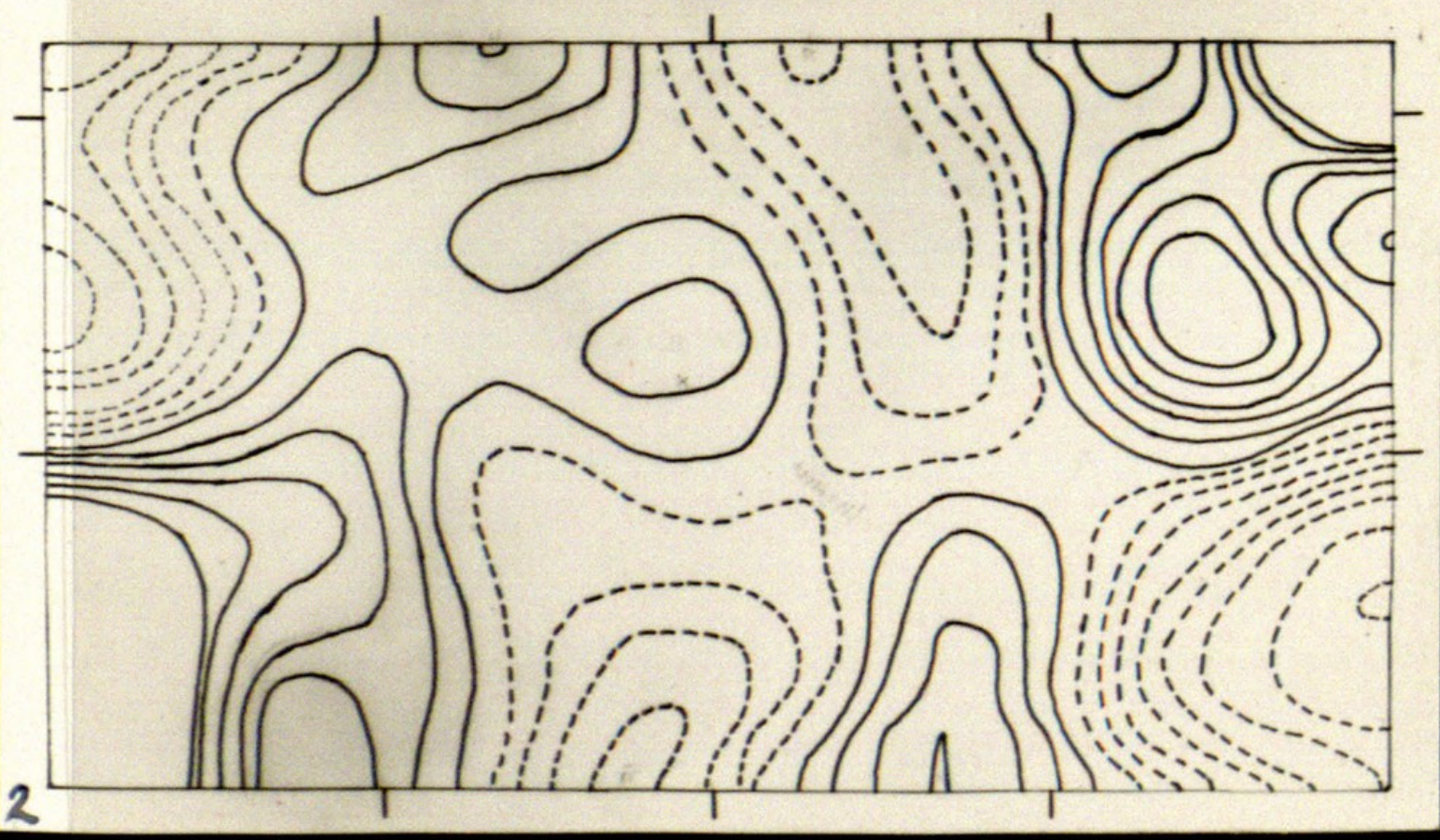
- signals reversed \therefore change orientⁿ bases, subsequent decrease \therefore decrease ^{orientⁿ}

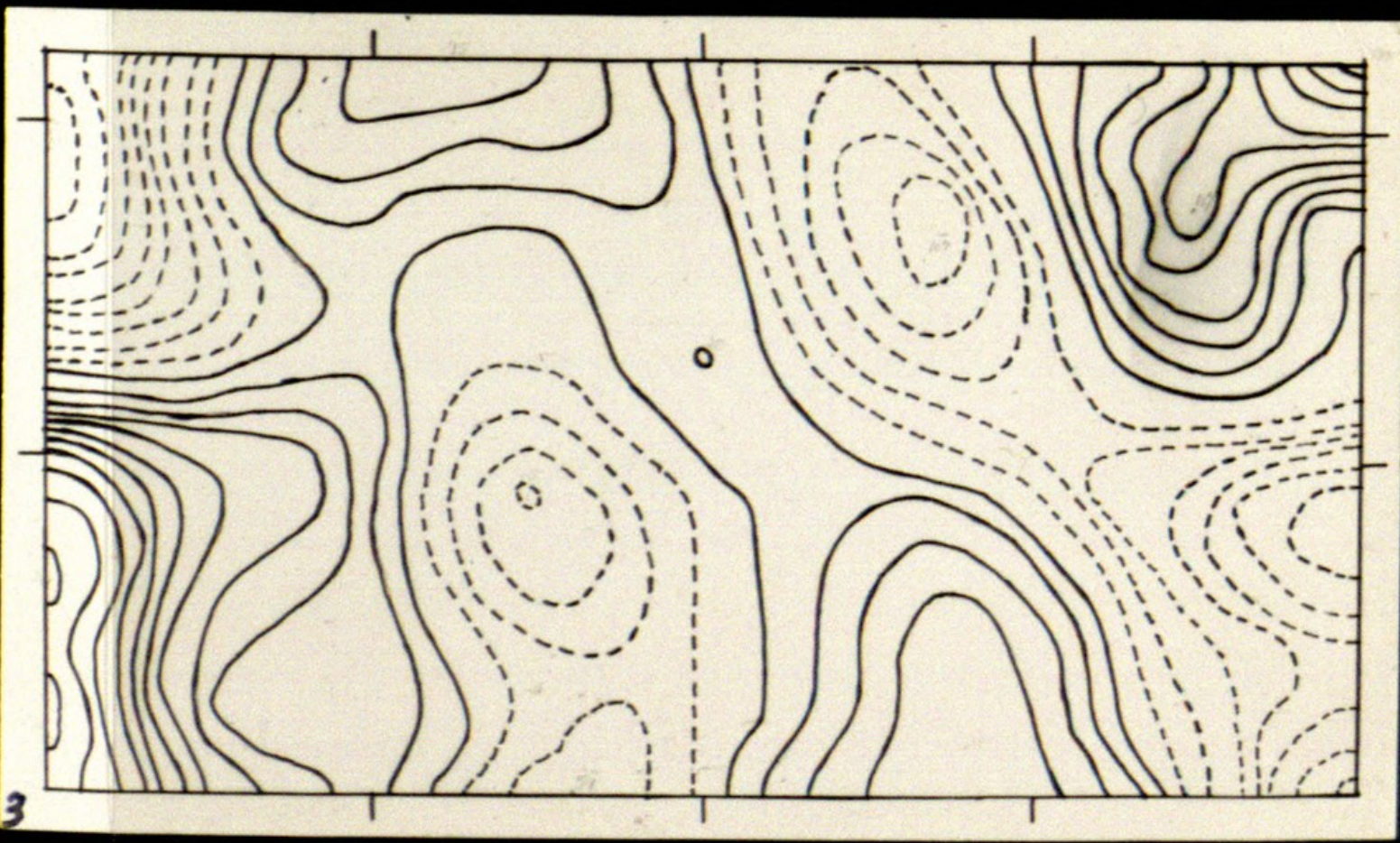
- partially bound water may be important in maintaining structure

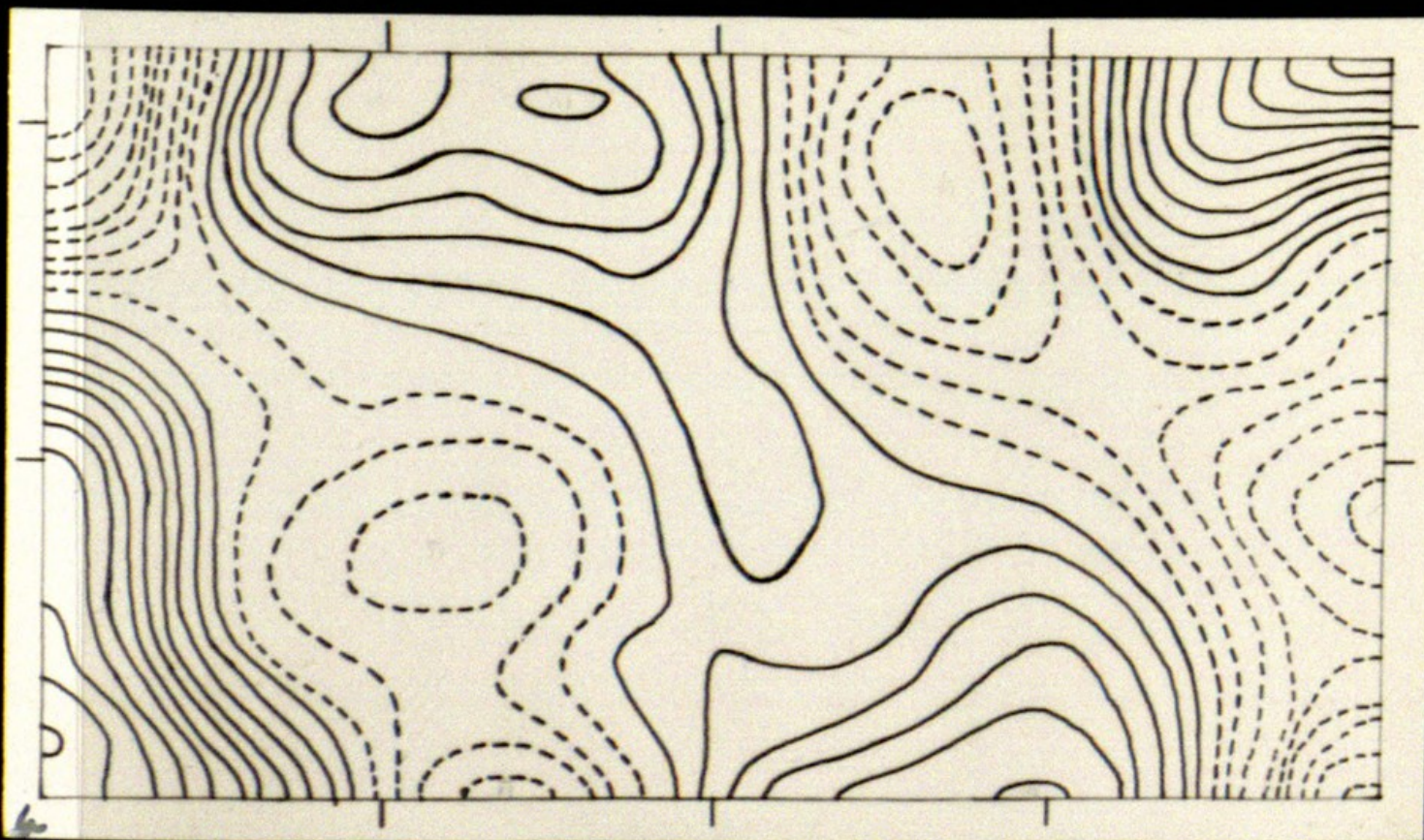
[+ve fibres only obs. in MeOH - does MeOH take part in structure?]

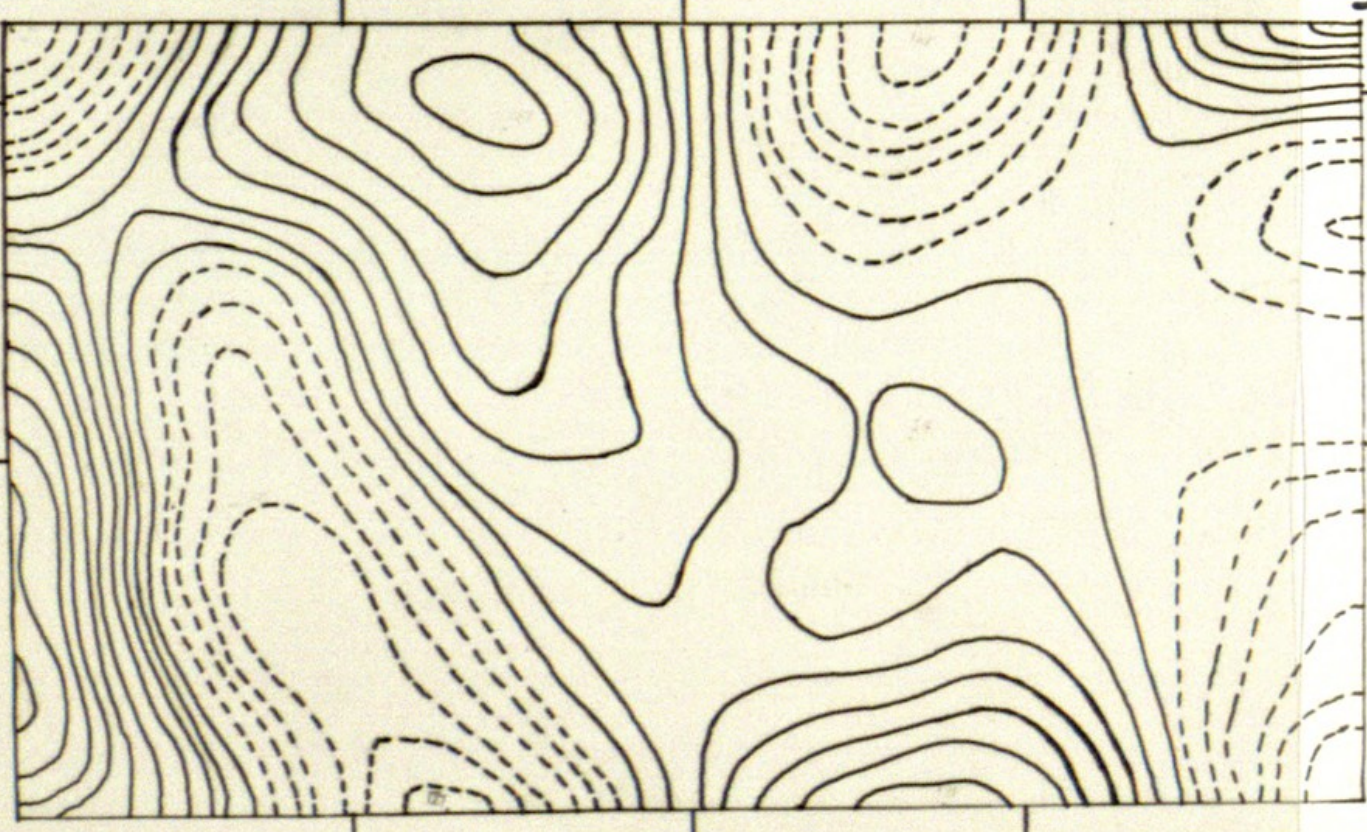


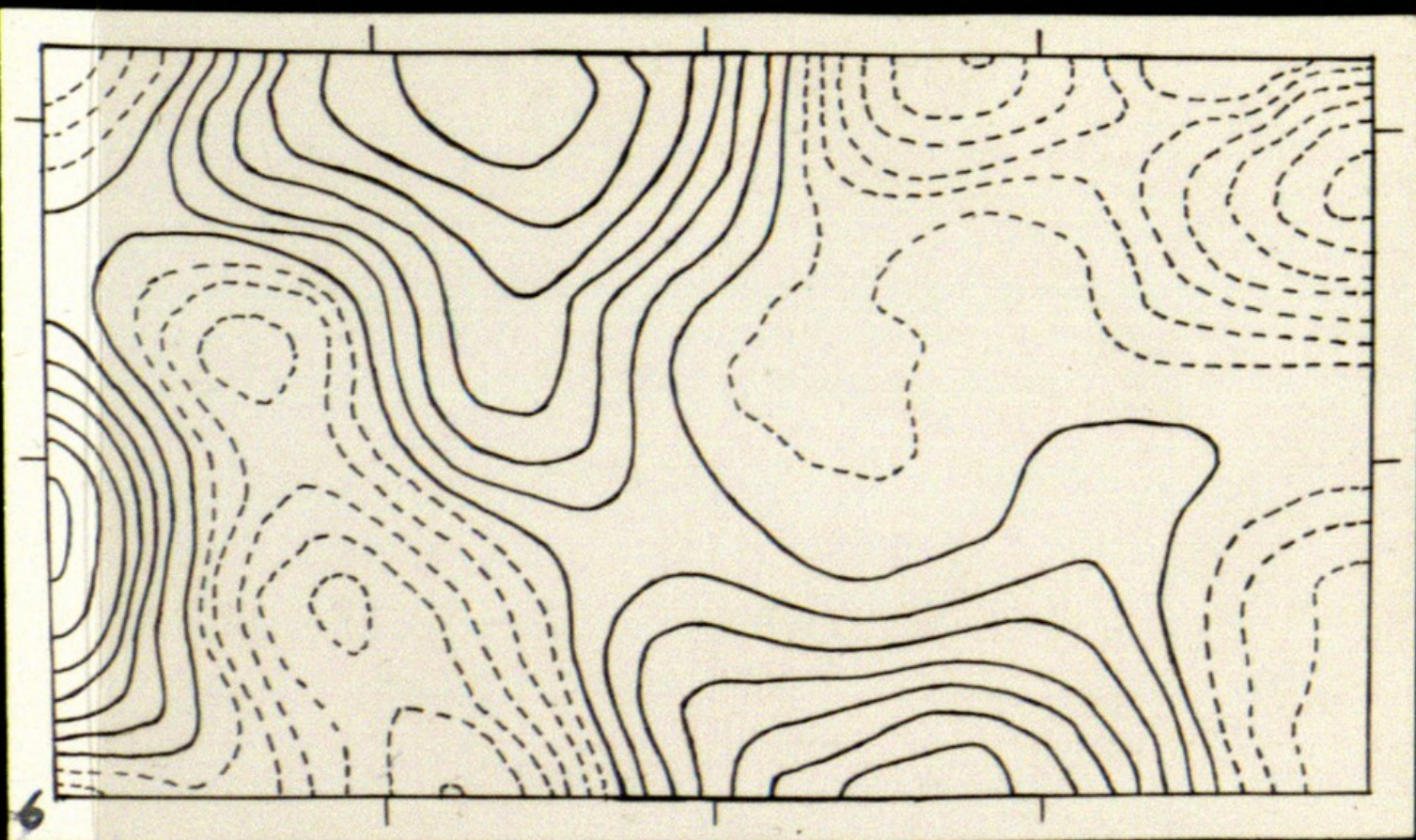


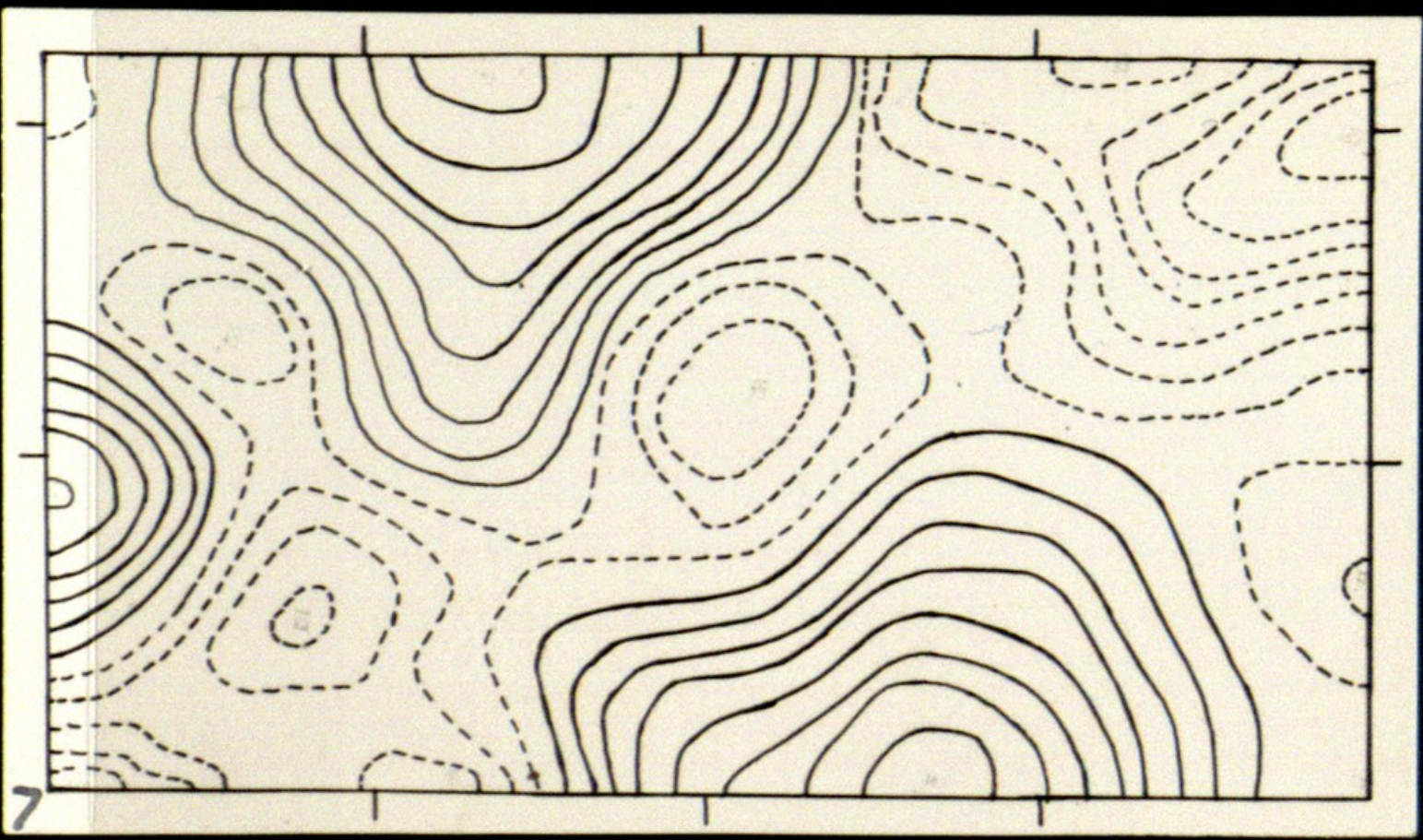


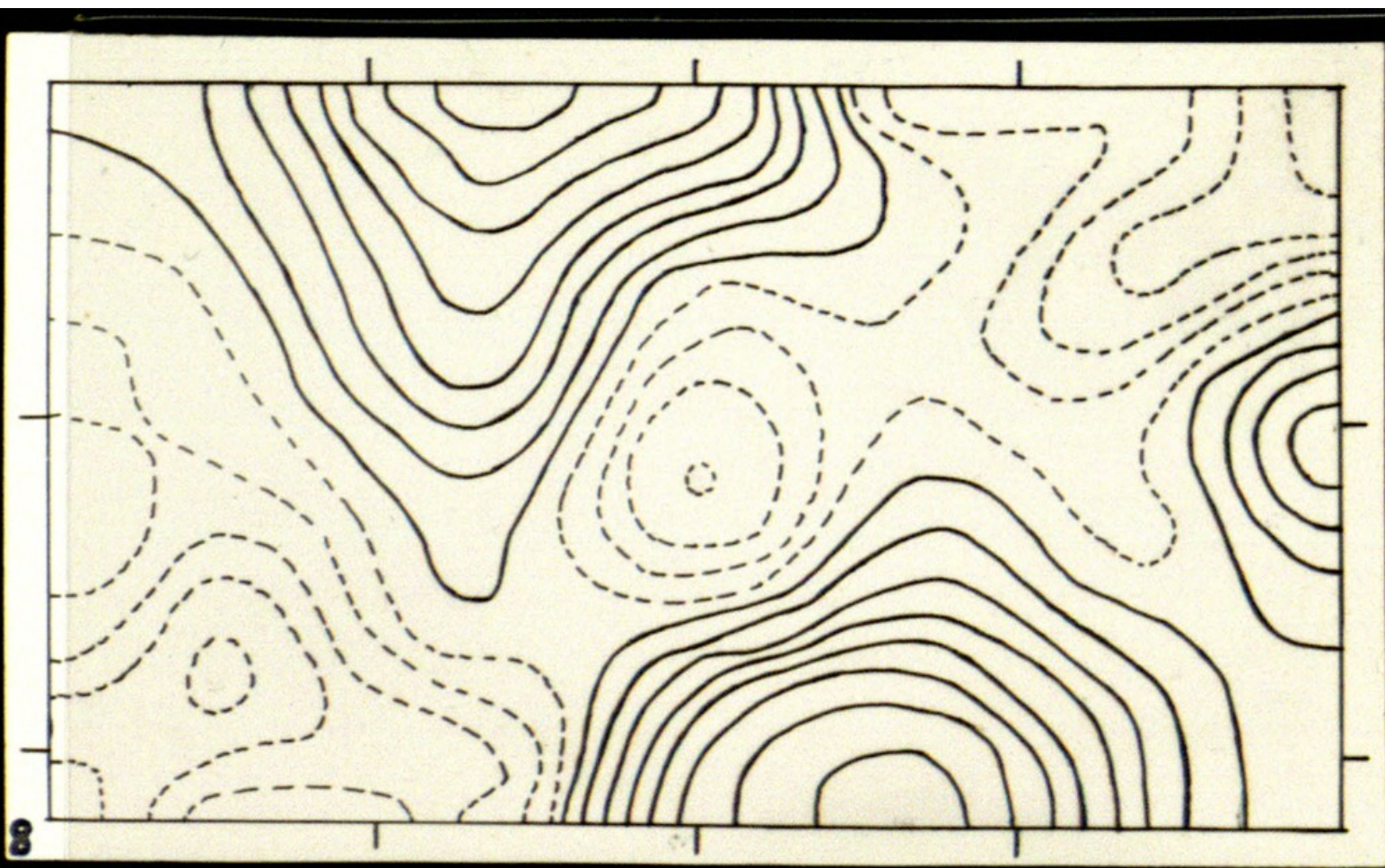


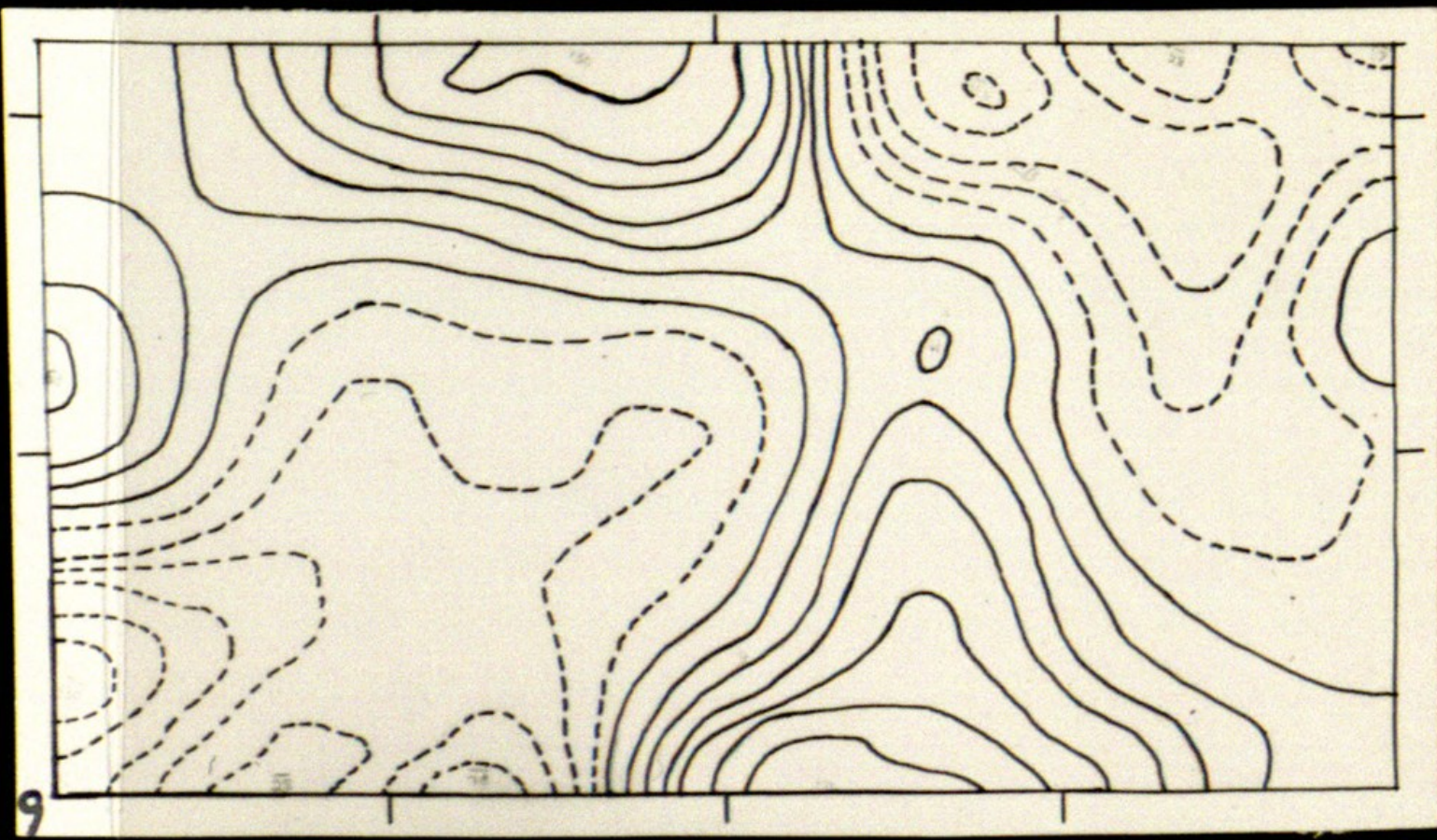


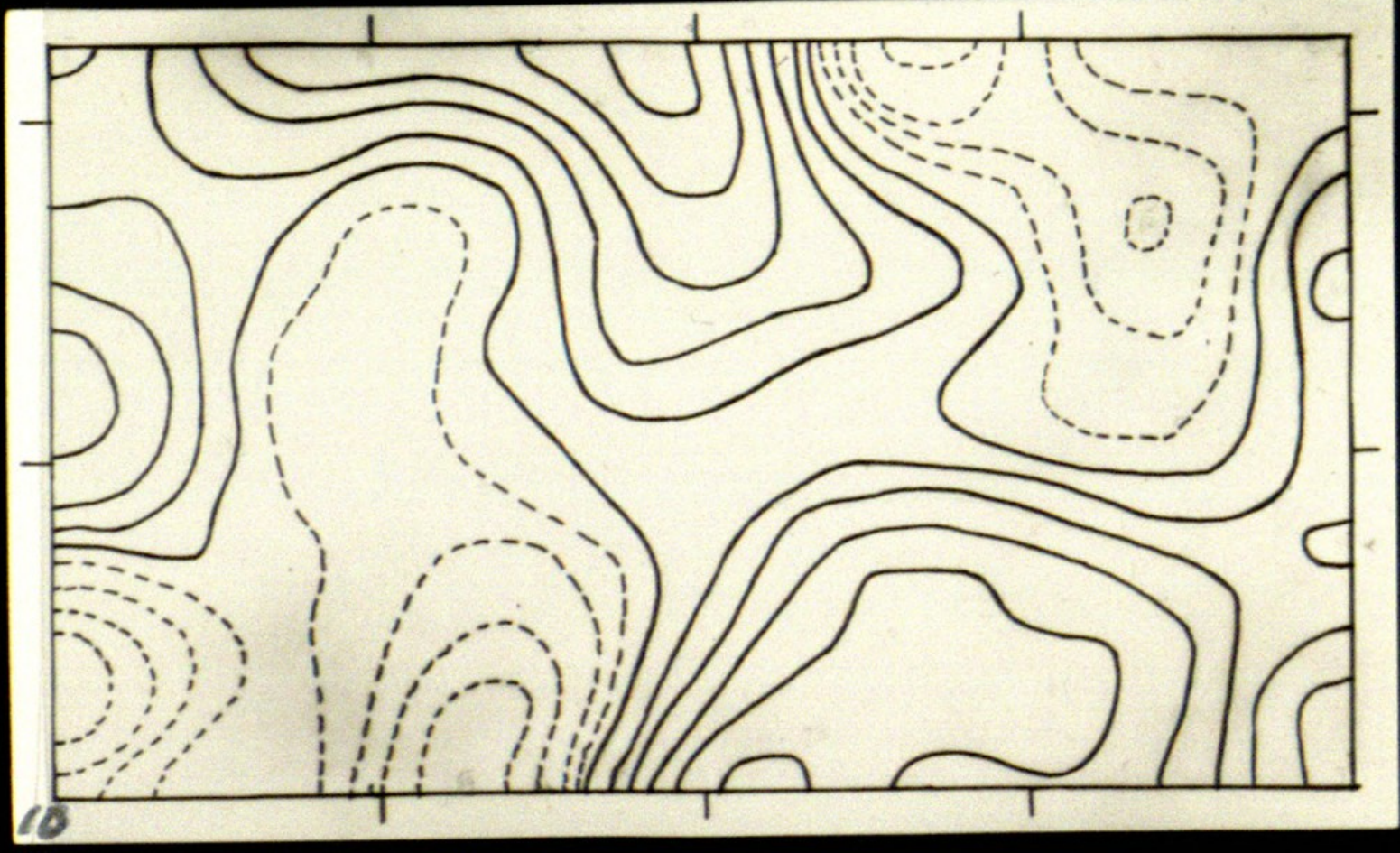


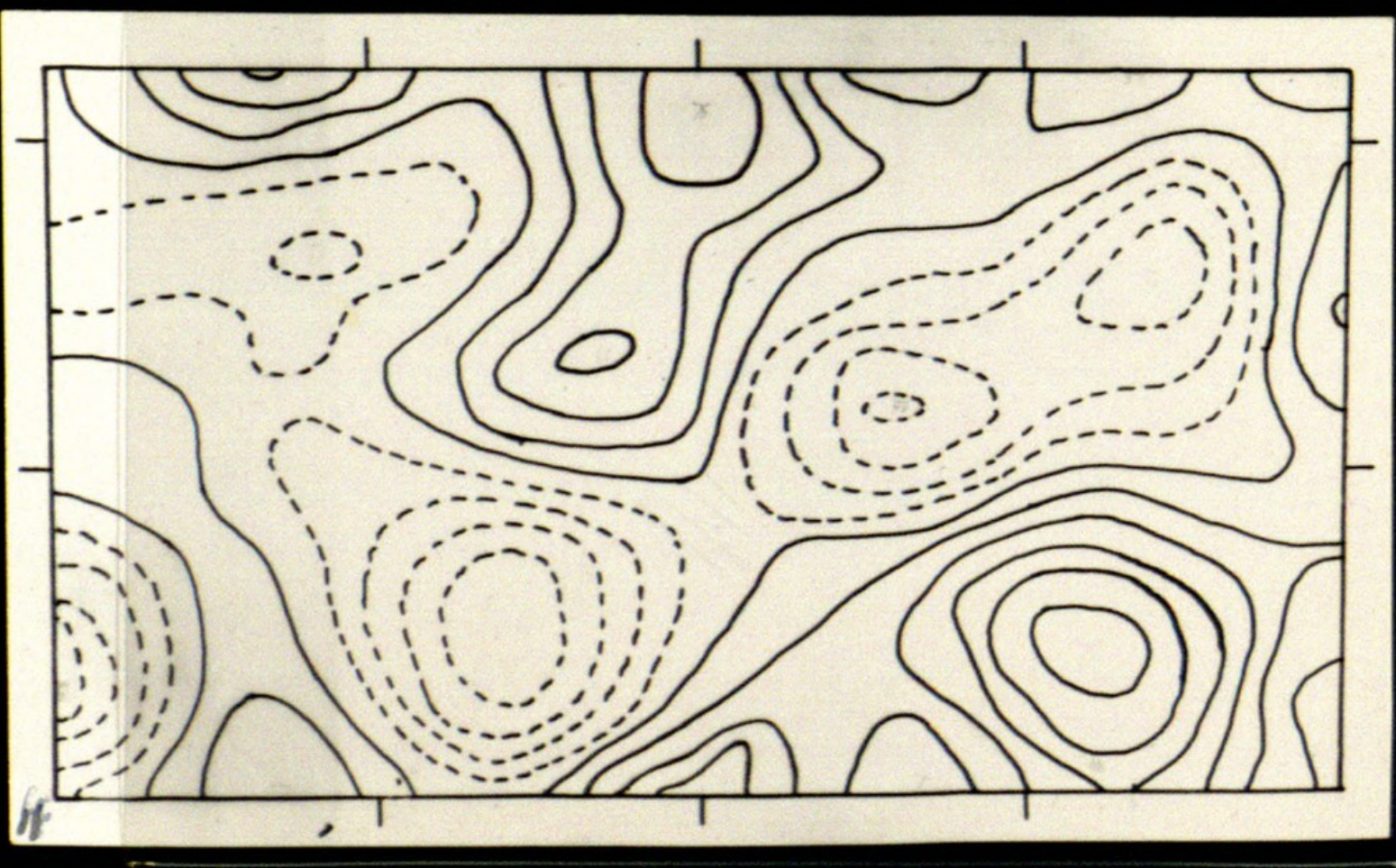


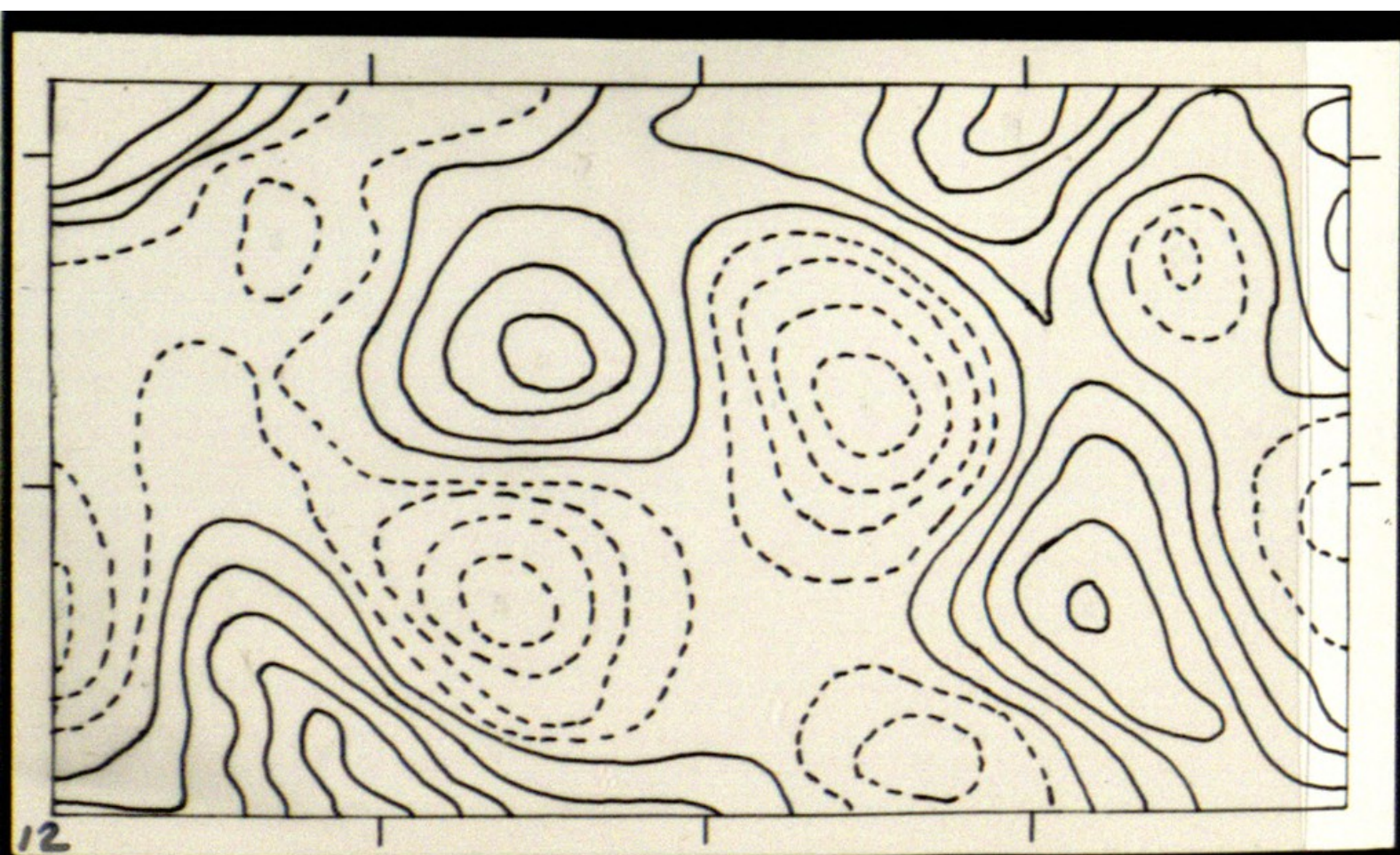


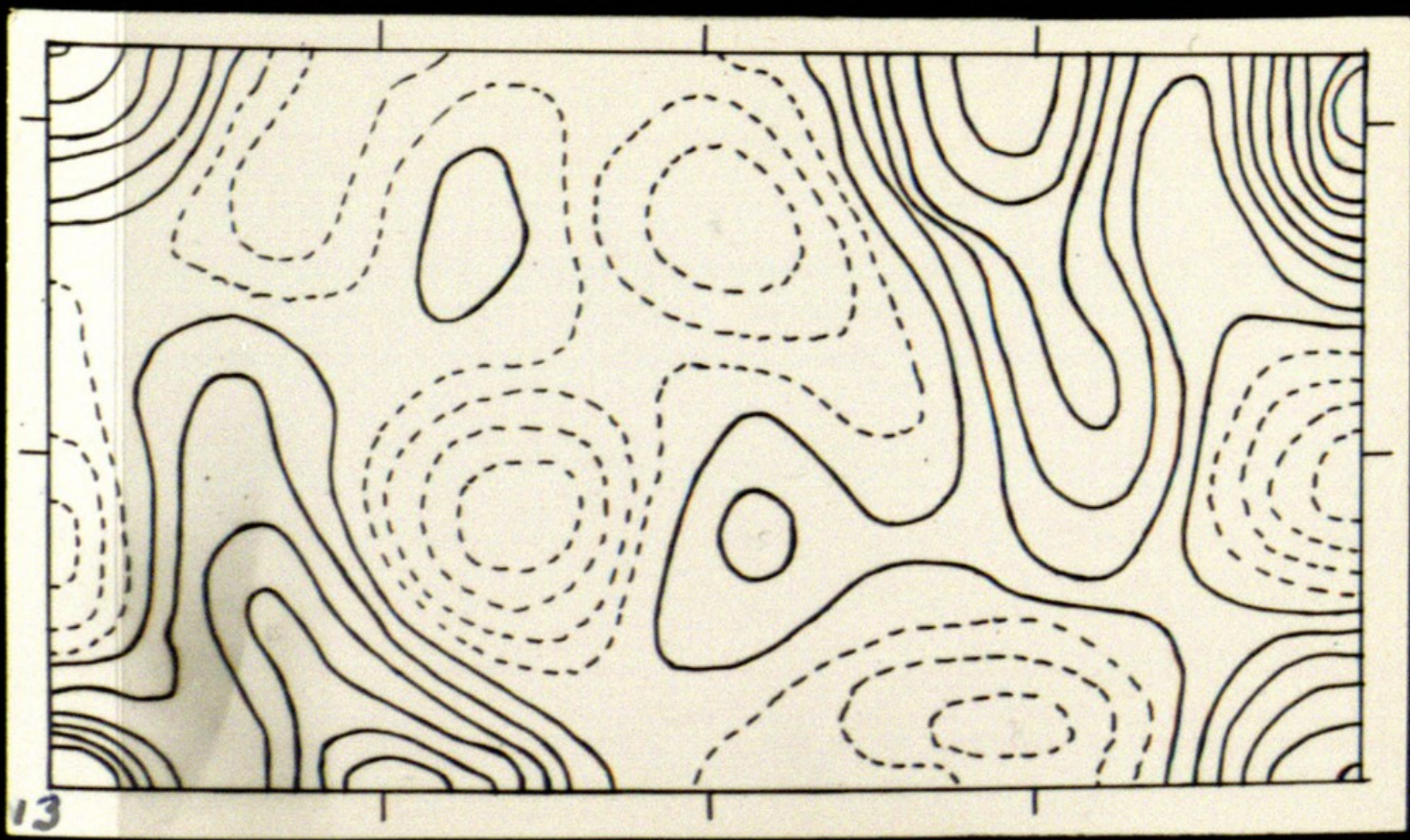


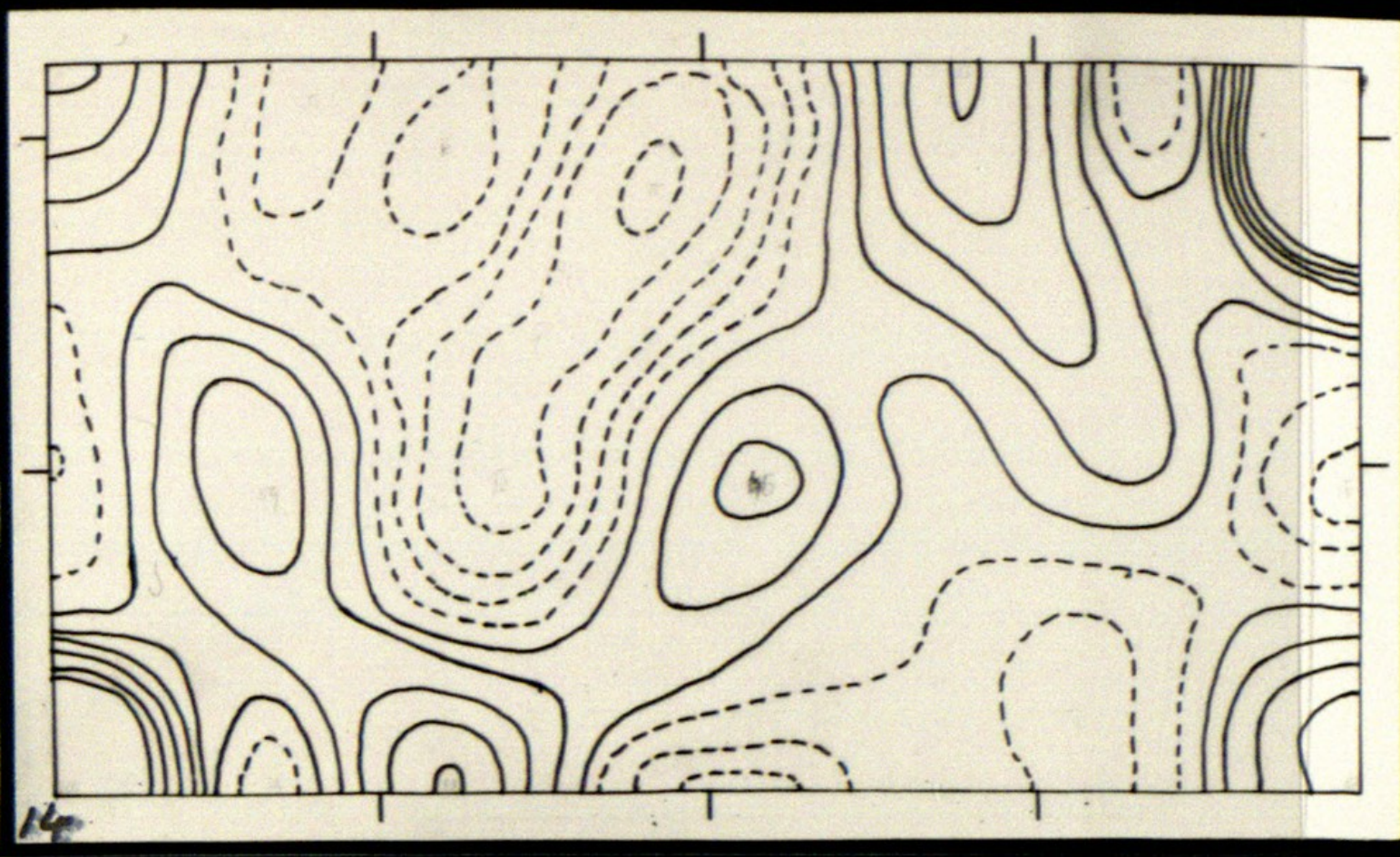


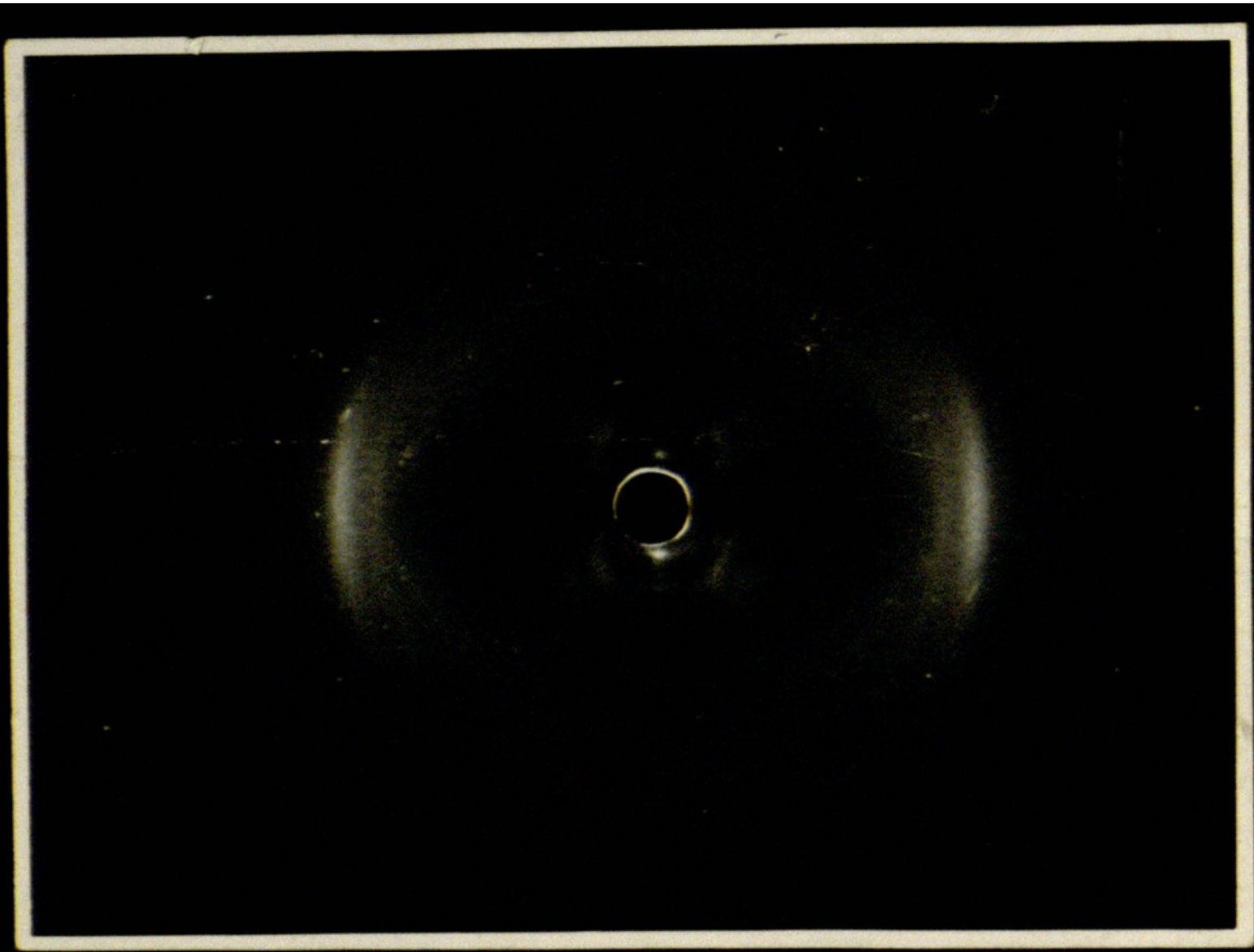


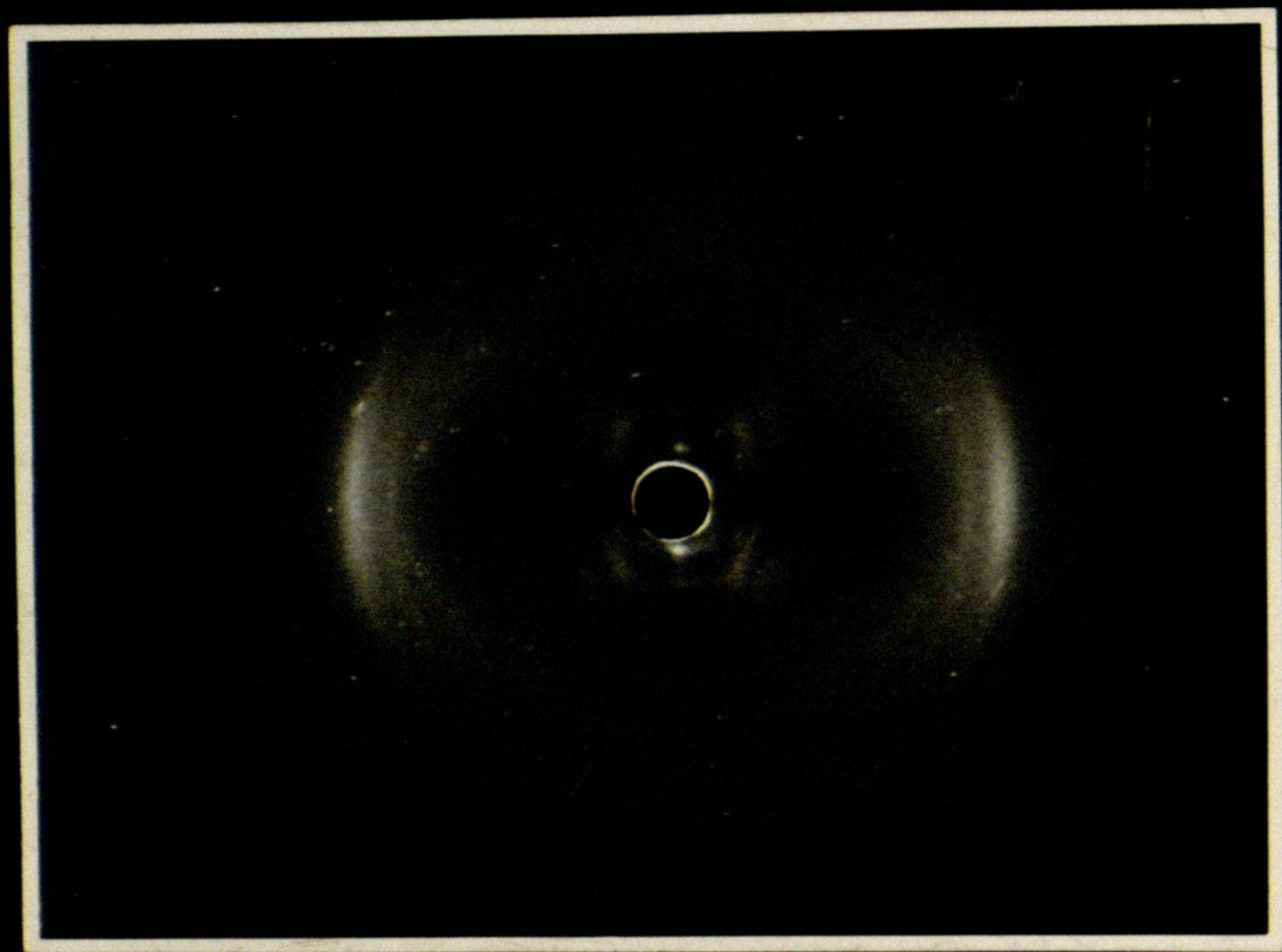


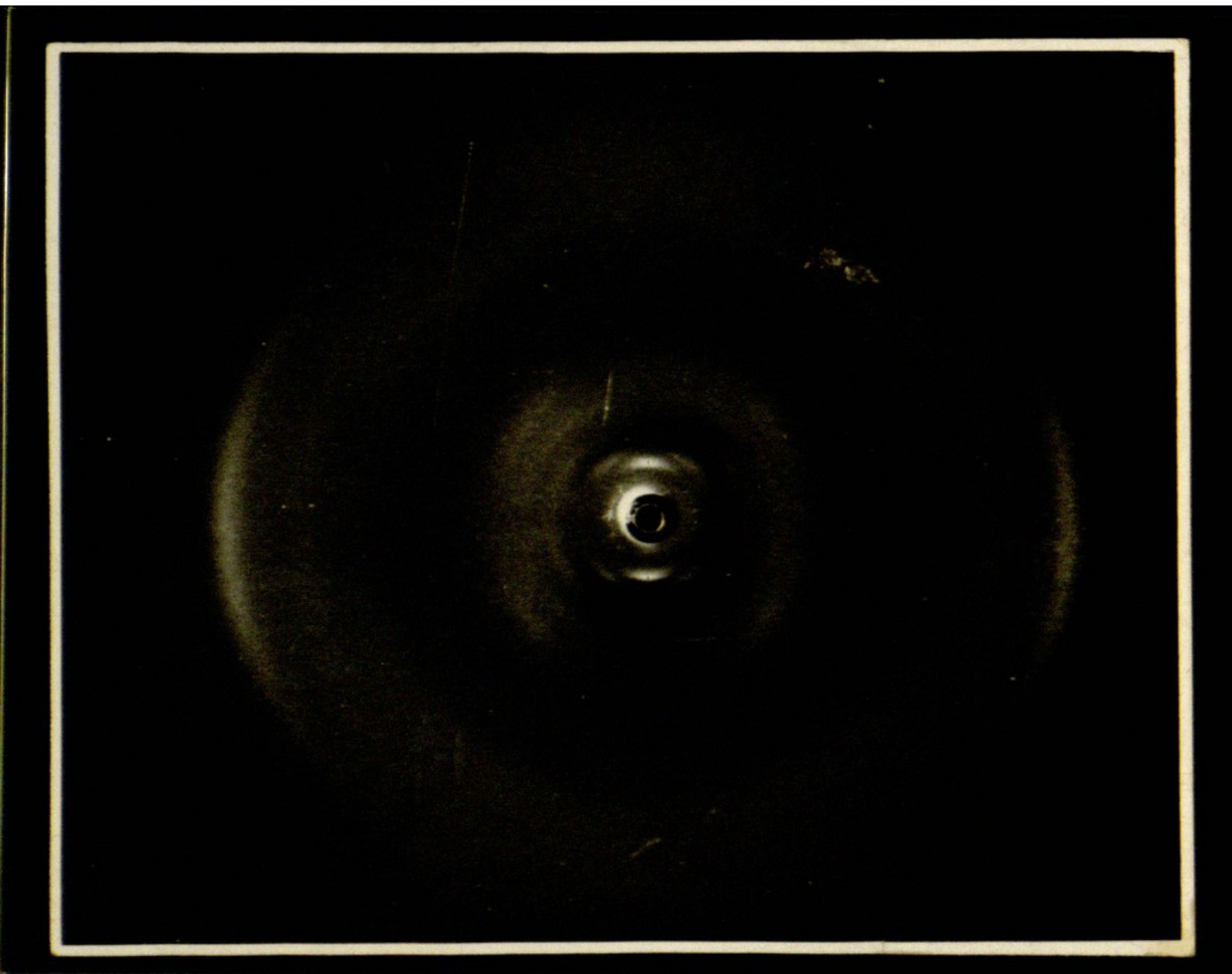










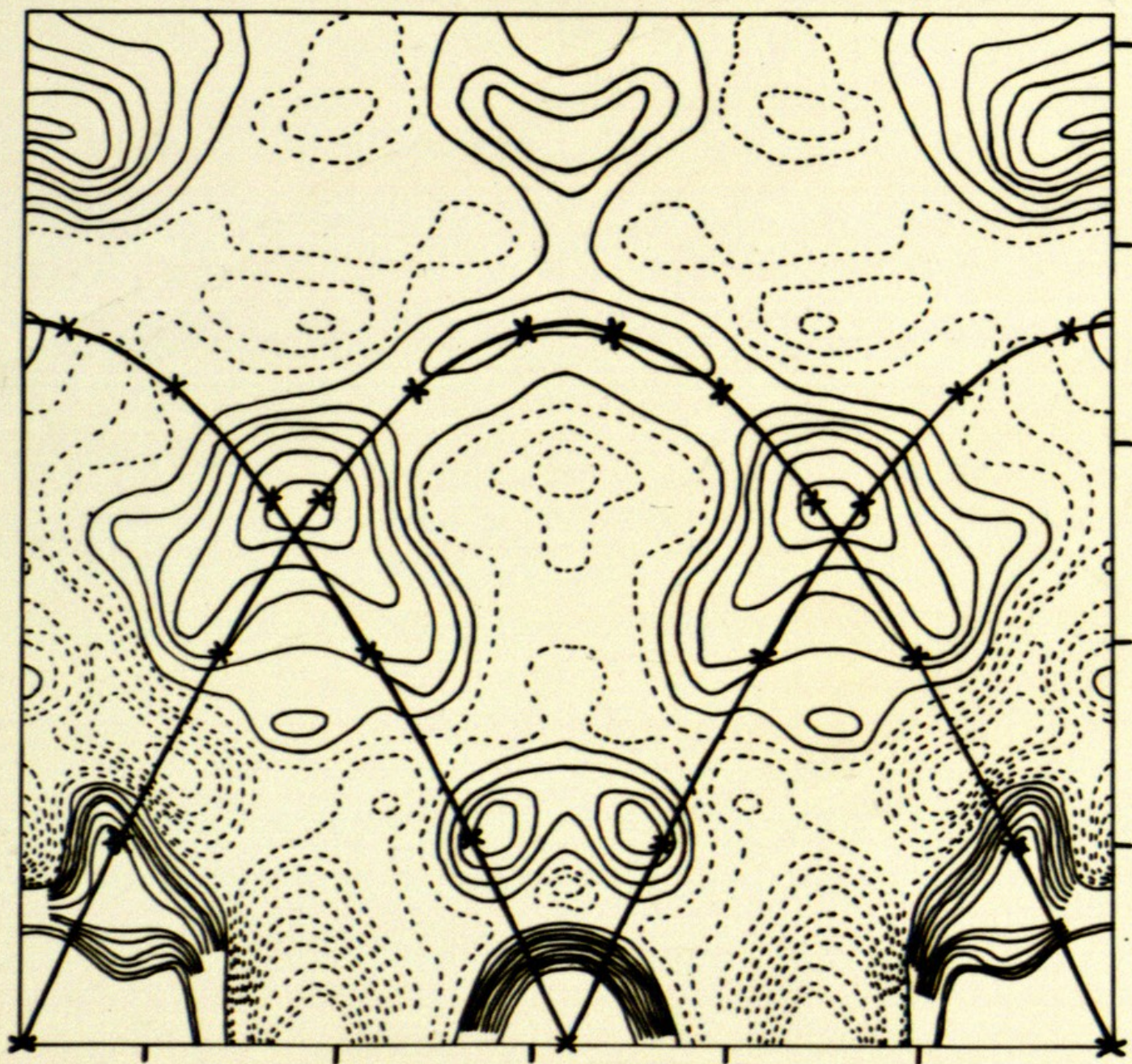


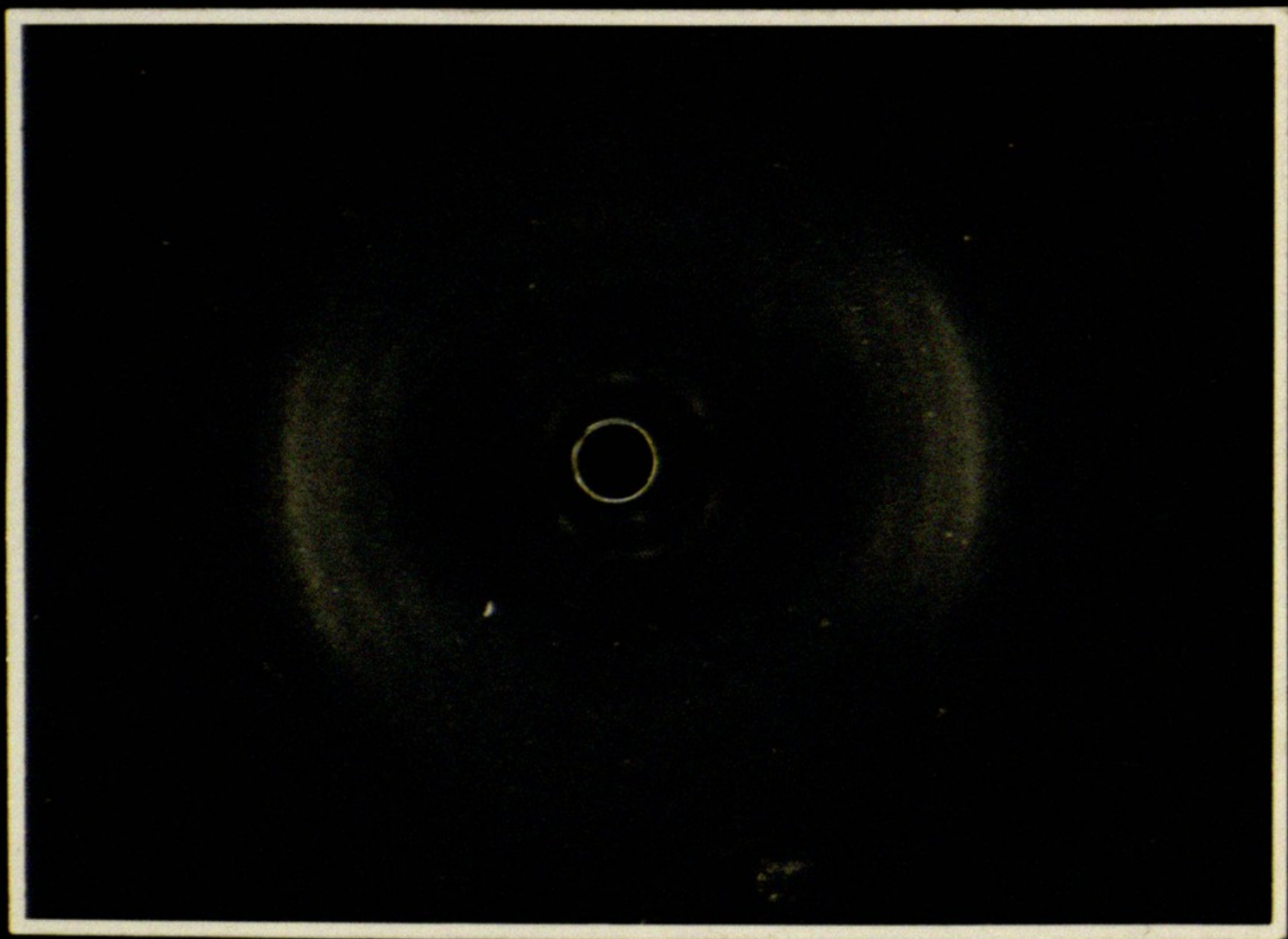
$$\begin{array}{r} 75 \\ 14 \end{array} \quad 5.3$$

$$\begin{array}{r} 65 \\ 13 \end{array} \quad \text{Thyph} \quad 5.0$$

Loligo Ne







Fibres of human Na DNA and nucleoprotein examined in polarized light

JC White & PC Elmes Nature 169 151 (Jan 26) 1952

by drying solⁿ in ~~the~~ Mon 2M NaCl solⁿ fine oriented fibres
occur in NaCl xtal. -ve birefringence

Solⁿ of ~~TDH~~ in NaCl in MeOH

→ fibres -ve at first but changing to +ve on prolonged

drying in MeOH

- reversible, → -ve immediately in wet atmosphere

Dyeing of nucleoprotein fibres

various dyes.

→ anomalous dispersion

ACTA CRYSTALLOGRAPHICA

FROM THE BRITISH CO-EDITOR AND TECHNICAL EDITOR

R. C. EVANS

CRYSTALLOGRAPHIC LABORATORY, CAVENDISH LABORATORY, CAMBRIDGE, ENGLAND

Telephone: CAMBRIDGE 55478

Telegrams: CRYSTALS, CAMBRIDGE, ENGLAND

In reply please quote 1043

22 July 1953

Dear Miss Franklin,

One or two small points about the proofs which you have just returned:-

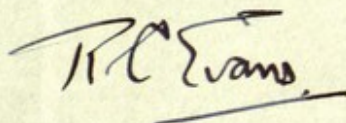
1. In the reference to the COLD SPRING HARBOUR SYMPOSIUM, the printer has queried the word 'quant'. We like to give such titles in full, and I should be glad to know what this abbreviation stands for.

2. In the short footnote which you wish to add, you refer to NATURE Volume 171 Pages 737 and 740. Will you please give me full details of these two references with the authors' names?

3. In the text you give the reference Clapp 1937, but in the bibliography as Clapp 1947. Will you please let me know which is right?

As soon as I have this information the proofs can go to press.

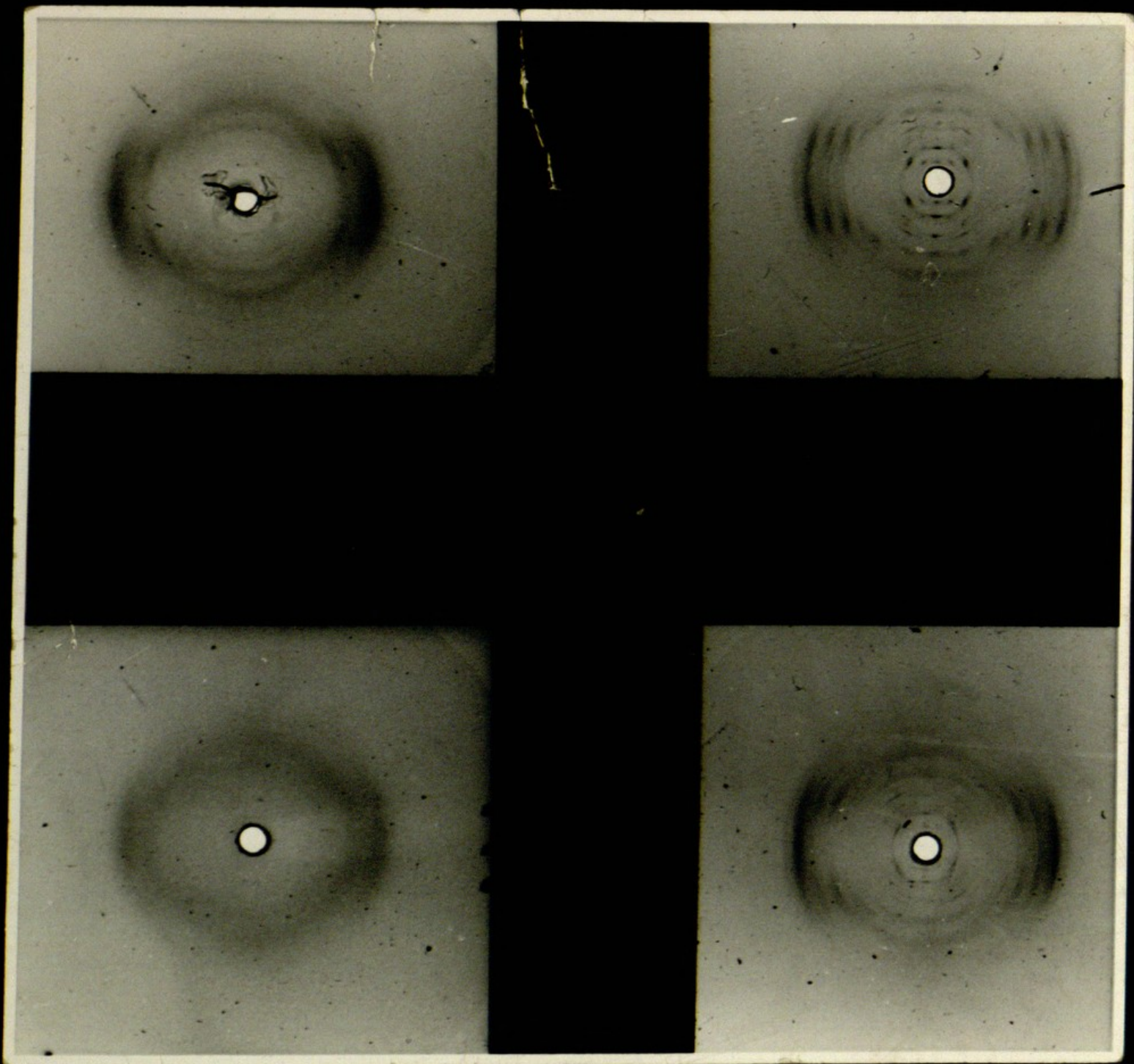
Yours sincerely,

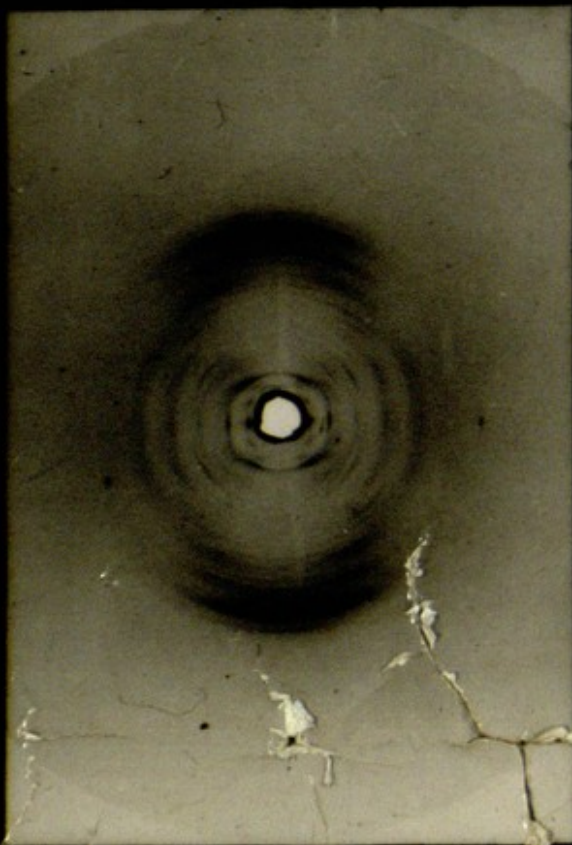
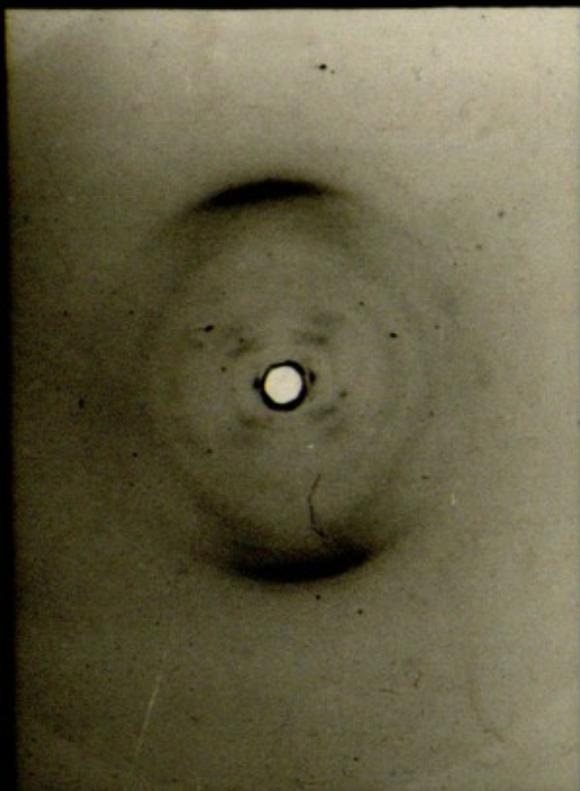
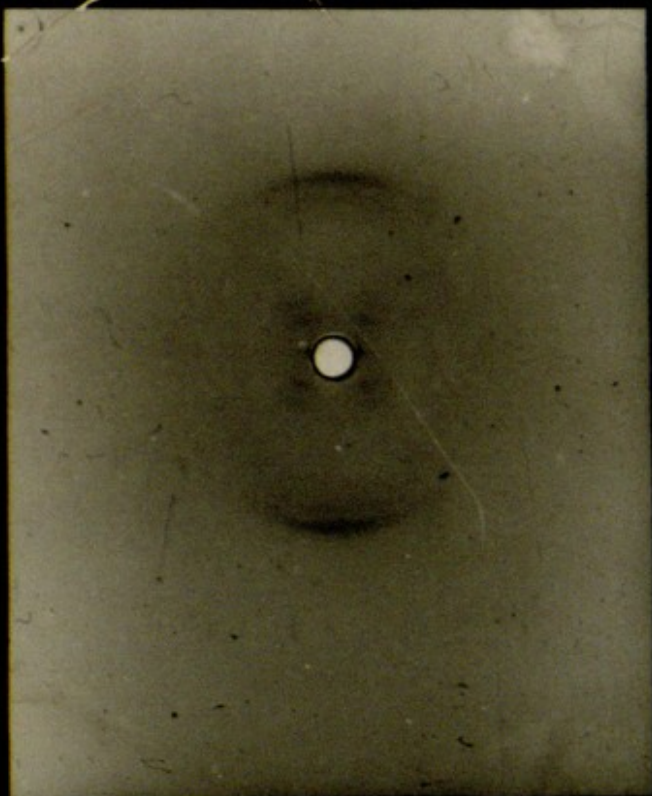


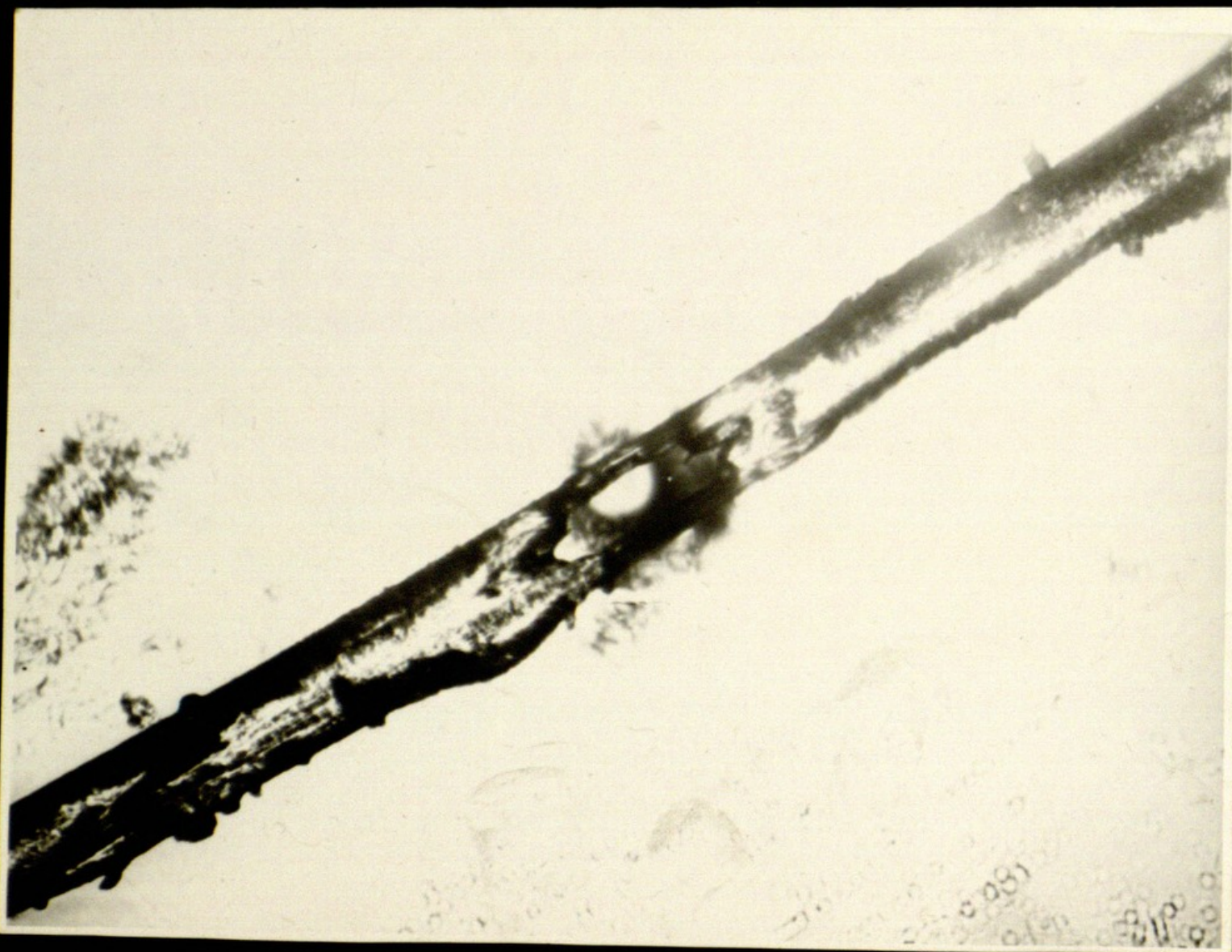
Miss R.E. Franklin,
Birbeck College,
Malet Street,
LONDON. W.C.1.

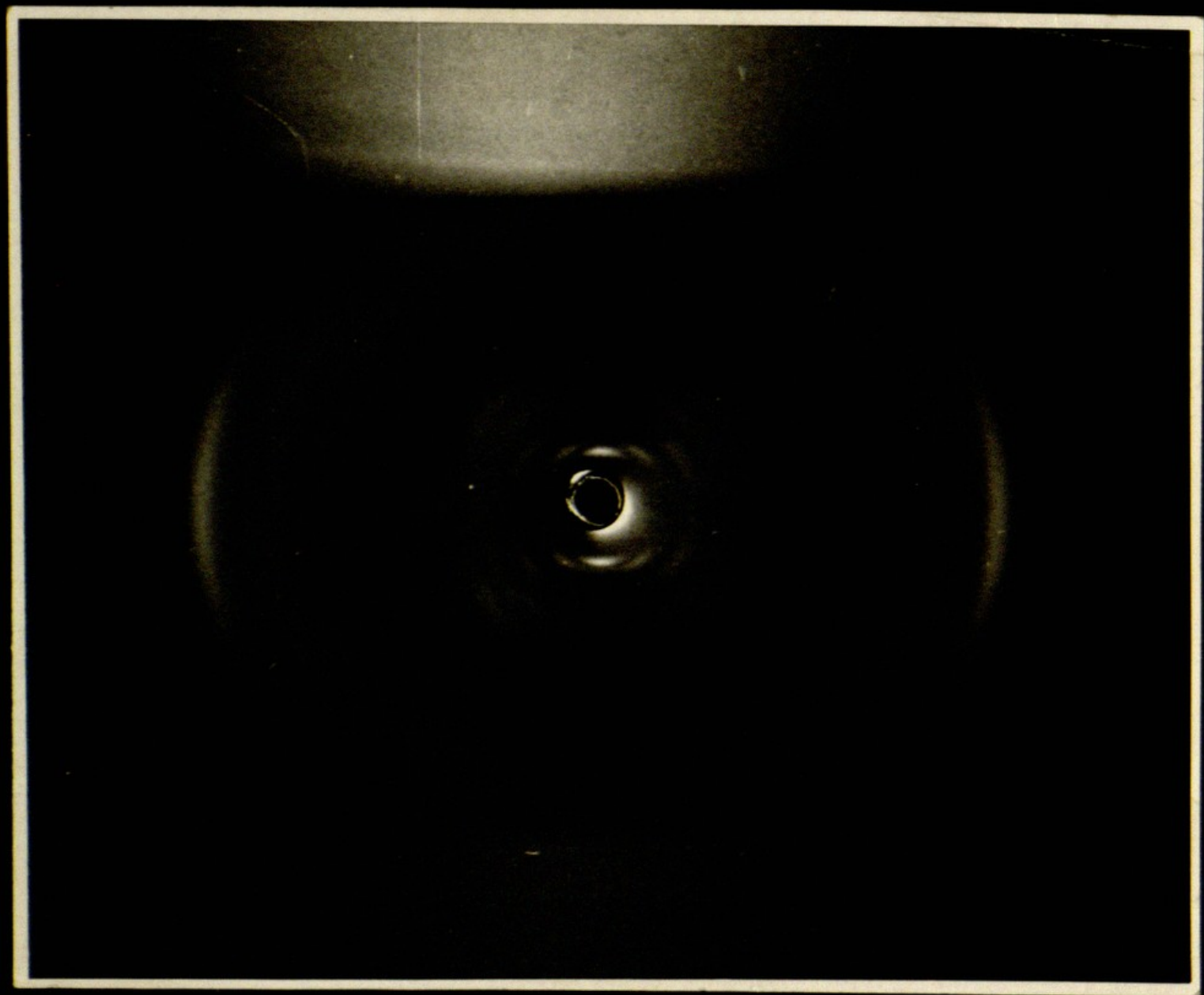






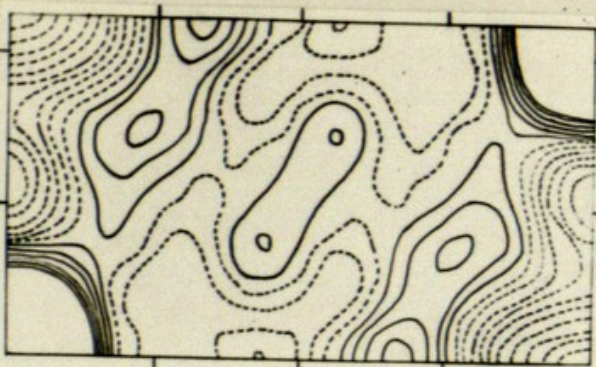




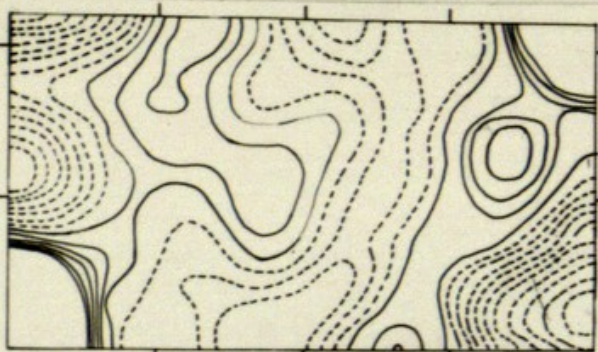


X³

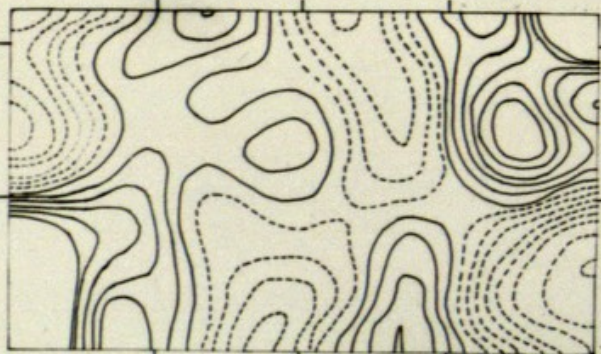
0



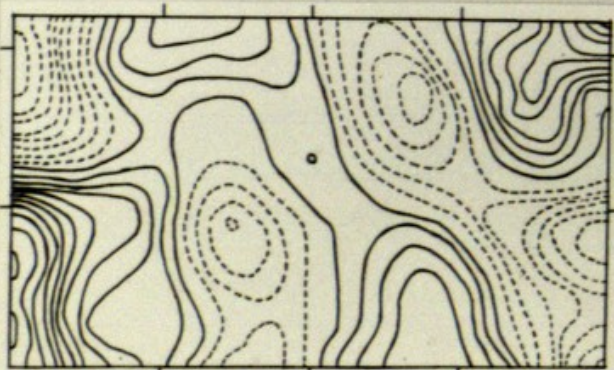
1



2



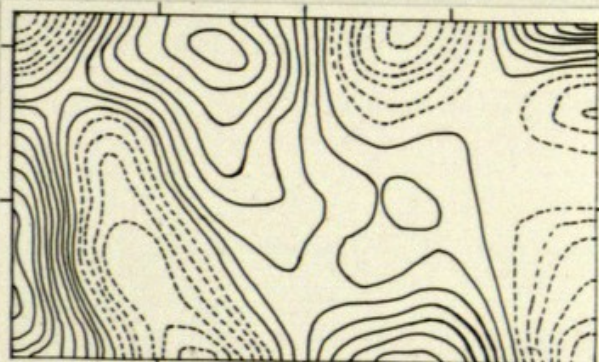
3



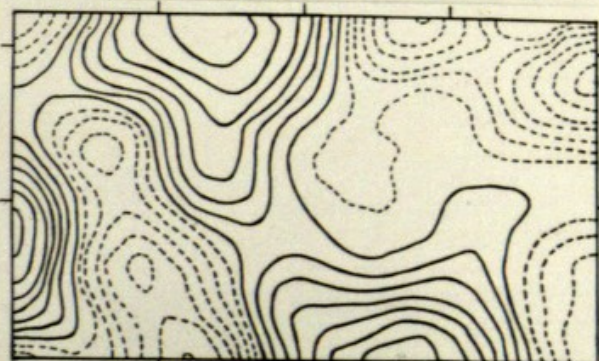
4



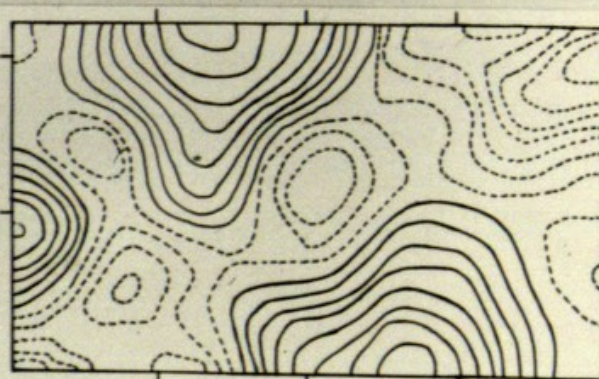
5



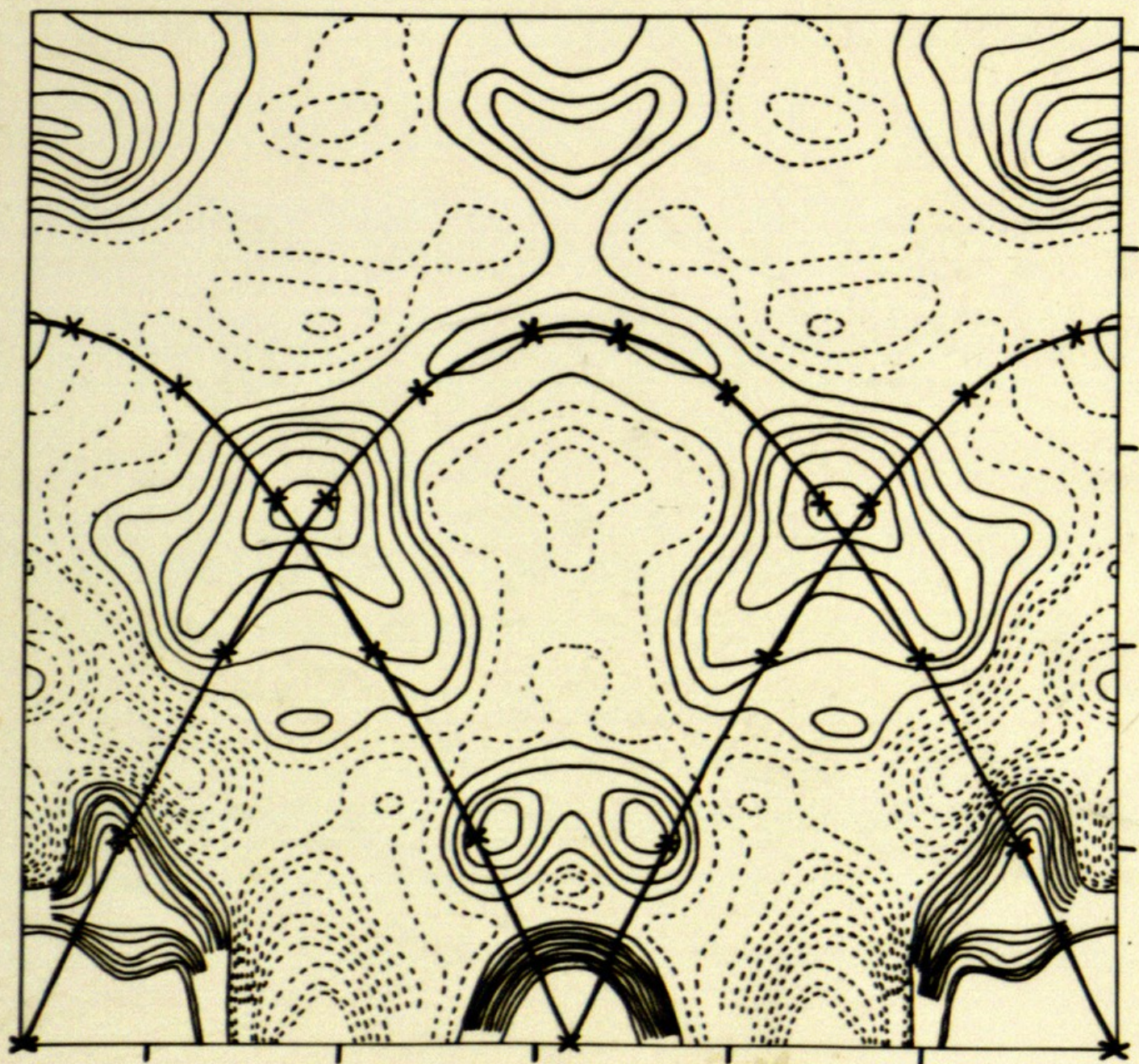
6



7



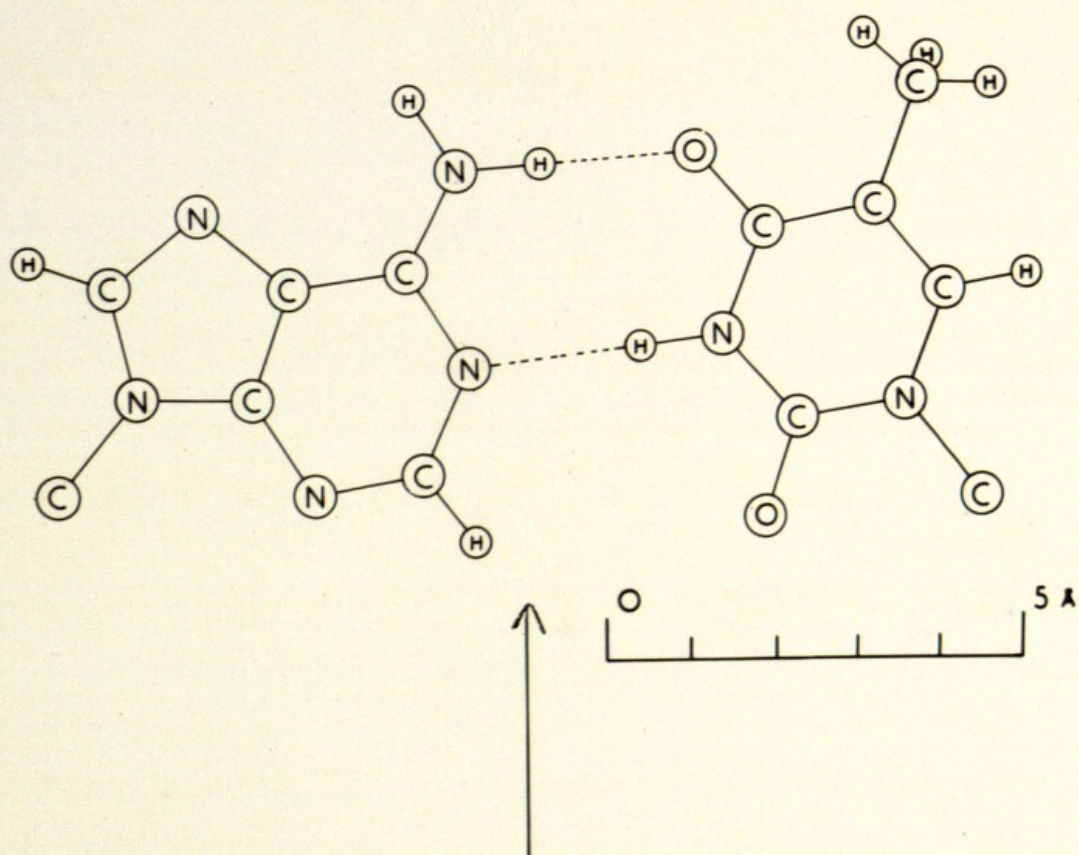
Q 873



ADENINE

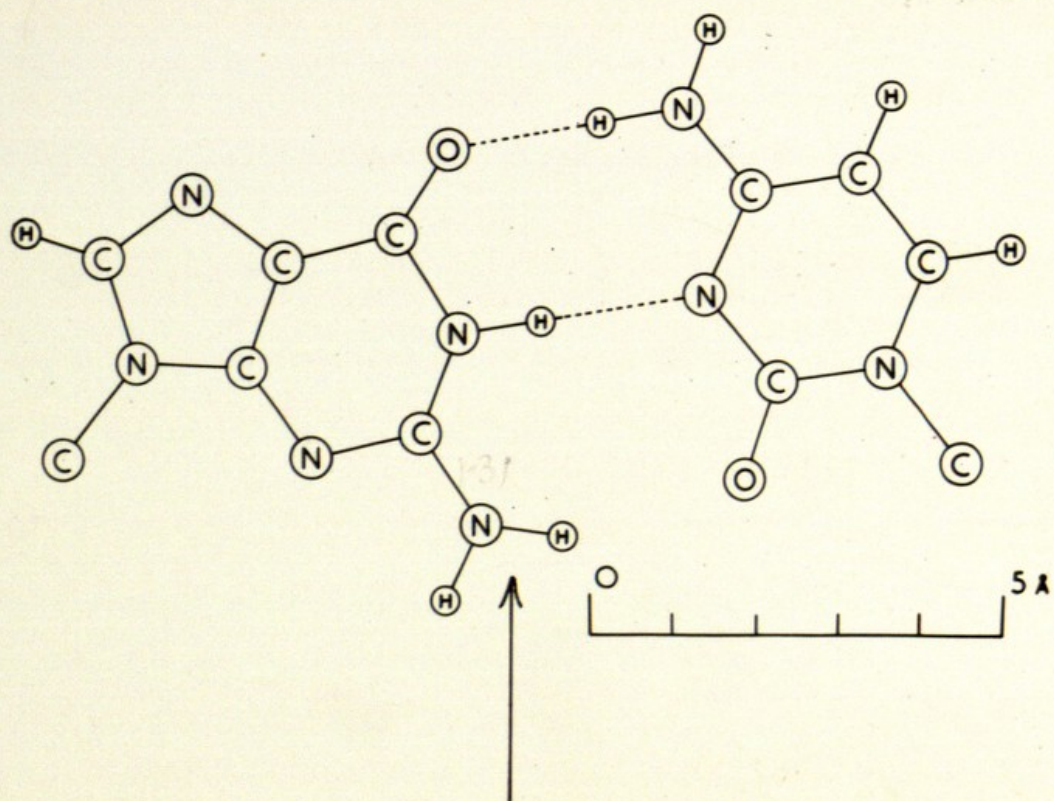
°

THYMINE

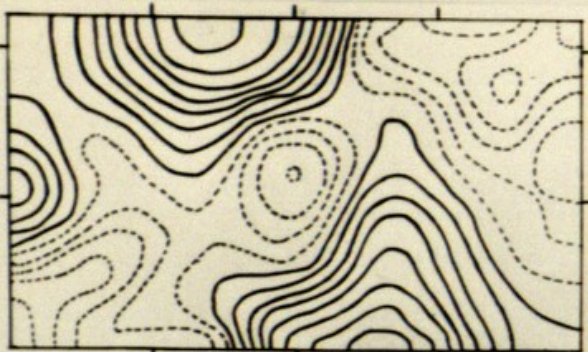


GUANINE

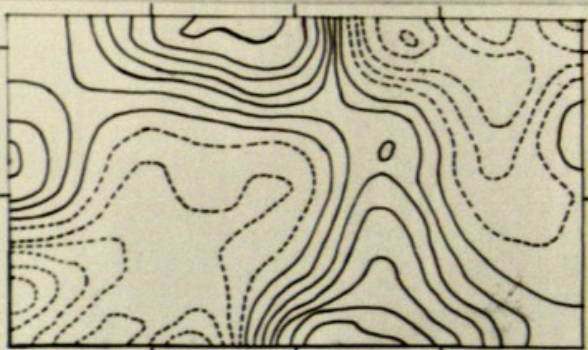
CYTOSINE



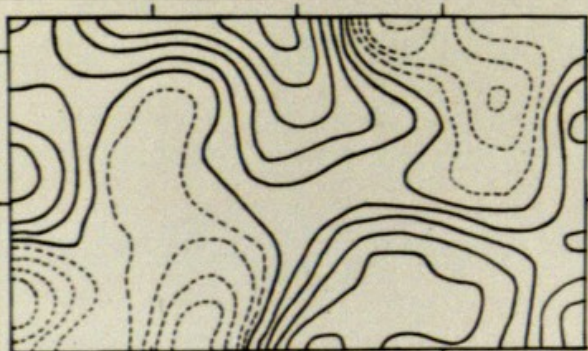
8



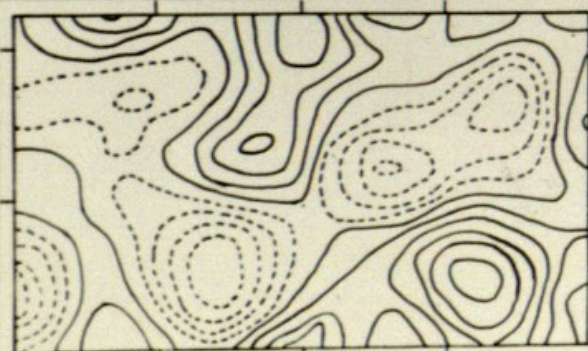
9



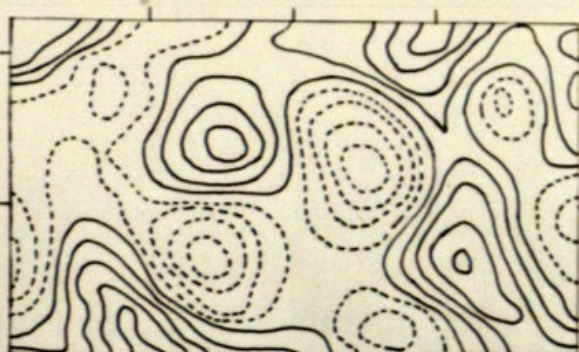
10



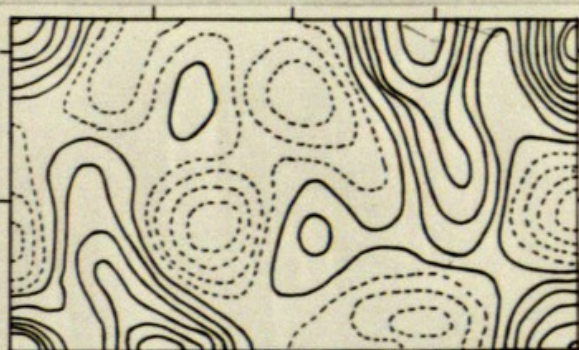
11



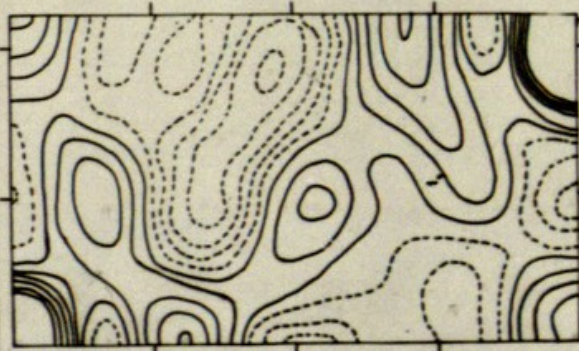
12



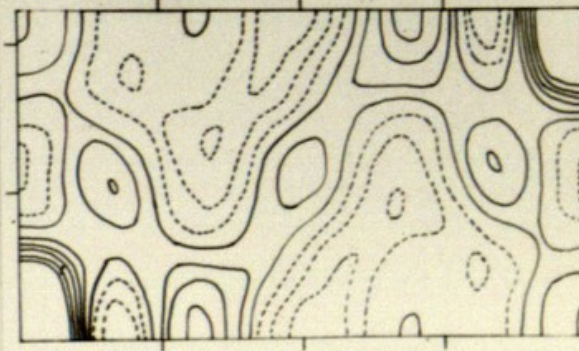
13



14



15



Q 874

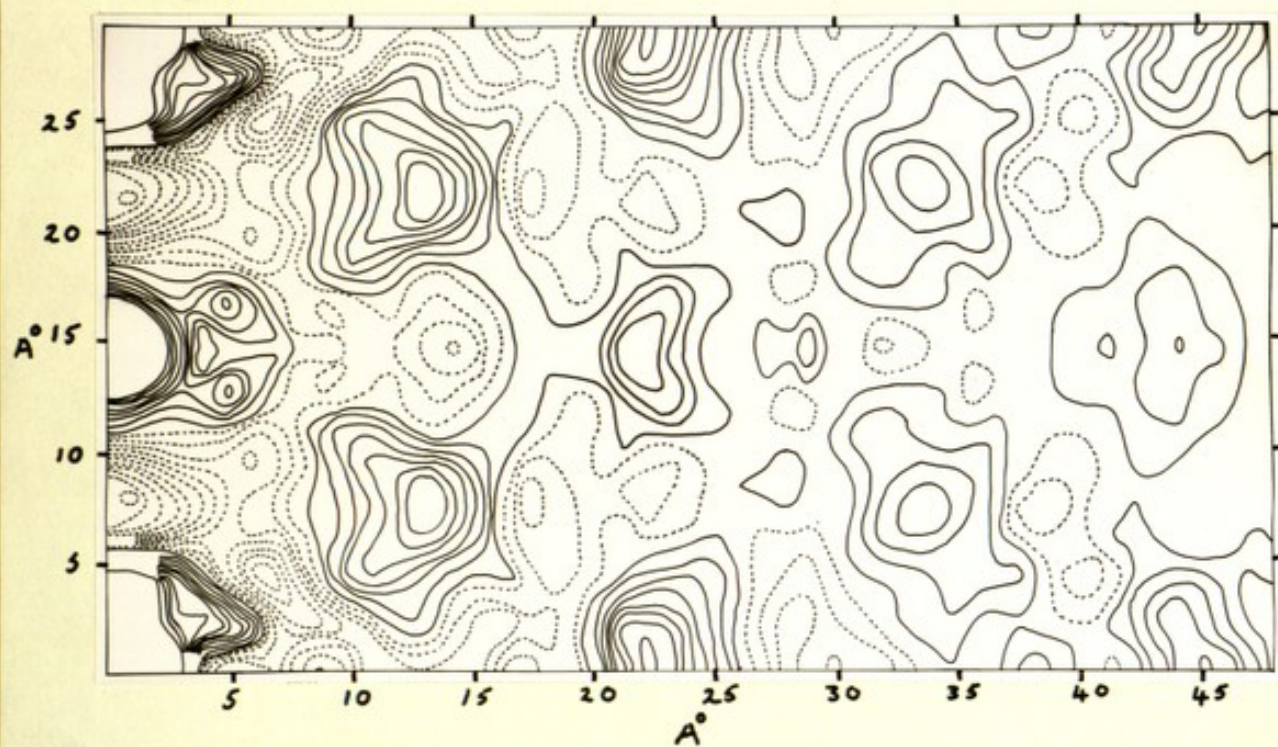


Fig 3

UNIVERSITÉ DE BORDEAUX

FACULTÉ DES SCIENCES

LABORATOIRE DE MINÉRALOGIE

20, Cours Pasteur

BORDEAUX

BORDEAUX, le 3 février 1953

Mademoiselle

Veuillez m'excuser de ne pas vous avoir répondu par retour de courrier ; les mémoires que vous me demandiez, faisant partie de l'Archiv original du CNRS, ne se trouvant qu'en microfilm et j'ai dû me les procurer pour vous les envoyer.

J'espère que le premier mémoire (Clastre, Garrido, Gay) pourra vous être utile à quelque chose ; en vérité je crains que cela ne vous serve pas beaucoup. Voici pourquoi :

il s'agit ^{de ce mémoire} ~~ici~~ du traitement d'un Patterson ponctuel (Patterson d'une structure d'atomes ponctuels). dans ce cas le résultat est immédiat, et la méthode des superpositions est une excellente chose. pour cette raison, la méthode est excellente quand il y a un atome lourd dans une molécule organique compliquée : la localisation de l'atome lourd est immédiate.

encore faut-il que les pics du Patterson des positions de l'atome lourd (considéré isolément) ne soient pas trop en "amas de pics" - si ces amas sont trop serrés il sera impossible de ~~de~~ individualiser les pics qui les composent. Parqu'il n'y a pas d'atomes lourds, dès que la structure est un peu compliquée, il est difficile d'analyser le Patterson, c'est à dire de le décomposer en pics individuels dont la Σ reconstitue le Patterson. Si la "ponctualisation" du Patterson ne peut être faite, la méthode ne doit pas être employée.

je vous signale cependant que je cherche à développer des méthodes susceptibles de conduire à une ponctualisation du Patterson même dans le cas de molécules organiques un peu compliquées. J'ai ainsi retrouvé la structure de l'isatine (déterminée par Cherdron et Goldschmidt) et ~~je~~ j'essaie d'appliquer les mêmes procédés pour établir la structure de l'antipyrine. Pour cela j'utilise la Transformée de Fourier des $\frac{|F|^2}{f^2}$ beaucoup plus claire, et même avec un certain succès (que je n'arrive pas à expliquer mathématiquement) la T. F. de $|F|$ ou de $\frac{|F|}{f}$: cela donne (je ne sais pas exactement) un "Patterson" très détaillé beaucoup plus détaillé que le vrai Patterson. Les pics s'y trouvent à très peu près aux mêmes endroits que dans le vrai Patterson (ceci a été vérifié sur de nombreux Pattersons de structures déjà ~~déterminées~~ connues : il semble qu'il suffise que les signes de \vec{F} soient suffisamment diversifiés.)

cela signifie que la Transformée des "Signes" de Facteurs de structures (en remplaçant les Facteurs de structure vrais par les valeurs +1 ou -1 suivant leur signe) est une fonction qui présente des maximums positifs aux mêmes points (à très peu près) que les centres atomiques : c'est un résultat surprenant mais que j'ai également vérifié sur quelques structures déjà connues.

J'utilise aussi des "reliefs" du Patterson (à la manière de G. von Eller) en dérivant le Patterson, c'est à dire en calculant la Transformée de Fourier des $h|F_{hkl}|^2$ de $k|F_{hkl}|^2$ de $l|F_{hkl}|^2$: cela permet de déceler sur le Patterson des accidents secondaires (ruptures de pente etc...) que le Patterson ne montre pas clairement.

Tout ceci en vue d'obtenir une connaissance (bien plus parfaite que celle dont on se contente d'habitude) de la fonction de Patterson. ce n'est qu'à ce moment que j'essaie de ponctualiser. et même encore, il faut faire état de nos connaissances chimiques : existence de chaîne, noyau benzénique pyrimidiques ou autres.

Tout ceci est bien compliqué, mais apporte des résultats au moins partiels sur la connaissance de la structure, qui peuvent compléter ceux qui appartiennent d'autre part la méthode de Harker Kasper, Karle et Hauptmann, Sayre et Cochran.

Veuillez m'excuser d'un si copieux laïus, peut être vous sera-t-il utile à quelque chose et croyez à mon meilleur souvenir

R. Gay

THE STRUCTURE OF SODIUM THYMONUCLEATE FIBRES

II. THE CYLINDRICALLY SYMMETRICAL PATTERSON FUNCTION

Rosalind E. Franklin and R. G. Gosling

Wheatstone Physics Laboratory
King's College London

SUMMARY

The positions and maximum photographic intensities of reflections have been measured on X-ray microphotographs of highly crystalline sodium thymonucleate fibres. A procedure is described for deducing from these measurements the integrated intensities of the reflections. These have been used to calculate the cylindrically symmetrical Patterson function. From this Patterson function it was possible to obtain the unit cell and hence to allot indices to all the 66 observed reflections. Confirmation of the correctness of the indexing was obtained from photographs of a single fibre which showed double orientation of the crystallites.

INTRODUCTION

In the preceding paper it was shown that by varying the water content of highly orientated fibres of sodium de-oxy-ribonucleate (NaDNA) different structural modifications could be obtained. The most highly ordered structure was that obtained when operating at about 75% R.H. (structure A). This has therefore been selected for a systematic quantitative study.

The fibre diagram of this crystalline structure (Franklin and Gosling, 1953, Plate I) shows 66 independent reflections distributed on nine well-defined layer-lines. During the course of attempts to index the reflections it became fairly clear that the unit cell was monoclinic c-face-centred, with the c-axis parallel to the fibre axis. However, owing to the inevitable errors of measurement, and to the ambiguities of indexing reflections at large angles of diffraction, it was not found possible, by direct inspection, to establish all the cell parameters with certainty. It was therefore decided to calculate the cylindrically symmetrical Patterson function described by MacGillavry and Bruins (1948). This function contains all the information which can be obtained from the fibre diagram without allotting to the reflections any indices other than their layer-line numbers, and is therefore periodic in the c-direction only. It is the function which would result from taking the true three-dimensional Patterson function, giving it cylindrical symmetry

2.
by rotating it about an axis through the origin and parallel to the fibre axis, and then taking a section through the axis of rotation.

The principal periodicities, or lattice translations, other than that corresponding to the layer-plane spacing, will be revealed as important peaks in this aperiodic Patterson function. They will, in general, be distinguished from other Patterson peaks in that their second (and higher) orders will be observed.

MacGillavry and Bruins (1948) have shown that the cylindrically symmetrical Patterson function $\phi(z, x)$ is given by the equations

$$\phi_l(x) = 2\pi/NV \int_0^\infty H(l, \xi') J_0(2\pi \xi' x) \xi' d\xi' \quad (1)$$

and
$$\phi(z, x) = \sum_l \phi_l(x) \cos 2\pi l z$$

(2)

Here $\xi' = \xi/\lambda$, where ξ is the

Bernal coordinate. x and λ is the wavelength of the incident radiation.

$H(l, \xi')$ is the intensity on the l th layer-line at a distance ξ' from the fibre axis in R-space.

$J_0(u)$ is the zero order Bessel function of u .

V is the volume irradiated
and N is the total number of periods in the fibre direction.

* MacGillavry and Bruins refer to ξ' (their ξ .) as the Bernal coordinate, but we have preferred to use Bernal's original notation in the discussion which follows, and so have introduced it here.

If each layer-line shows only discrete reflections whose integrated intensities can be measured, the integral in equation

→ (1) may be replaced by a summation, and

$$\phi'_l(x) = \sum_{\xi'} I(l, \xi') J_0(2\pi \xi' x). \quad (3)$$

where $I(l, \xi')$ is the integrated intensity of a reflection occurring on the l th layer-line at a distance ξ' from the fibre axis,

and

$$\phi'_l(x) = NV \cdot \phi_l(x).$$

EXPERIMENTAL

Measurements were made on photographs taken with a specimen-film distance of 15 mm. using the Phillips micro-camera and an Ehrenberg-Spear fine-focus tube as described in the preceding paper. A constant stream of hydrogen at 75% relative humidity was passed through the camera during the exposures.

In order to search for further reflections on or near the fibre-axis direction, photographs were also taken with the fibre inclined to the X-ray beam at a series of angles in the range 85° to 70° . A micro-camera was designed specifically for this purpose and will be described elsewhere. The specimen-film distance and collimator dimensions were the same as those of the Phillips micro-camera.

These photographs revealed only one reflection not observed with the fibre perpendicular to the X-ray beam. This reflection lies on the 11th layer-line on, or close to, the fibre-axis direction. It is, however, a weak reflection and in the quantitative work described here its intensity,

when corrected for geometrical factors, is negligibly small.

For the measurement of the R-space co-ordinates and the intensities of the 66 independent reflections standard methods could not be applied owing to the small size of the photographs, and to the variety of shapes and sizes of the photographic spots. A description of the methods used is given below.

Measurement of R-space co-ordinates

For the measurement of the positions of reflections the microphotographs were projected on a white cardboard screen using a magnification of about 10. The centres of the reflections were then marked on the card and their x and y co-ordinates measured. For the outer reflections an indication of the length of the arcs was also recorded. The use of the projector rather than a travelling microscope was found not only to be much less fatiguing, but also to provide a more reliable estimate of the positions of weak reflections and a more convenient method of making measurements on curved^{ed} layer-lines.

For calibration of the scale of the projected photographs, photographs taken with a Unicam single-crystal camera were used. In this way, the very strong equatorial reflection was shown to correspond to a spacing of 11.3Å. Using this value, the appropriate demagnification factor for converting the measured x and y co-ordinates to the scale of a Bernal chart was calculated, and hence the ξ and ζ values of each reflection were obtained.

Correction for tilting of the fibre axis

A correction must be applied to the measured ξ and ζ values owing to the fact that it is almost impossible to place the fibre

exactly perpendicular to the X-ray beam.

Fig. 1 (a) illustrates the diffraction conditions when the fibre-axis deviates from the ideal position by a small angle γ . A plane parallel to the layer-lines and at a distance from the R-space origin 0 given by $\zeta_s = \sin \gamma$ will give a straight line l_s on the flat film. Layer planes above ζ_s will form layer lines which are less curved and have reflections more widely separated than if the fibre were normal to the direct beam. Layer planes lying below ζ_s will form layer-lines more highly curved having reflections closer to the meridian. The general form of the layer lines will be as indicated in Fig. 1 (b).

Let ζ_1 and ζ_2 be the apparent ζ -values measured above and below the equator respectively for a given set of reflections corresponding to a spacing $d = \lambda/\rho$. It can be shown that the required value of ζ for the perpendicular fibre is given by

$$\zeta = \zeta_1 \cos \gamma + \frac{1}{2} \rho^2 \sin \gamma = \zeta_2 \cos \gamma - \frac{1}{2} \rho^2 \sin \gamma \quad (4)$$

whence

$$\tan \gamma = (\zeta_2 - \zeta_1) / \rho^2 \quad (5)$$

and

$$\zeta = \cos \gamma \cdot (\zeta_2 + \zeta_1) / 2 \quad (6)$$

Measurements of ζ_1 , ζ_2 and ρ can therefore be used to determine γ .

Most of our measurements were made on photographs for which γ was found to be about 8° . Values of ζ obtained with the aid of equations (4) and (5) from measurements made on reflections in the first 9 layer-lines are shown in Table 1. Each value is a mean of measurements on at least 3 reflections. Neglecting the value obtained for the 3rd layer-

line, where the reflections are weak and difficult to measure accurately, the mean value of γ is 0.0547. This gives c , the fibre-axis repeat period, as 28.1A.

TABLE I

L :	1	2	3	4	5	6	7	8	9
γ :	.0550	.0540	.0533	.0545	.0552	.0548	.0545	.0546	.0551

Having established in this way the layer-line spacing, values of ξ can now be obtained with improved accuracy for reflections on the higher layer-lines. For these, the most accurately observable parameter is the radius of the circle on which the four equivalent photographic spots must lie. This gives $\rho (= \lambda/d)$, and ξ -values were therefore determined from the relationship

$$\xi^2 = \rho^2 - \left(\frac{\lambda}{c}\right)^2$$

Measurement of intensities

The variety of shapes and sizes of the photographic spots makes it impossible to estimate directly the integrated photographic intensity. It is necessary therefore either to explore each spot photometrically, or to estimate its maximum intensity and to consider separately the question of spot size and shape. The latter alternative was adopted. Not only would the photometric method involve a very large amount of work, but, in the micro-photographs available, the grain-size is too large in relation to the spot-size for photometry to be applied with any degree of accuracy. Use of fine-grain films would lead to excessive exposure times and thus remove the advantage gained from the use of the micro-technique.

The maximum intensity of each spot was estimated visually by comparison with a standard scale. For the preparation of this scale the ultra-fine collimating system of a low-angle camera * (slit width 8μ) was used to photograph the direct beam, with exposure times varying from 3 to 90 seconds. A set of streaks of width comparable with that of the spots on the micro-photographs was obtained. The fibre-photograph was projected, as for the measurement of the positions of reflections, and the scale displaced by hand across the photograph in the projector. The standard streaks were placed as close as possible to the spot whose intensity was being measured in order to eliminate, as far as possible, the effect of varying intensity of the background.

We must now consider how the measured values of photographic maximum intensity are related to the R-space integrated intensities of reflections. The relationship will depend on the following factors:-

(i) True diffraction breadth The breadth of the reflections, measured along a line joining the reflection to the origin, is approximately constant over the whole photograph. It may therefore be assumed that the true diffraction breadth is everywhere small compared with the geometrical broadening (direct beam size) and can be neglected.

(ii) Spread of reflections in R-space due to disorientation of the crystallites

(a) If the crystallites are perfectly aligned with respect to the fibre axis but in random orientation about this axis, each reflection will be spread over a circle of radius $\frac{g}{\lambda}$. Maximum intensities must therefore

be multiplied by

in order

* Designed by K.P. Norris.

8.

be multiplied by ξ/λ in order to relate them to integrated intensities. (This accounts for the factor $2\pi\xi' = 2\pi\xi/\lambda$ which occurs in Equation (1) but not in Equation (3)).

(b) Imperfect alignment of the crystallites with respect to the fibre axis results in a small angular spread, ϕ , (fig. 2) of each reflection along an arc of a circle with centre at the origin and the fibre axis as diameter. The length of this arc in R-space is equal to $S\phi$, where S is its distance from the origin. The R-space maximum intensity must therefore be multiplied by S to relate it to the integrated intensity.

(iii) Geometrical factors involved
in the transfer of R-space effects to the photographic film

We have seen that each reflection will be spread, in R-space, over a small volume of circular symmetry with mean radius ξ/λ , and axis on the fibre axis. An axial section of this volume (Fig. 2) shows two elements each of area $ds \cdot dl$ where ds is the true diffraction breadth of the reflection and dl , the length of the arc resulting from disorientation of the crystallites with respect to the fibre axis. We must now consider the effect on the photographic maximum intensity of the oblique intersection of ds and dl with the reflecting sphere.

When a reflection intersects the reflecting sphere obliquely two extreme effects are possible.

(a) If the diffraction breadth is much less than the geometrical breadth then the photographic spot-size is independent of the diffraction breadth, and oblique intersection leads only to increased photographic intensity. This is normally true in single-crystal work and is corrected for in the Lorentz factor.

(b) If the diffraction breadth is much greater than the geometrical breadth then oblique intersection with the reflecting sphere leads to increased spot breadth on the film but does not influence the maximum intensity.

In the present case we have seen that (a) is true for the dimension ds . Since ds makes an angle θ with the surface of the reflecting sphere, the observed maximum intensity must be multiplied by $\cos \theta$ to relate it

to the integrated intensity.

In general, the effect of oblique intersection of dl with the reflecting sphere is important for all reflections which occur at a large angular displacement from the equator. However, in the present work it happens that all such reflections occur at diffraction angles large enough for the length of the photographic arcs to be much greater than the geometrical broadening (direct beam size). Oblique intersection of dl and the reflecting sphere is therefore without effect on the maximum intensity for these reflections (see (iii) (b) above) and no special correction is required.

For reflections at small diffraction angles and small angular displacement from the equator, the influence, on the photographic maximum intensity of the geometrical broadening in the direction of dl is important. dl is given by $s\phi$ where ϕ is the angular spread due to disorientation. To obtain ϕ a visual estimate was made of the $\frac{1}{2}$ -peak length of the arcs for equatorial reflections at large θ . (Since the value of the correction to be applied is in any case small, this method of estimation was considered adequate).

This value of ϕ was then used to obtain the R-space lengths, dl , of arcs occurring at small θ . The lengths dl' of the photographic arcs for reflections at small θ were then obtained, from the dl values and the known diameter of the direct beam (by the method of Jones (1938)). If the effect of oblique intersection be neglected, the ratio of the R-space maximum intensity to the photographic maximum intensity is given by dl'/dl . The measured maximum intensity values must therefore be multiplied by this factor.

It is shown below that any error introduced by neglecting the obliquity correction for the reflections at small θ has little effect on the resulting Patterson function.

We are now in a position to list all the corrections which must be applied to the observed maximum intensity values. They are as follows:

1. Multiply by S/λ (see (ii) a above)
2. Multiply by $\cos \theta$ (see (iii) a above)
3. Multiply by s (see (ii) b above)

4. For reflections at small θ , multiply by d_1'/d_1
5. Multiply by the polarisation factor $(1 - \cos 2\theta)/2$ ²/_{1 + cos 2 θ} .
6. Correction for the influence of the angle of incidence of the diffracted X-rays on the film (Cox and Shaw, 1930).
7. Correction for variation of specimen-film distance with θ for a flat film.
8. Absorption correction

Correction 8. was negligible throughout. Moreover, in the range of θ used in this study, corrections 2, 5, 6 and 7 taken together never exceed 10%, which is well within the limit of experimental error of our intensity measurements. Only corrections 1, 3 and 4 were therefore used.

For the complete set of intensity measurements 12 films were used. These were obtained from two exposures on each of two different specimens, using three films for each exposure. The total range of intensities measured in this way was from 1 to 96, and agreement obtained between different sets of measurements was better than 20% for all except a few of the weakest reflections. Some slight further error may have been introduced by the approximations involved in obtaining integrated from maximum intensities, but such error will vary only smoothly and slowly with s and will not, therefore, have a major influence on the main features of the Patterson diagram.

Artificial temperature factor

Since the corrected intensities showed little, if any, tendency to decrease with increasing θ an "artificial temperature factor" was applied. Intensities were multiplied by $e^{-a^2 s^2}$ where $a = 0.456$, a value chosen to reduce to 0.3 of its value the intensity of the furthest equatorial reflection observed.

Calculation of the cylindrical Patterson function

Values of $J_0(u)$ were available only for values of u up to 40 (Brit. Asso. 1937, Clapp, 1937). In order to cover the desired range of $2\pi s'x$ in the present work, values of $J_0(u)$ for u up to 76 were required. These were calculated from the approximation formula $J_0(u) = \frac{\sin u + \cos u}{\sqrt{\pi u}}$.

The results obtained are tabulated in the Appendix.

Values of the corrected intensities, $\bar{I}(\ell, \xi')$, were then assembled for each layer-line, ℓ , and the summations of equation (3) were carried out at intervals of 1A in x in the range $x=0$ to 50A. For each value of x , the required Patterson function is then given as a function of z by the cosine series of equation (2).

RESULTS

The resulting cylindrically symmetrical Patterson function is shown in Fig. 3.

Before seeking in any way to interpret this function it seemed desirable to have some idea of the extent to which it might be influenced by possible errors in the intensity measurements. The greatest possible source of error lies in the two strongest spots, those at 11.3A on the equator and at 12.4A on the 2nd layer-line. Each of these is clearly an unresolved doublet, a fact which was allowed for only by making a visual estimate of the breadth of the arc. Moreover, in the case of the 2nd layer-line doublet, no correction was made for oblique intersection with the reflecting sphere (see above) and the intensity value adopted was therefore somewhat too high. It was estimated that, for these reflections, the maximum possible error from all sources was about 30%. The Patterson function was therefore calculated for values of x up to 26A for these two doublets alone, and one-third of it subtracted from the function shown in Fig. 4. It is clear that the principal features of the function are substantially unaltered by this procedure, and that the effect of experimental error in intensity measurements is therefore not important.

The Patterson function shows a number of strong, well-defined peaks, and among these we must look for the lattice translations,

The first important region of high density occurs at $x=12-14$ A and $z=5-9$ A. However, it can readily be shown that it is impossible to index the equatorial reflections on the basis of a unit cell in which one parameter has an x -component of about 13A.

The peaks around $x=22$ A, $z=2$ A, and $x=40$ A, $z=0$ were next selected as possibly containing lattice vectors. These agreed well with the

$\frac{b}{a} \sin \beta$ ratio of 1.82 indicated by the application of a Bunn chart to the equatorial reflections, and led to the satisfactory indexing of all the

66 observed reflections on the basis of a face-centred monoclinic unit cell having the following parameters

$$a = 22.0\text{\AA}$$

$$b = 39.8\text{\AA}$$

$$c = 28.1\text{\AA}$$

$$\text{and } \beta = 96.5$$

Agreement between calculated and observed values of ξ was generally better than 1%, and in no case worse than 2%.

It was found that for the larger values of θ on the equator and the first and second layer-lines no reflection could be indexed unambiguously; reflections which should have been well-resolved and single were absent. This result is clearly not fortuitous. It seems to imply that the presence or absence of observable reflections in this region is not of great significance; single reflections are not strong enough to be distinguished from the rather strong diffuse background, and only where the geometry of the reciprocal lattice is such that two or more reflections reinforce one another can a photographic effect be observed. On this account the introduction of an "artificial temperature factor" mentioned above is more than usually important.

When all possible indices of the observed reflections are taken into account the total number of reflections is increased from 66 to 92.

Space group

Owing to the relatively small number of reflections observed, and to the ambiguity of indexing the reflections at large θ , systematic absences cannot be detected with certainty. However, since the asymmetric carbon atoms of the sugar rings preclude the existence of a plane of symmetry, C_2 is the only space-group possible.

Double orientation

A fortunate accident provided a rather satisfactory confirmation of the correctness of the indexing scheme. One fibre, of diameter about 40μ , was found to give a photograph showing strong double orientation. That is, the crystallites were not in random orientation about the fibre

axis, and gave, as a result, something intermediate between a rotation and an oscillation photograph. This photograph is shown in Plate I. It will be seen that many pairs of equivalent reflections in adjacent quadrants have markedly different intensities.

A list was drawn up in which those reflections which were strongest in the top left-hand quadrant of this photograph were labelled L and those strongest in the top right-hand quadrant were labelled R. It was then found that all reflections labelled L had been allotted indices $hk\ell$ whereas all R reflections had indices $hk\bar{\ell}$. The distribution of the observed reflections among the different quadrants in R-space as determined independently by the process of allotting indices is thus directly confirmed by comparison with the distribution revealed in this photograph.

It was thought that the double orientation shown in Plate I was probably due either to a mechanical accident to the fibre, or to preferential orientation of the crystallites which lie near the surface.

Two series of attempts to reproduce the effect in other fibres have, however, been unsuccessful. Firstly, single fibres were placed on a glass slide and flattened by rolling a glass rod along the direction of the fibre-axis. When air-dried fibres were used this resulted in a transformation to the unstable, optically positive state (Wilkins et al, 1951) which is highly disordered; that is, it had the same effect as excessive stretching. If, on the other hand, the fibres were rolled while at 75% relative humidity they remained optically negative but showed subsequently the less highly ordered structure B (Franklin and Gosling, 1953, Plate 4). Secondly, X-ray photographs were taken of single fibres displaced with respect to the collimator in such a way that only a small region near the surface of the fibre was exposed to the X-rays. In this way several well-orientated photographs of structure A were obtained, but they showed no trace of double orientation.

Density Determination

The density of NaDNA at various humidities was measured by the following method.

Homogeneous lumps of dry Na DNA were prepared by allowing pieces of swollen gel to dry slowly, stirring them gently at first to allow trapped

14.
air to escape. The lumps were then dried over P_2O_5 at room temperature for several weeks. To measure the density of the dry substance, each lump was placed in CCl_4 in a test-tube, and the temperature allowed to rise slowly from below $-10^\circ C$ until the lump just sank. In this way a density range of about 1.65 to 1.58 g/cc, corresponding to temperatures from $-10^\circ C$ to $25^\circ C$, can be satisfactorily covered. The density of dry Na DNA was found to be $1.625 \pm 0.002 \text{ g/cc}$ at $4 \pm 1^\circ C$, in good agreement with Astbury's value of 1.63 (Astbury 1947).

By using, in the same temperature range, $CHCl_3$ in place of CCl_4 densities between about 1.54 and 1.48 g/cc can be measured. Lumps of Na DNA were maintained at the required relative humidity until equilibrium was reached, then immersed in the appropriate liquid (CCl_4 or $CHCl_3$) the temperature of which was rapidly adjusted to give a density measurement. In this way the density of Na DNA at 75% R.H. was found to be $1.521 \pm 0.002 \text{ g/cc}$ (corresponding to a temperature of $2^\circ C$ to $4^\circ C$ in $CHCl_3$). The water uptake of the lumps at 75% R.H. was 32 - 42%.

Number of nucleotides per unit cell

We are now in a position to assign upper and lower limits to the number of nucleotides per unit cell. The value cannot be fixed precisely owing to the uncertainty in the quantity of water in the crystallites (Franklin and Gosling 1953); this in turn leads to some uncertainty in the density of the crystallites, which may well be slightly greater than the value measured for the bulk material at 75% R.H.

In Table 2 we show the number of nucleotides per **face**-centred unit cell, calculated for water contents of the crystallites corresponding to from 4 to 8 molecules of water per nucleotide, and assuming a density of 1.521 g/cc for the crystallites.

DISCUSSION

It has been shown that the use of the cylindrically symmetrical Patterson function has enabled the unit cell to be established for the most highly ordered state of the sodium desoxy-ribonucleate obtained from calf thymus. For subsequent stages in the elucidation of this

structure, methods used in the determination of structure of single crystals can therefore be applied. Work on the three-dimensional Patterson function is now in progress and will be described in a later paper. Since this is a much more powerful instrument than the cylindrical function, no attempt will be made to introduce hypotheses concerning details of structure at the present stage. A few comments of a general nature may, however, be made.

The Patterson function shows rather few peaks of remarkably high intensity relative to that of the peak at the origin. Since the unit cell contains a very large number of atoms (of the order of 1000 excluding hydrogen and water) it seems probable that the main features of the function represent phosphate - phosphate interactions, these being the heaviest group in the structure.

It will be observed that the face-centred monoclinic unit cell is near-hexagonal in projection. Nevertheless, there is evidence to suggest that the symmetry of the structural unit itself is far from cylindrical. Although the nature of the accident which produced double orientation of the crystallites in a fibre (Plate I) is unknown, it seems unlikely that it could have occurred at all if the individual crystallites had a high degree of symmetry about the fibre axis. Moreover, when the reflections are indexed it is found that nearly all the strong spots have indices $(hk\bar{l})$; the total intensity in $(hk\bar{l})$ reflections is about twice that in the (hkl) 's.

REFERENCES

- Astbury, W.T., (1947) Cold Spring Harbour Symp. on Quant. Biology, p. 56.
- British Association for the Advancement of Science, (1937), Mathematical Tables Vol. 6 Part 1. Cambridge University Press.
- Clepp, M.M., (1937), J. Maths and Phys., 16, 76.
- Cox, E.G. and Shaw, W. F. B., (1930), Proc. Roy. Soc., A 127, 71.
- Franklin, R.E. and Gosling, R. G., (1953), Acts Crystallographica.
- Jones, F.W., (1938), Proc. Roy. Soc., A166, 16.
- MacGillavry and Bruins, (1948), Acts Crystallographica 1 156.

TABLE 2

Number of nucleotides per unit cell

Mean molecular weight of dry nucleotide = 330			
Density of NaDNA at R.H. 75% = 1.521			
No. molecules water per nucleotide	Mol. Wt. nucleotide and water	Water content, per cent	No. nucleotides per unit cell
4	402	21.8	55.8
5	420	27.3	53.5
6	438	33.0	51.2
7	456	38.2	49.1
8	474	43.6	47.4

HEADINGS TO FIGURES

1. a) Diagram showing reciprocal lattice planes and reflecting sphere for tilted fibre. (a).
1. b) Appearance of photograph for diffraction conditions shown in (a).
-1-
X = position of equivalent reflections with fibre normal to X-ray beam.
• = position of equivalent reflections for fibre inclined at $(90 - \gamma)$ to X-ray beam.
2. Diagram illustrating spread of reflection in reciprocal space.
3. Cylindrical Patterson function of NaDNA (structure A).
4. Function shown in Fig. 3, with contribution of strong reflections reduced by one third.

HEADING TO PLATES

Plate 1. Single fibre, about 40μ diameter. Specimen-film distance 15 mm. Exposure about 100 hours. Photograph showing double orientation.

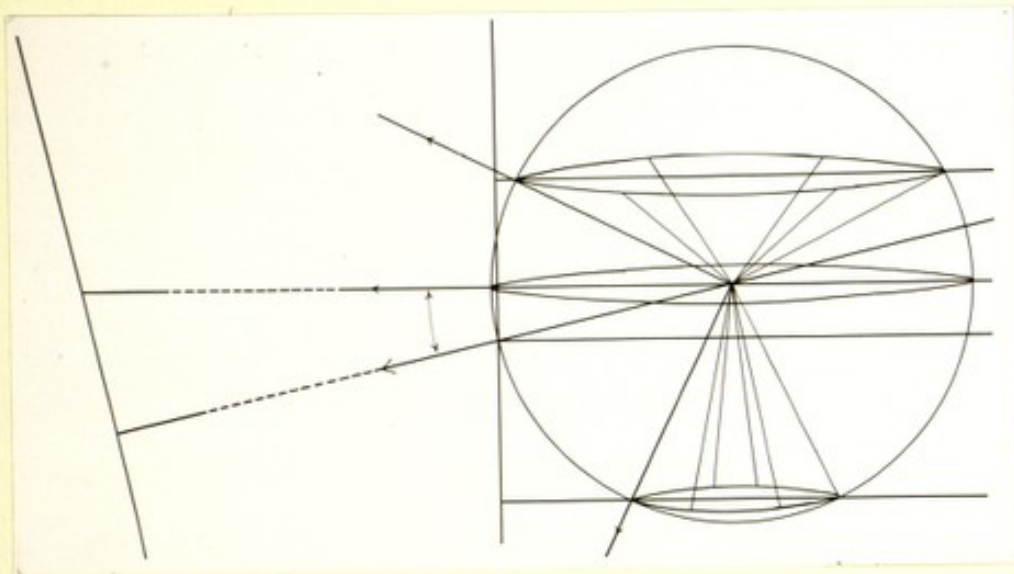


Fig 1a

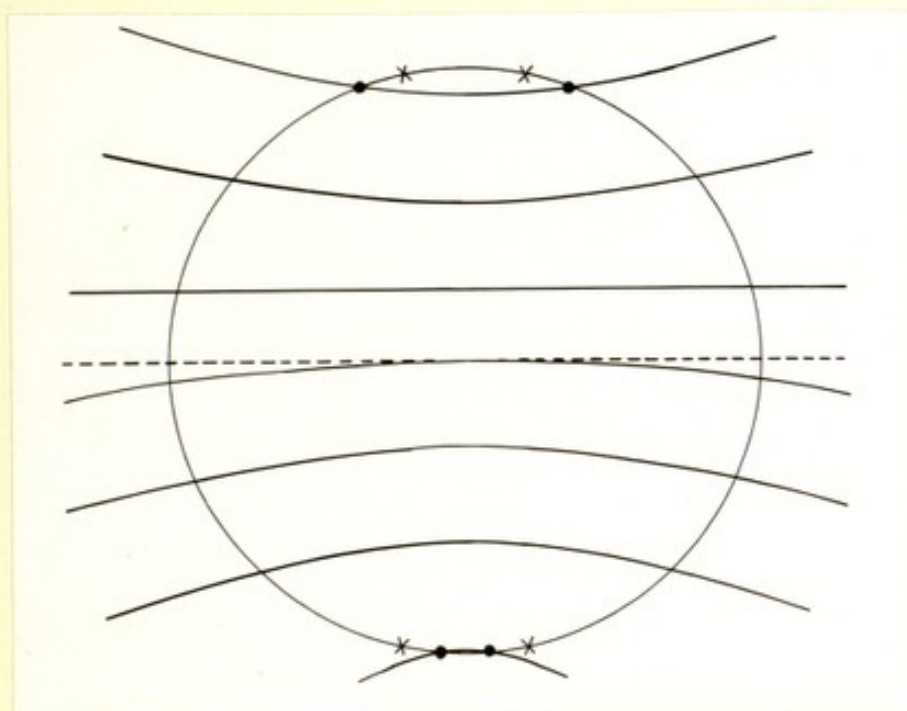


Fig 1b

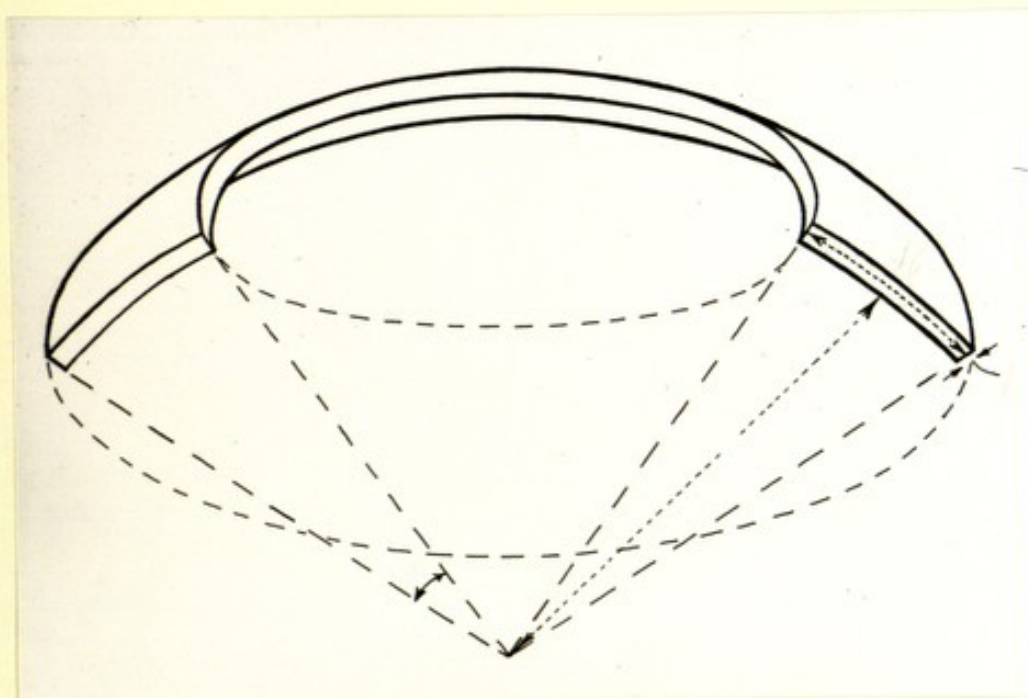


Fig 2

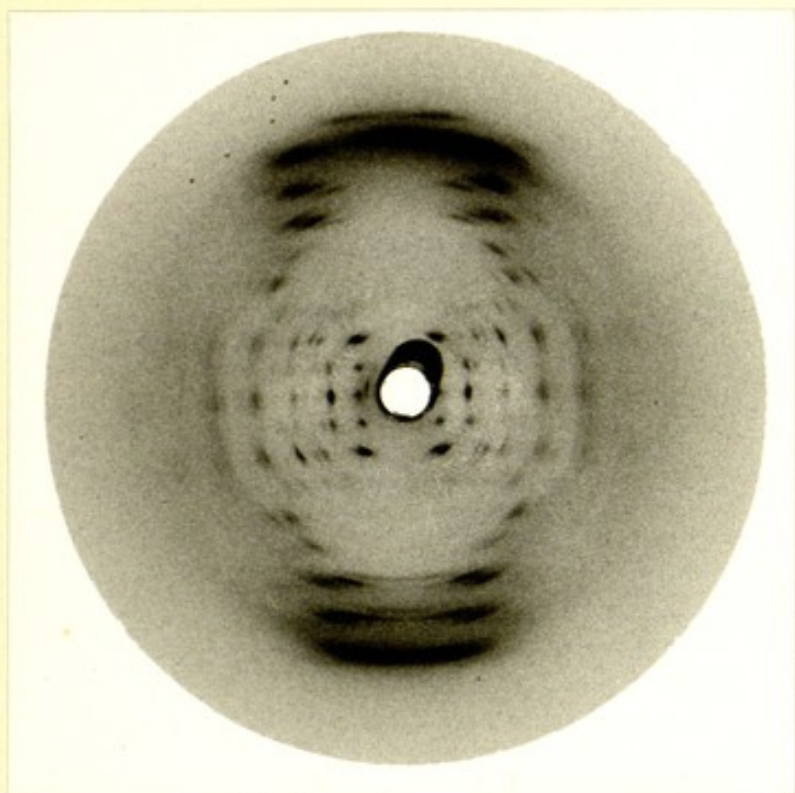


Plate 1